UNIVERSIDAD DE EXTREMADURA

TESIS DOCTORAL

ANÁLISIS Y VALIDACIÓN DE MATERIALES DESTINADOS AL DISEÑO DE INJERTOS VASCULARES DE INGENIERÍA TISULAR

DAVID DURÁN REY

Programa de Doctorado en Salud Pública y Animal

Conformidad de los directores:

Fdo. Dr. D. Francisco Miguel Sánchez Margallo

Fdo. Dra. Dña. Verónica Crisóstomo Ayala

Esta tesis cuenta con la autorización del director y codirectora de la misma y de la Comisión Académica del programa. Dichas autorizaciones constan en el Servicio de la Escuela Internacional de Doctorado de la Universidad de Extremadura.

2023

Esta tesis doctoral ha sido financiada parcialmente a través de la ayuda *PD18077* para la financiación de contratos predoctorales y de las ayudas GR18199 y GR21201 a Grupos de Investigación Catalogados, todas de la Consejería de Economía, Ciencia y Agenda Digital de la Junta de Extremadura/FSE y FEDER. Su realización se ha llevado a cabo en las Unidades U21-Experimental Operating Rooms, U22-Animal Housing y U24-Medical Imaging de la ICTS distribuida NANBIOSIS, localizadas en el Centro de Cirugía de Mínima Invasión Jesús Usón. Otra parte del presente trabajo fue realizado en el "Centro de Física das Universidades do Minho e do Porto (CF-UM-UP)" y en el "Institute of Science And Innovation for Bio-Sustainability (IB-S)" de la Universidad de Minho en Braga (Portugal).

Índice

Abreviaturas

DSC	Calorimetría de barrido diferencial (D*ifferential Scanning Calorimetry*)
ePTFE	Politetrafluoroetileno expandido (expanded Polytetrafluoroethylene)
ES-NO	Fibras electrohiladas no orientadas (E*lectrospun Non-Oriented fibers*)
ES-O	Fibras electrohiladas orientadas (E*lectrospun Oriented fibers*)
ES-O (0°)	Fibras electrohiladas orientadas en la misma dirección de la fuerza aplicada
ES-O (90°)	Fibras electrohiladas orientadas perpendicularmente a la dirección de la fuerza aplicada
FTIR	Espectroscopía de infrarrojos (*Fourier Transform Infrared Spectroscopy*)
hiPSCs	Células madre humanas pluripotentes inducidas (*human induced Pluripotent Stem Cells*)
HUVECs	Células endoteliales de vena umbilical humana (Human Umbilical Vein Endothelial Cells)
ISO	Organización Internacional de Normalización (*International Organization for Standardization*)
PET	Tereftalato de polietileno (Polyethylene Terephthalate)
PM	Membrana porosa (*Porous Membrane*)
PVDF	Fluoruro de polivinilideno (P*oly(vinylidene Fluoride)*)
SF	Fibroína de seda (*Silk Fibroin*)
TEVG	Injerto vascular de ingeniería tisular (T*issue-Engineered Vascular Graft*)

Summary

Cardiovascular diseases are the leading causes of death worldwide. The stenosis or blockage of blood vessels results in a decrease in blood flow and causes tissue damage due to inadequate nutrient supply. Conventional surgery is the main surgical option for the treatment of these diseases through the use of autologous vascular grafts. However, in certain patients, especially the elderly, the use of these grafts is not possible. In this situation, tissue-engineered vascular grafts are a promising therapeutic option that can replace or restore the biological functions of blood vessels.

The aim of this PhD thesis is to analyze and validate the physicochemical and biological properties of materials that can be used for the development of tissue-engineered vascular grafts. To this end, this research has been divided into several chapters. The first chapter addresses the current state of development of tissue-engineered vascular grafts, focusing on the methods and procedures used in the development of these grafts, as well as the advances and challenges in this field. The second chapter focuses on the manufacture and analysis of basic architectures designed with silk fibroin and poly(vinylidene fluoride) using various tissue engineering techniques. These studies provided information on the physicochemical and biological properties of the polymers, the results of which were used to determine they are optimal for vascular graft engineering, and select the best manufacturing method.

In summary, we have validated silk fibroin and poly(vinylidene fluoride) polymers for the development of tissue-engineered vascular grafts. Promising results have been obtained with electrospinning technology, establishing a new branch of research in the field of materials and tissue engineering.

Resumen

La principal causa de muerte en el mundo se relaciona con patologías del sistema cardiovascular. El estrechamiento o la obstrucción de los vasos sanguíneos provocan una reducción del flujo sanguíneo y daños en los tejidos debido a un aporte deficiente de nutrientes. La cirugía convencional mediante el uso de injertos vasculares autólogos es la principal opción quirúrgica para el tratamiento de estas patologías. Sin embargo, en determinados pacientes, especialmente en aquellos de avanzada edad, puede no ser posible utilizar estos injertos. Por este motivo, los injertos vasculares basados en ingeniería tisular resultan prometedores como tratamiento quirúrgico, los cuales tienen la capacidad de sustituir o reparar las funciones biológicas de los vasos sanguíneos.

Esta tesis doctoral tiene como objetivo primordial el análisis y validación de las propiedades fisicoquímicas y biológicas de materiales destinados al diseño de injertos vasculares de ingeniería tisular. Para ello, el presente trabajo se ha divido en dos bloques temáticos. El primer bloque se centra en el estado actual del desarrollo de los injertos vasculares de ingeniería de tejidos para conocer datos relativos a los materiales y metodologías empleados en el desarrollo de estos injertos, así como esclarecer los avances y desafíos hallados en este campo. El segundo bloque aborda la fabricación y análisis de estructuras básicas diseñadas con fibroína de seda y fluoruro de polivinilideno mediante diversas técnicas de ingeniería tisular. Estos estudios aportaron información de las características fisicoquímicas y biológicas de los polímeros, cuyos resultados sirvieron para comprobar si son óptimos para el diseño de injertos vasculares, así como hallar la mejor metodología para su desarrollo.

En definitiva, la presente tesis doctoral ha permitido la validación de los polímeros de fibroína de seda y fluoruro de polivinilideno para su uso en el diseño de injertos vasculares de ingeniería tisular. Hemos obtenido unos resultados prometedores con la tecnología del electrohilado, estableciendo una línea de investigación en el ámbito de materiales e ingeniería tisular.

Introducción

1. Perspectiva histórica: Injertos vasculares de ingeniería tisular

Las patologías relacionadas con el sistema cardiovascular son la principal causa de muerte en el mundo [1]. La reducción del flujo sanguíneo provocado por el estrechamiento o bloqueo de los vasos nativos genera daño tisular debido al suministro insuficiente o inadecuado de nutrientes. Además, la inactividad física, dietas no saludables, el consumo de alcohol y tabaco, entre otros, son factores de riesgo conductuales que aumentan la aparición de estas patologías, previéndose una tasa de mortalidad mundial superior a 20 millones de personas en el año 2030 [2,3].

La intervención farmacéutica y quirúrgica es requerida en la mayoría de las ocasiones. Entre los tratamientos, destacan las cirugías endovasculares, como la angioplastia, procedimiento que se emplea para paliar estas patologías mediante el dilatación de la estenosis [2]. A pesar de ello, la cirugía convencional mediante el uso de injertos vasculares autólogos sigue siendo la principal opción para el tratamiento de estas patologías, siendo la vena safena, arteria radial o la arteria mamaria interna las de elección para reestablecer el flujo sanguíneo [4].

Estos injertos vasculares autólogos pueden no estar disponibles en ciertos pacientes, especialmente en aquellos de edad avanzada o que presenten alguna patología vascular previa. Por esta razón, se introdujeron los primeros injertos sintéticos en la década de 1950. Esta circunstancia supuso el origen de nuevos avances en farmacología, ciencia de los materiales y metodologías de fabricación [5,6].

En términos generales, estas prótesis sintéticas resisten muy bien el enroscamiento y las diferentes presiones vasculares [7]. Se han obtenido muy buenos resultados clínicos en sustituciones arteriales de gran diámetro [8], como por ejemplo en *bypass* aortoilíacos (**Fig. 1**). El politetrafluoroetileno expandido (ePTFE) o el tereftalato de polietileno (PET), son materiales sintéticos utilizados en el diseño de injertos sintéticos comerciales. Sin embargo, se hallaron problemas clínicos al usarse estas prótesis comerciales en vasos de pequeño diámetro (<6 mm de diámetro) debido

a la disminución de la permeabilidad vascular y aparición de trombos [6]. Ante esta situación, surgieron los primeros injertos vasculares de ingeniería de tejidos (TEVGs; *tissue-engineered vascular grafts*) como alternativa, cuyo objetivo es diseñar injertos vasculares capaces de sustituir o reparar las funciones biológicas de los vasos sanguíneos.

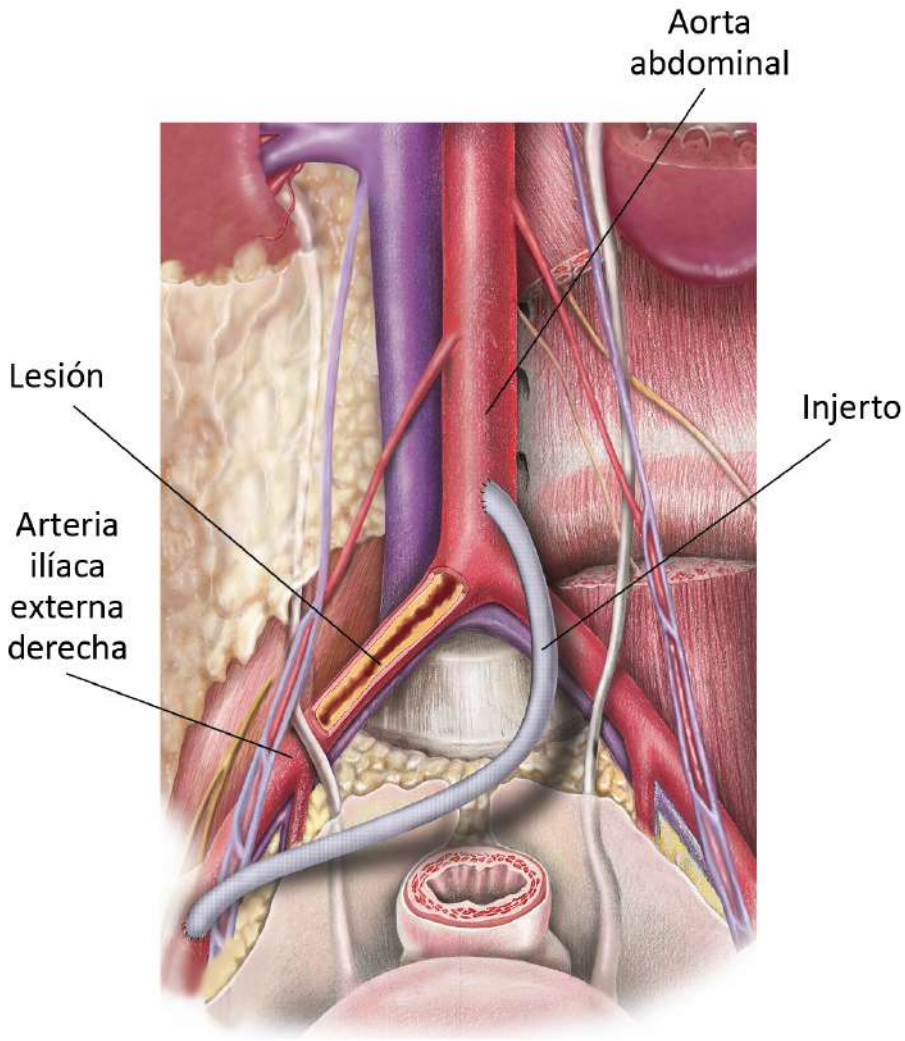

Figura 1: *Bypass* aortoilíaco derecho donde el injerto vascular permite la circulación de la sangre desde la aorta abdominal hacia la arteria ilíaca externa derecha.

Weinberg y Bell fueron quienes crearon el primer TEVG que imitaba las tres capas histológicas de las arterias [9]. Este injerto estaba diseñado a partir de un tubo de colágeno, una fina malla de Dacron y cultivo de células, tales como células endoteliales aórticas bovinas, células del músculo liso y fibroblastos procedentes de la adventicia. Este TEVG no fue implantado en modelos *in vivo*, ya que el punto de rotura de este injerto era de 300 mmHg, siendo bastante inferior con respecto al de los vasos nativos, los cuales presentan valores superiores a 1500 mmHg [10,11]. Posteriormente, L'Heureux et al. consiguieron desarrollar un TEVG completamente biodegradable, el cual estaba formado por colágeno a partir de células del músculo liso y fibroblastos, y cultivados con células endoteliales [12]. Este injerto mostró tener una resistencia a la rotura similar a la de los vasos nativos, pero la permeabilidad de los TEVGs solo duró una semana.

Estudios posteriores diseñaron injertos vasculares utilizando materiales sintéticos, como fue el caso de Hoerstrup et al., donde desarrollaron un TEVG diseñado con polímeros sintéticos (ácido poliglicólico/poli-4-hidroxibutirato) y cultivado con miofibroblastos y células endoteliales [13]. Surgieron una amplia variedad de injertos vasculares fabricados con materiales sintéticos, cuya aplicabilidad estuvo restringida debido a la aparición respuestas inmunes por parte del organismo [14]. En 2001, se realizó un estudio en humanos [15], donde los autores diseñaron un andamio biodegradable compuesto por un copolímero de L-lactida y ε-caprolactona, reforzado con ácido poliglicólico, y sembrado con células autólogas de médula ósea. Este injerto fue utilizado para reemplazar la arteria pulmonar debido a un defecto cardíaco congénito que producía niveles bajos de oxígeno en un paciente pediátrico.

Actualmente, y después de más de medio siglo de investigaciones, existe un amplio abanico de estudios destinados a mejorar el desarrollo y diseño de estos TEVGs aprovechándose de las nuevas tecnologías y materiales.

2. Principios básicos para el diseño de injertos vasculares de ingeniería tisular

La ingeniería tisular es un campo interdisciplinar que aprovecha la biología celular y los principios de la ingeniería para diseñar y desarrollar estructuras que restauren, imiten o mejoren las condiciones biológicas de los tejidos y órganos [16]. Por tanto, los injertos vasculares diseñados mediante ingeniería tisular tienen como objetivo sustituir o reparar las funciones biológicas de los vasos sanguíneos dañados. En términos generales, los TEVGs deben ser capaces de remodelarse, crecer, autorrepararse y responder al entorno inmediato [7]. Estos injertos deberían diseñarse con una conformación similar o idéntica a los vasos sanguíneos nativos, siendo importante estudiar su organización histológica antes de proceder a su desarrollo.

Histológicamente, las paredes arteriales y venosas se dividen en tres túnicas diferentes: íntima, media y adventicia (**Fig. 2**). La íntima, capa concéntrica más interna, provee a los vasos de una capa lisa. Esta estructura está formada principalmente por células endoteliales, las cuales son claves para prevenir la coagulación y regular el intercambio de oxígeno y nutrientes, así como controlar la señalización del componente muscular a la capa media [17]. Debemos destacar la existencia de una serie de válvulas venosas procedentes de unos repliegues de la capa íntima, cuya principal función es evitar el reflujo y estancamiento de la sangre, especialmente en las partes inferiores del cuerpo [18]. La túnica intermedia está constituida por una población densa de células musculares lisas, dilatándose y contrayéndose de forma coordinada cuando reciben señales de las células endoteliales de la capa íntima, de tal manera que pueden regular la función contráctil a medida que cambia la presión de los vasos sanguíneos [19]. Por último, la túnica adventicia compone la capa más externa, formado principalmente por fibras de colágeno y fibroblastos. A diferencia de la capa íntima que proporciona elasticidad al vaso sanguíneo, la capa adventicia aporta rigidez [19,20].

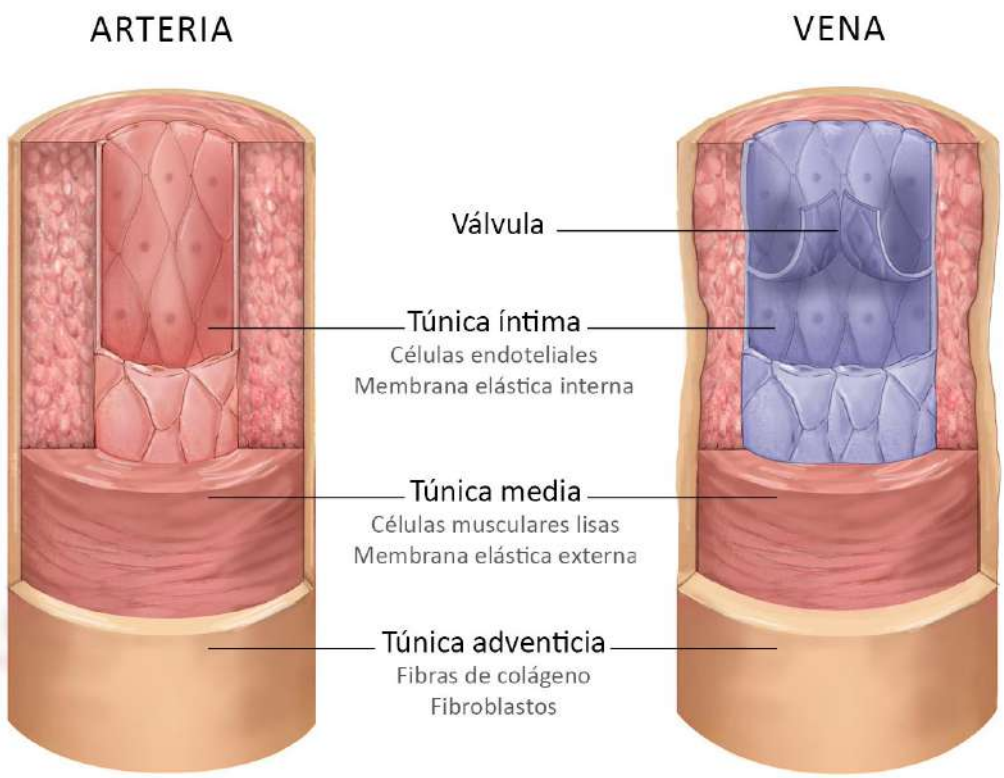

Figura 2: Ilustración histológica de una arteria y una vena con sus respectivas capas y componentes principales.

A la hora de diseñar un TEVG, hay que tener en cuenta una serie de características propias del injerto, tales como sus propiedades fisicoquímicas (resistencia mecánica, elasticidad, grado de cristalinidad del polímero, etc.) y biológicas (biocompatibilidad, adhesión y proliferación celular, etc.). Los TEVGs deben, en primera instancia, evitar la rotura tras su implantación y ser flexibles para acomodar el flujo sanguíneo, así como ser capaces de aguantar una presión pulsátil [6]. Además, los TEVGs tiene que estar diseñados con materiales no inmunogénicos y no trombogénicos, evitando la aparición respuestas inmunes e inflamación por parte del paciente y la formación de trombos, respectivamente [7]. Finalmente, las células utilizadas en la fabricación del TEVG (endoteliales, musculares, fibroblastos, etc.), así como las procedentes del organismo, deben de ser capaces de adherirse y proliferar en el injerto, de tal manera que exista una integración entre las células del huésped y el TEVG, mejorando la biocompatibilidad y regeneración del tejido [6].

2.1. Materiales utilizados en el diseño de andamios vasculares

Un TEVG debería estar formado por un andamio o scaffold, el cual da forma y resistencia mecánica al injerto. La arquitectura del andamio puede presentar porosidades, las cuales permiten y mejoran la adhesión y proliferación en el propio injerto. Idealmente, los andamios deberían ser biodegradables, reemplazándose por el nuevo tejido funcional procedente del organismo [7]. Sin embargo, esta degradación del andamio debe producir productos no tóxicos y que sean fácilmente liberados por el organismo [21]. Por otra parte, los andamios tienen que ser biocompatibles, no trombogénicos y presentar unas propiedades mecánicas (resistencia mecánica, elasticidad, etc.) aptas para su implantación, capaces de aguantar la presión pulsátil del flujo sanguíneo y evitar su rotura [6,22]. Debemos destacar que, aunque se recomienda usar andamios, se pueden desarrollar TEVGs sin ellos, por lo que los injertos están únicamente formados por células [23,24]. En cuanto a los tipos de materiales que pueden ser utilizados en el diseño de andamios vasculares, existe una amplia variedad, siendo principalmente naturales y sintéticos (**Tabla 1**).

Tabla 1. Resumen de las ventajas e inconvenientes de los materiales que pueden ser utilizados en el diseño de los TEVGs.

Materiales	Ventajas	Inconvenientes
Naturales	Biocompatibilidad Adhesión y proliferación celular Componentes de vasos nativos	Propiedades mecánicas Precio elevado Procesado complejo
Sintéticos	Propiedades mecánicas Económicos Rapidez de fabricación	Reacción inmune Hidrofóbicos Toxicidad en productos degradados

La principal ventaja de los polímeros naturales es su gran biocompatibilidad [25]. Estos materiales pueden obtenerse de una multitud de fuentes, como los tendones o la piel. Algunos ejemplos son el colágeno, el cual presenta baja antigenicidad, reduciendo la aparición de respuestas inmunitarias, y mejora la adhesión y proliferación celular [26,27], o la elastina, la cual previene la hiperplasia de la túnica

íntima [28]. No obstante, los andamios vasculares fabricados con estos polímeros naturales presentan propiedades mecánicas, tales como la resistencia a la rotura o elasticidad, inferiores a los vasos nativos [29,30]. Además, el procesado de estos polímeros es complejo, de larga duración y caro [25,28].

Por otro lado, los materiales sintéticos, como el ácido poliglicólico, el ácido poliláctico y la policaprolactona, destacan por su comportamiento mecánico, los cuales son capaces de adaptarse a las diferentes necesidades clínicas en términos de elasticidad y flexibilidad [31]. Entre todos ellos, debemos destacar el ácido poliglicólico, ya que diferentes estudios demostraron que este polímero puede soportar presiones equivalentes a la aórtica e incluso tener una resistencia mecánica superior a la de la vena safena [32,33]. Además de las propiedades mecánicas, los materiales sintéticos son económicos y fáciles de obtener, consiguiendo tiempos de fabricación cortos. Sin embargo, algunos polímeros presentan una baja biocompatibilidad, provocando reacciones inmunes, y generalmente presentan un comportamiento hidrofóbico, el cual interfiere en la adhesión y proliferación celular [28]. Por otro lado, muchos de estos polímeros son degradables, cuyos productos de descomposición pueden ser tóxicos para el organismo [25,34].

2.2. Tipos de células utilizadas en ingeniería de tejidos vasculares

Las células usadas en ingeniería de tejidos deben ser no inmunogénicas, funcionales y fáciles de obtener. La necesidad de utilización de un injerto vascular puede ser inmediata, por lo que se requieren tiempos de cultivos y procesado celulares cortos, así como un correcto funcionamiento celular y que no estén alteradas su comportamiento fisiológico. En la **Tabla 2** se resumen las principales técnicas de siembra celular aplicadas en los TEVGs [31,35].

Tabla 2. Principales tipos de siembra celular aplicadas en los TEVGs.

Siembra Celular	Técnica	Ventajas	Inconvenientes
Estática	Suspensión y cultivo celular directamente sobre el lumen o el exterior del andamio.	Económico Procedimiento sencillo Evita daño celular	Mala eficiencia de siembra celular Distribución no homogénea de las células
Dinámica	Siembra rotacional, al vacío y tensión de fluido.	Distribución y penetración homogénea de las células Eficiencia de siembra celular	Técnicas complejas Mayor susceptibilidad a la contaminación Condiciones específicas para cada técnica
Electroestática	Altera las cargas eléctricas del andamio para promover adhesión celular.	Alta eficiencia de siembra celular Acelera maduración celular	Las células solo se adhieren a la superficie Existen pocos estudios de viabilidad celular
Magnética	Uso de perlas magnéticas para seleccionar células deseadas y aplicación de un campo magnético externo.	Cultivo celular completo y homogéneo	Necesidad de evaluar posibles efectos secundarios

Por otro lado, existe un amplio abanico de fuentes celulares. A continuación, se resumen los principales tipos celulares utilizados en la producción de TEVGs.

Células autólogas

Son aquellas procedentes del propio paciente, por lo que la principal ventaja es la ausencia de reacción inmune [36]. Algunos ejemplos son las células endoteliales o las células del músculo liso, las cuales son muy importantes para la estructura y función de los vasos sanguíneos, como ya se ha explicado. En un estudio clínico realizo por Herrmann et al., se fabricaron TEVGs de 3-6 mm de diámetro mediante la obtención de injertos de vena safena procedentes de donantes de órganos, se descelularizaron y recelularizaron con células endoteliales autólogas. Estos injertos vasculares se implantaron en cirugías de *bypass* coronario de 12 pacientes con una edad media de

69 años, los cuales tuvieron una supervivencia de 9 años. Los resultados del final del estudio mostraron la presencia de estenosis en el injerto de 7 pacientes, y una permeabilidad del 50% [37]. Comentar como limitación de que el hecho de que estas células sean autólogas implica la obtención de las mismas mediante biopsia. Por otro lado, el uso de TEVG suele ser destinado a personas de avanzada edad, por lo que la capacidad proliferativa y regenerativa de estas células autólogas es limitada. Además, la realización de la biopsia y cultivo celular son procedimientos largos y costosos [34].

Células madre embrionarias

Estas células proceden, como su propio nombre indica, de embriones en la fase de blastocisto, por lo que presentan la capacidad de diferenciarse en cualquier célula de las capas germinales [38], tales como células endoteliales o células del músculo liso [34]. Sundaram et al. consiguieron desarrollar TEVGs de pequeño diámetro utilizando estas células. Los resultados *in vitro* demostraron la capacidad de las células madre embrionarias para diferenciarse en células del músculo liso y de ser cultivadas en TEVGs de ácido poliglicólico. Histológicamente, los injertos mostraron similitudes con respecto a los vasos nativos en términos de celularidad y expresión de marcadores de células de músculo liso [39]. Existen pocos estudios con el uso de estas células, ya que hay riesgo de rechazo inmunitario y tumorigenicidad, así como problemas éticos derivados de su uso en humanos [34,40].

Células madre mesenquimales

Las células madre mesenquimales son células madre adultas capaces de autorrenovarse y obtener células de linaje mesodérmico [41]. Estas células se obtienen en una multitud de fuentes, tales como el cordón umbilical o el tejido adiposo. Además, son capaces de secretar factores inmunosupresores, reduciendo las respuestas inmunogénicas [42,43], e incluso pueden promover la angiogénesis [44]. Zhao et al. fabricaron TEVGs de 2 mm de diámetro diseñados con células madre mesenquimales autólogas procedentes de la médula ósea. Los injertos fueron

implantados en la arteria carótida de 4 conejos durante 4 semanas, los cuales fueron permeables durante todo el estudio, no hallando signos de respuesta inmune, estenosis o formación de trombos [45]. Por otro lado, Jiao et al. desarrollaron injertos vasculares de 3 mm de diámetro a partir de arterias carótidas porcinas descelularizadas, las cuales fueron cultivadas con células madre mesenquimales procedentes de médula ósea. Tras un tiempo de cultivo de 7 días, se observaron células endoteliales en la capa interna de los TEVGs, así como la existencia de marcadores mecanorreceptores y de angiogénesis [46]. Sin embargo, durante el procesamiento *in vitro* de las células madre mesenquimales, éstas pierden rápidamente su capacidad de diferenciación, presentando una limitada e insuficiente expansión celular [34,42,47]. Además, se han reportado algunos casos en los que el tratamiento con estas células puede provocar trombosis debido a un incremento de los factores procoagulantes y de la respuesta inflamatoria [48,49].

Células progenitoras endoteliales

La sangre o la médula ósea son fuentes en las que se pueden obtener y aislar las células progenitoras, las cuales tienen el potencial diferenciarse en células endoteliales [34]. Las células procedentes de la sangre del cordón umbilical son más estables que las de la sangre periférica, pero su utilización es escasa debido a que no todos los pacientes pueden tener acceso a su propio cordón umbilical [50]. Los injertos vasculares desarrollados con las células progenitoras muestran potencial para la endotelización [51], así como un mantenimiento de la permeabilidad vascular [52]. Allen et al. demostraron que las células endoteliales procedentes de células progenitoras presentaban un crecimiento, fenotipo y funciones similares a las de los vasos nativos [53]. En otro estudio realizado por Muniswami et al., se cultivaron células progenitoras endoteliales en TEVGs descelularizados, los cuales se implantaron en la aorta abdominal de 3 ratas durante 1 semana. Los resultados mostraron que los injertos vasculares expresaban marcadores endoteliales y no se hallaron respuestas inmunogénicas [54]. Sin embargo, el uso de estas células está limitado debido a su dificultad de aislamiento y existencia de heterogeneidad relacionada con su potencial

angiogénico y especificidad tisular, así como desconocimiento de las características y mecanismos exactos de diferenciación de las células progenitoras endoteliales [42,54].

Células madre humanas pluripotentes inducidas

Las células madre humanas pluripotentes inducidas (hiPSCs; *human induced pluripotent stem cells*) son capaces de generar células específicas para el diseño de TEVG. Estos tipos de células pueden llegar a presentar propiedades similares al de las células madre embrionarias, ya que se generan a partir de la reprogramación genética de las células somáticas mediante factores de transcripción de pluripotencia [55]. Las principales características de estas células son su gran capacidad de autorrenovación y diferenciación en cualquier célula somática, como por ejemplo las células endoteliales y las células musculares lisas. Además, las células somáticas pueden proceder del paciente, evitando reacciones inmunogénicas [56,57]. En un estudio reciente realizado por Luo et al., se diseñaron TEVGs sembrando hiPSCs en un andamio de ácido poliglicólico, las cuales se diferenciaron en células del músculo liso. Los injertos con un diámetro de 3 mm se implantaron en la aorta abdominal de 6 ratas durante 60 días, los cuales permanecieron permeables durante todo el seguimiento y no se observaron reacciones inmunogénicas [58]. A pesar de todas las ventajas de las hiPSCs, existe el riesgo de teratogénesis y tumorigénesis debida a la activación no deseada de genes de pluripotencia [59-61]. Todavía se requieren más estudios para asegurar su aplicación clínica.

2.3. Metodologías aplicadas en el diseño de injertos vasculares

Como se ha descrito con anterioridad, los diferentes materiales y células modifican las propiedades fisicoquímicas y biológicas del injerto. La arquitectura de un TEVG es clave para el correcto funcionamiento del injerto, ya que su estructura interna modifica el comportamiento del mismo y su función, e influye en la adhesión y proliferación celular del huésped en el propio injerto [21,62]. La metodología empleada debería dar lugar a estructuras con poros, ya que es importante que las

células del huésped proliferen en el injerto vascular para que exista una integración entre las células del huésped y el TEVG [6], como se comentó anteriormente. Así pues, la metodología empleada en el diseño y desarrollo de los TEVGs influye directamente en la arquitectura del injerto, existiendo una amplia variedad de técnicas destinadas a la fabricación de injertos vasculares. A continuación, se exponen las principales metodologías usadas en la fabricación de TEVGs (**Fig. 3**).

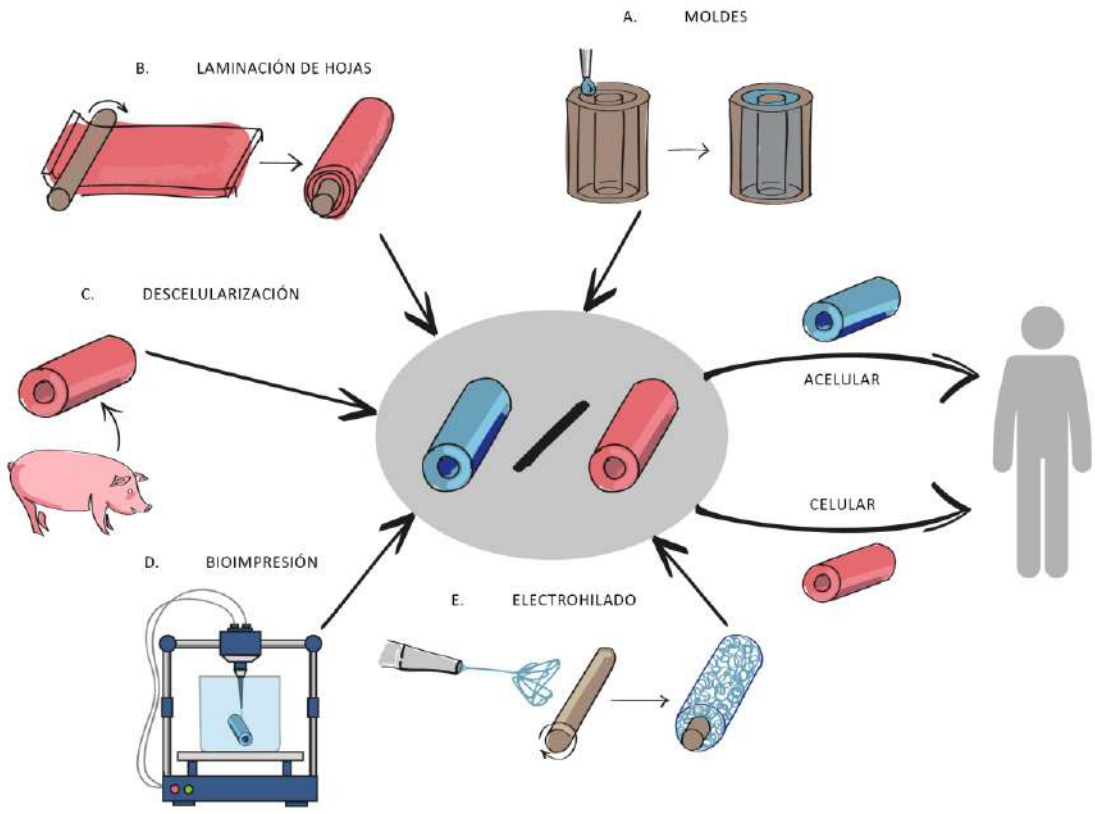

Figura 3: Principales metodologías utilizadas en la fabricación de injertos vasculares de ingeniería tisular, siendo **(a)** el uso de moldes, **(b)** laminación de hojas cultivadas con células, **(c)** obtención de un injerto vascular procedente de fuentes xenogénicas y descelularizarlo, **(d)** bioimpresión 3D, y el **(e)** electrohilado. Una vez fabricados, se puede llevar a cabo el cultivo celular del injerto, implantándose con o sin células.

Uso de moldes

Es una técnica relativamente sencilla en la que se utilizan moldes para fabricar estructuras tubulares con una morfología similar a los vasos sanguíneos nativos. En términos generales, la solución polimérica, ya sea con materiales naturales o sintéticos, se inyecta dentro de un molde cilíndrico. Dicho molde presenta un tubo interior, cuyo tamaño coincide con el diámetro interno deseado del injerto, y una pared externa, la cual delimita el grosor de la pared del TEVG [6].

Otras técnicas, como la lixiviación de sales, pueden utilizarse para crear injertos vasculares con porosidad. Sin embargo, las propiedades mecánicas de estos injertos, tales como la resistencia mecánica o la elasticidad, suelen ser insuficientes para su implantación, por lo que esta metodología puede combinarse con otras para mejorar dichas características y proporcionar resistencia adicional al TEVG, como la inserción de una malla o el revestimiento con fibras de electrohilado [63]. Un ejemplo de esta metodología sería el estudio de Jiao et al., donde diseñaron injertos vasculares con un diámetro de 3-6 mm utilizando moldes en los que se introdujo una solución de gelatina/alginato cargado de células madre con factores de crecimiento. Estas células se diferenciaron en células endoteliales y células de músculo liso para imitar la túnica íntima y media, respectivamente, y se añadió una capa externa de ácido poliláctico-glicólico para mejorar la resistencia mecánica de los injertos vasculares [64].

Laminación de hojas

En primer lugar, se diseñan láminas de células y, posteriormente, se enrollan sobre una estructura tubular para crear una morfología tridimensional [6]. Tradicionalmente se ha utilizado el laminado celular secuencial, el cual consiste en el cultivo de varias láminas celulares, dando lugar a un injerto multicapa formado exclusivamente por células. Debido a que se trata de un proceso largo, existe la opción de cultivar largas láminas con diferentes grupos celulares y, posteriormente, obtener en un solo paso un injerto vascular multicapa.

Por otro lado, se pueden mejorar las propiedades de los injertos combinándolos con otras técnicas, como el moldeo o el electrohilado [63]. Baba et al. diseñaron un TEVG con un diámetro de 4 mm utilizando láminas de fibra de vidrio sembradas con fibroblastos, células musculares lisas y células endoteliales, imitando las capas adventicia, media e íntima, respectivamente. Los resultados *in vitro* demostraron que la maduración de las capas en un biorreactor mejoró significativamente la resistencia mecánica del injerto vascular [65]. A pesar de que esta técnica permite la obtención de TEVGs diseñados con células autólogas, evitando respuestas inmunes por parte del organismo, así como diseñar estructuras biológicas muy similares a los vasos sanguíneos nativos, se trata de un proceso complejo y laborioso. Se necesitan biopsias para poder conseguir las células del huésped para, posteriormente cultivarlas y realizar la técnica de laminación. Además, estas láminas celulares son muy susceptibles a dañarse durante el proceso [63].

Descelularización

Consiste en la obtención de una matriz extracelular eliminando todas las células de un tejido u órgano mediante el uso de agentes físicos, químicos y enzimáticos [66,67]. Esta matriz extracelular puede ser obtenida a partir de fuentes alogénicas o xenogénicas, ya que en general la composición de la matriz extracelular es similar a la del ser humano, o a partir del cultivo de células autólogas en un andamio diseñado con materiales naturales o sintéticos y posteriormente descelularizada, donde se promueve la proliferación de las células del huésped [68-70]. En un estudio realizado por Liu et al., se fabricaron un TEVG de 2 mm mediante la descelularización de una membrana amniótica humana, cuya resistencia mecánica fue mejorada añadiendo externamente una capa electrohilada de policaprolactona y fibroína de seda. Este injerto fue implantado en la aorta abdominal de 10 ratas durante 24 semanas. Los resultados mostraron una rápida endotelización y una resistencia mecánica similar a la de la aorta nativa [71].

La descelularización permite al TEVG mantener una composición y arquitectura similar a las de los vasos sanguíneos nativos, por lo que presentan una

biocompatibilidad, adhesión y proliferación celular similar a ellos [72-74]. Al eliminar todo el material celular y antigénico, se disminuye el riesgo de reacciones inmunogénicas e inflamatorias [75]. Sin embargo, esta metodología implica un procesamiento complejo, donde las técnicas de descelularización pueden dañar la matriz extracelular, empeorando las propiedades mecánicas [76].

Impresión 3D y Bioimpresión

La impresión 3D es una técnica innovadora en el área de ingeniería tisular, ya que tiene la capacidad de diseñar y fabricar estructuras complejas con gran reproducibilidad [28]. La utilización de esta metodología comprende la obtención de imágenes del tejido u órgano diana mediante resonancia magnética o tomografía computarizada, diseño de la estructura utilizando un software informático, elección de una tinta imprimible y el desarrollo de un objeto 3D por medio de una impresora 3D [77]. Sin embargo, su aplicación en el campo de injertos vasculares ha sido poco estudiada debido a la generación de estructuras duras y rígidas [28], restringiendo su empleo en la planificación y enseñanza de procedimientos vasculares [78,79]. Por este motivo, la impresión 3D se utiliza en mayor medida en la fabricación de tejidos duros, tales como el hueso o el cartílago [67,80].

Un derivado de la impresión 3D es la bioimpresión, en la cual se utiliza una biotinta, es decir, la combinación de un polímero (colágeno, fibrina, alginato, etc.) y células (células del músculo liso, endoteliales, fibroblastos, etc.), obteniendo estructuras en 3D con células [81]. Existen una amplia variedad de estudios en los que se han diseñado y desarrollado injertos vasculares mediante bioimpresión. Algunos ejemplos son la fabricación de TEVGs combinando gelatina y fibroblastos [82], o el uso de una biotinta de metacrilato de gelatina cargado con células de músculo liso y posteriormente el cultivo de células endoteliales en la superficie interna de la estructura tubular [83]. La bioimpresión permite el diseño y fabricación de TEVGs con una adecuada densidad y distribución celular. Sin embargo, la resistencia y fuerza

mecánica son inferiores con respecto a los vasos nativos, estando limitado su implantación [28,77,84].

Electrohilado

El electrohilado o *electrospinning* es una técnica versátil utilizada para producir nanofibras de polímero, ya sea natural o sintético, mediante la aplicación de una corriente eléctrica [63,85]. En términos generales, el electrohilado se realiza mediante una jeringa en el que se encuentra la solución del polímero, una bomba para impulsar el émbolo de la jeringa, una cánula con punta roma por la que sale el polímero, un colector metálico donde se acumulan las fibras resultantes, y fuentes de alimentación de alto voltaje para generar un campo eléctrico (**Fig. 4**). En el caso del electrohilado destinado a TEVG, el colector tiene forma cilíndrica, cuyo grosor coindice con el diámetro interno del injerto vascular.

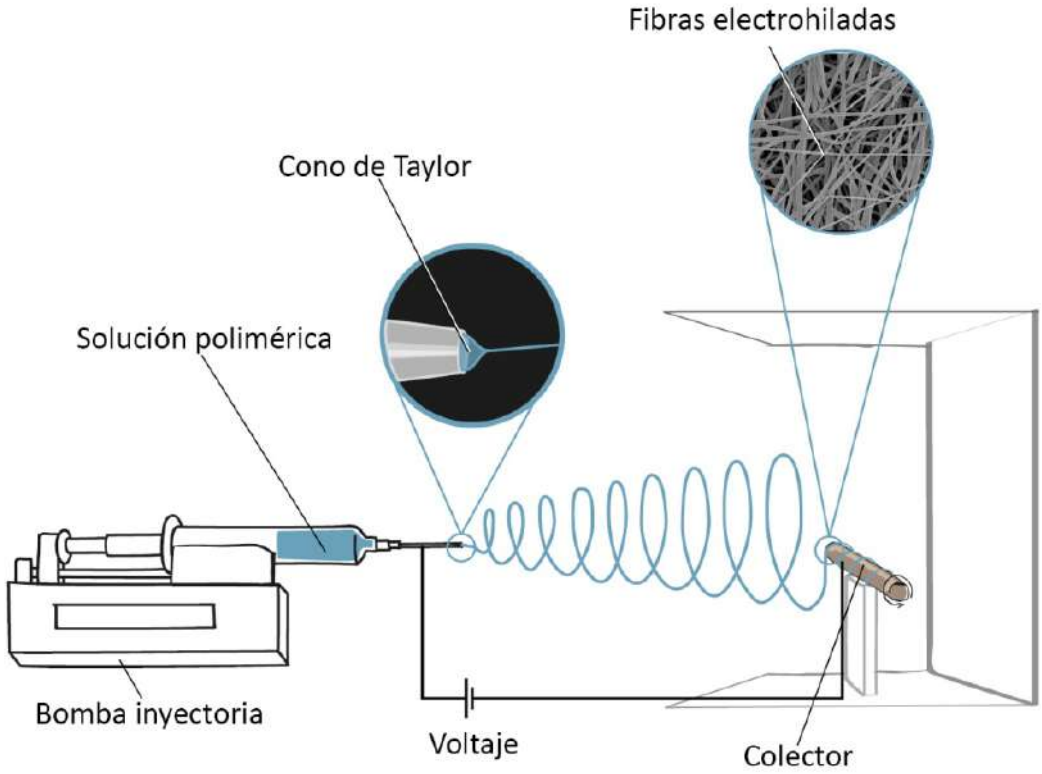

Figura 4: Representación de la configuración básica del electrohilado.

El factor clave de esta técnica es el empleo de un campo eléctrico entre la punta de la aguja y el colector metálico. Resumidamente, el electrohilado se puede dividir en las siguientes fases [85,86]:

1) Al principio, la solución del polímero se mantiene en la aguja por tensión superficial. Al aumentar el voltaje, las cargas electrostáticas se acumulan en la punta de la aguja, haciendo que la solución se reorganice formando un cono conocido como "cono de Taylor" [87].
2) Cuando la fuerza generada por el campo eléctrico logra superar la tensión superficial, se genera un chorro o *jet* del cono, en el que la solución fluye estable y uniformemente en línea recta desde la jeringa hacia un colector metálico cargado en sentido opuesto.
3) A medida que el chorro avanza se generan una serie de complejas inestabilidades en el chorro, provocando movimientos de flexión [88].
4) La evaporación del disolvente se produce durante el desplazamiento de la solución desde la jeringa al colector, lugar donde se forman las fibras de polímero.

El electrohilado es una metodología que permite realizar estructuras formadas por fibras de polímero, creando andamios con porosidades. Esas estructuras son capaces de replicar la arquitectura y propiedades mecánicas de los vasos sanguíneos nativos [89]. Además, diferentes estudios han demostrado que esta técnica mejora la adhesión y proliferación celular [90,91]. Por otro lado, existen una serie de parámetros, ya sean de la solución, del propio proceso de electrohilado o ambientales, que modifican la morfología de las fibras de polímero. En la **Tabla 3** se resumen los efectos de estos factores [63].

Tabla 3. Parámetros que afectan a la morfología de las fibras del polímero electrohiladas.

Parámetros		**Efecto en la Morfología de la Fibra**	**Referencias**
Solución	Viscosidad	Con un aumento en la viscosidad se obtienen fibras continuas, y con una disminución se forman partículas en lugar de fibras.	Shenoy et al. [92]
	Concentración del polímero	A mayor concentración, mayor diámetro de fibras.	Gu et al. [93]
	Tensión superficial	Cuando aumenta la tensión superficial de la solución, se necesitan valores más altos de voltaje.	Lee et al. [94]
Intrínsecos del electrohilado	Velocidad de flujo	Se puede incrementar el diámetro de las fibras con un aumento de la velocidad de flujo. Cuanto mayor sea la velocidad de flujo, mayor es la probabilidad de que se creen defectos en las fibras por una evaporación insuficiente del disolvente.	Zarghman et al. [95]
	Voltaje	A mayor voltaje, menor diámetro de fibra.	Deitzel et al. [96]
	Distancia aguja-colector	Cuanto menor es la distancia aguja-colector, menor es la evaporación del disolvente, generando defectos y modificaciones en el diámetro de las fibras.	Gaumer et al. [97]
Ambientales	Humedad	Cuanta más baja sea la humedad, se obtienen superficies más lisas. Cuanto mayor sean los valores de humedad, mayor cantidad de poros se generan en la superficie de las fibras.	Casper et al. [98] De Vrieze et al. [99]
	Temperatura	Afecta a la velocidad de evaporación del disolvente y a la viscosidad de la solución.	De Vrieze et al. [99]

3. Cirugía en injertos vasculares

El injerto vascular diseñado debe poseer unas propiedades fisicoquímicas y biológicas aptas para su implantación. Además, su diámetro y longitud tienen que ser similares al lugar anatómico donde se vaya a realizar la sustitución vascular. Una vez desarrollado el TEVG, es importante llevar a cabo correctamente la cirugía reconstructiva mediante la realización de una anastomosis vascular (**Fig. 5 y 6**), cuyo objetivo es la unión del injerto con el vaso nativo, consiguiendo sellar ambos extremos, sin hemorragia y usando el menor número posible de suturas.

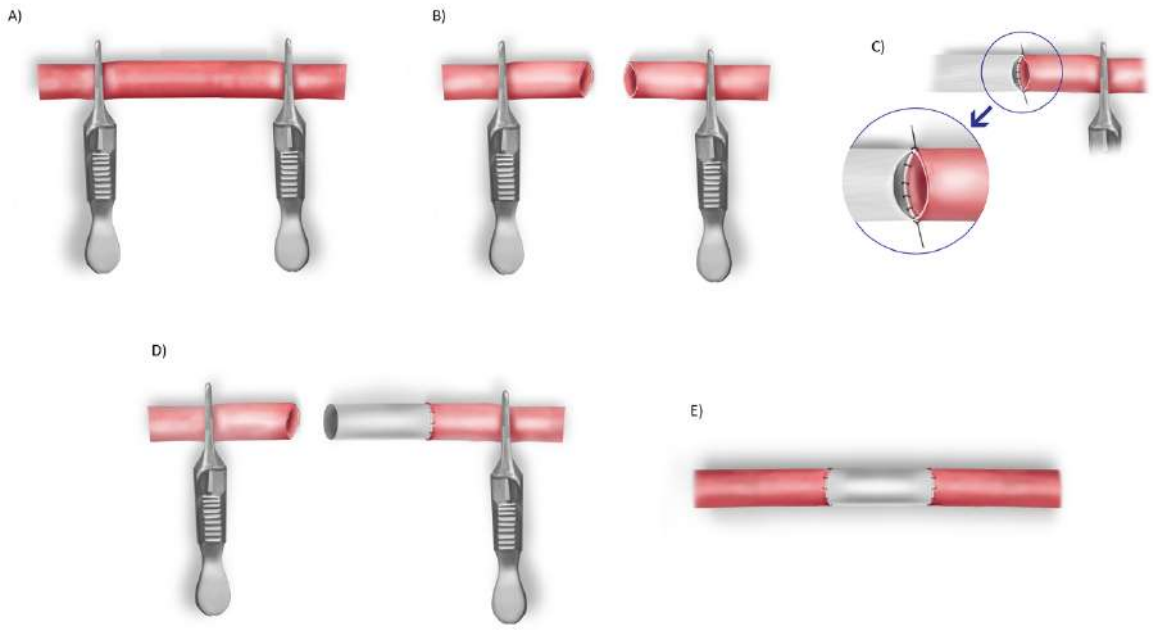

Figura 5: Implantación de un injerto vascular mediante anastomosis término-terminal. **a)** colocación de clamps hemostáticos, los cuales se sitúan lo más proximal y distal posible del vaso disecado; **b)** sección de la arteria o vena diana; **c)** sutura del injerto vascular empezando por un extremo de la anastomosis dejando puntos guía para facilitar la manipulación del vaso sanguíneo y del injerto; **d)** suturada toda la circunferencia en un lado, se realizan los mismos procedimientos en el extremo contrario; **e)** completada la anastomosis, se procederá a la retirada de los clamps vasculares y comprobación de si existen fugas de sangre tras la eliminación de los clamps, las cuales se tratan con suturas adicionales.

Aunque Alexis Carrel describió por primera vez la triangulación para realizar de forma segura una anastomosis, actualmente existe una amplia variedad de técnicas que se pueden llevar a cabo en dicho procedimiento quirúrgico [100,101]. En términos generales, se recomienda dejar 2 o 3 puntos guíaS con cabos largos para facilitar la manipulación del vaso y del injerto durante la cirugía [102]. La única diferencia entre ambas técnicas es la separación entre los puntos guía, siendo de 180° o 125°, respectivamente. Por otro lado, las suturas pueden realizarse de manera interrumpida o continua. A pesar de que la aplicación de sutura continua es más rápida y muestran resultados de permeabilidad similares que el patrón de puntos sueltos, se han hallado problemas asociados a estenosis vasculares. Por esta razón, la sutura interrumpida se aplica a anastomosis de pequeño calibre (menor de 6 mm), mientras que la continua a injertos de mediano-gran tamaño (mayor de 6 mm) [103,104].

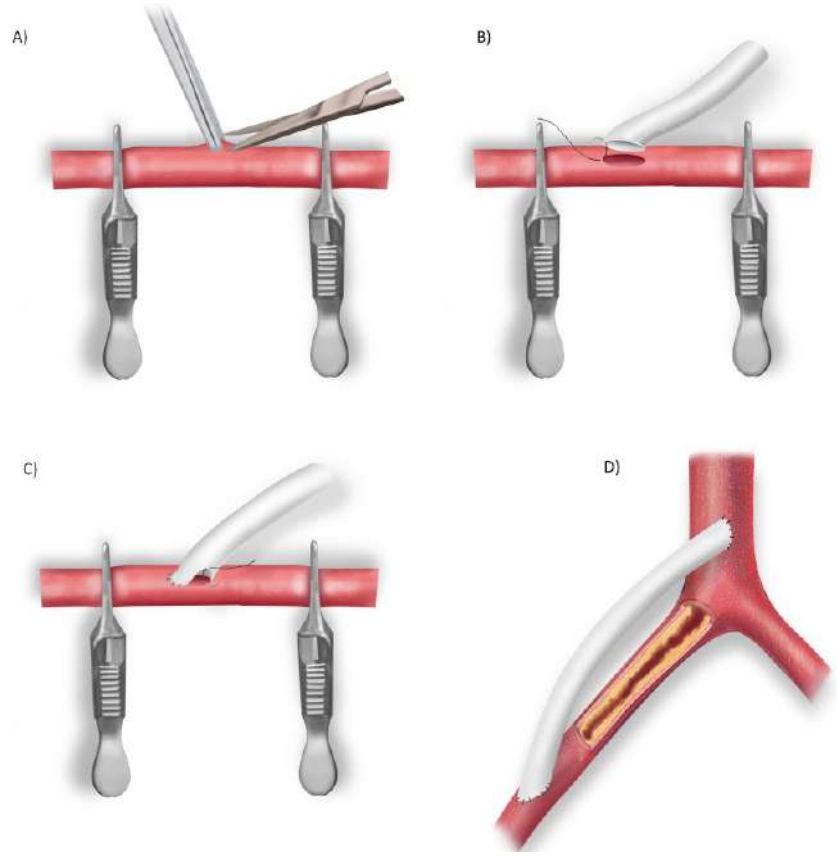

Figura 6: Implantación de un injerto vascular mediante anastomosis término-lateral, donde **a)** colocación de clamps hemostáticos y realización de una arteriotomía o venotomía en la superficie del vaso diana; **b-c)** sutura de un extremo del injerto vascular con respecto a el defecto creado previamente; **d)** se llevan a cabo los mismos procedimientos en el extremo contrario del injerto y el vaso diana, retirada de los clamps vasculares, y consecución de la revascularización de una arteria o vena mediante un *bypass*.

3.1. Fisiopatología vascular

Durante la cirugía vascular hay una serie de factores que se deben de tener en cuenta para asegurar el resultado clínico tras la realización de la anastomosis. Concretamente, el espasmo vascular y la formación de trombos son los principales problemas que pueden aparecer durante y tras la cirugía. Existe una multitud de causas que pueden provocar ambos procesos, tales como maniobras bruscas, sequedad de los tejidos, tensión o desgarros en la línea de sutura, etc. Todos estos factores provocan la disminución del calibre del vaso debido contracción de las fibras musculares lisas, en el caso del espasmo vascular [105], y la activación de las vías de coagulación y mecanismos trombogénicos, provocando la agregación de plaquetas y aparición de trombos [106].

No obstante, el espasmo vascular y la trombosis se pueden prevenir. Algunas de las estrategias son:

- Minimizar el daño quirúrgico [105,107], ya sea con el uso de clamps atraumáticos, uso correcto del material quirúrgico, evitar tensión en la línea de sutura, etc.
- Mantener la capa íntima, ya que está formado por células endoteliales, las cuales son clave para prevenir la coagulación y controlar la señalización del componente muscular a la capa media [17,108].
- Utilización de sustancias anticoagulantes como la heparina, la cual regula la actividad plaquetaria y evita la formación posterior de coágulos o trombos [102,109].
- Utilización de diferentes fármacos para prevenir los espasmos, como la lidocaína [110]. Este fármaco se puede utilizar antes de realizar la anastomosis debido a su efecto vasodilatador.
- Uso de suero atemperado localmente para prevenir que los tejidos se enfríen y se sequen. Además, se puede diluir junto a sustancias anticoagulantes para prevenir la formación de coágulos en el lumen vascular. Según se cree el defecto y antes de finalizar el último punto de la anastomosis, también se

puede lavar con suero salino heparinizado y atemperado para eliminar los restos de sangre [102,110].

3.2. Pruebas diagnósticas de permeabilidad vascular

Tras la finalización de la cirugía, es importante el seguimiento posoperatorio del paciente para comprobar la evolución, así como la permeabilidad del injerto. Existen varios métodos para analizar y diagnosticar la evolución del injerto vascular, destacando la ecografía y angiografía.

Ecografía

Se trata de un método no invasivo en el que se registra el flujo de la sangre gracias a la emisión y recepción de ultrasonidos. Se puede diagnosticar la presencia de coágulos, estenosis, flujometría, oclusiones vasculares, existencia de permeabilidad vascular, etc. [111,112]. Para la realización de este método diagnóstico, se debe colocar gel entre la sonda o transductor y la piel para permitir una adecuada trasmisión de los ultrasonidos. El funcionamiento consiste, en términos generales, en la emisión de ultrasonidos mediante la sonda, los cuales se trasmiten por los diferentes tejidos. Parte de estas ondas atraviesan el tejido, mientras que otras se reflejan y vuelven al transductor, obteniendo una imagen en escala de grises [113], que es lo que se conoce como Modo B. Los tejidos que no dejan pasar los ultrasonidos (hiperecoico), se verán de color blanco. Por otro lado, las zonas donde los ultrasonidos atraviesan los tejidos (anecoico), corresponden con las partes de color negro.

Existen varios modos durante la ecografía, los cuales permiten detectar e interpretar las zonas en las que existe movimiento. Para el diagnóstico de la permeabilidad vascular, se pueden diferenciar [113]:

- Modo Doppler espectral: representación gráfica de la variación de velocidad del flujo sanguíneo con respecto al ciclo cardíaco.

- Modo Doppler Color: representa la velocidad media y dirección flujo sanguíneo. En función de la dirección del flujo, se representa en una escala de colores. Puede ser de color rojo, si el flujo se acerca al transductor, y de color azul, si se aleja de la sonda.
- Modo Power-Color: permite valorar la intensidad o potencia del flujo sanguíneo. A diferencia de los anteriores, no cuantifica la velocidad ni dirección del flujo. Sin embargo, tiene una mayor sensibilidad a la existencia de permeabilidad vascular. Se representa la existencia movimiento con una escala de rojos.

Angiografía

Representa un método diagnóstico mínimamente invasivo que consiste en un examen de diagnóstico de los vasos sanguíneos mediante la utilización de rayos X y medios de contraste. Con este método se pueden identificar aneurismas, estenosis, malformaciones vasculares, trombos, etc. [114,115].

Generalmente, para el acceso vascular se emplea la técnica de *Seldinger* [116]. Esta técnica consiste en la punción percutánea con una aguja hasta localizar el vaso sanguíneo, dentro de la cual se avanza una guía. Una vez que la guía se encuentre dentro de la arteria, se retira la aguja y se introduce un catéter o introductor sobre la guía hasta estar en la localización deseada. Finalmente, se extrae la guía. La arteria femoral sigue siendo el acceso arterial más habitual y común, aunque actualmente existen otras alternativas como la arteria braquial, axilar o poplítea [117]. Por otro lado, se tiene que elegir adecuadamente el tipo de catéter en función de la anatomía específica del vaso diana. Algunos de los parámetros que se deben tener en cuenta para la elección del catéter son la longitud, diámetro del vaso, o la presencia de ramas, entre otros. Algunos ejemplos son la utilización del catéter *Judkins* para la cateterización de vasos coronarios [118,119], o el catéter *Headhunter* para vasos cerebrales o arteria carótida [120,121].

Justificación Unitaria de la Tesis

La mayor causa de muerte en el mundo son patologías relacionadas con el sistema cardiovascular. Un aporte deficiente de nutrientes debido a la estenosis u obstrucción de los vasos sanguíneos puede provocar daños irreparables en el tejido afectado. Se prevé un aumento progresivo de la mortalidad por patologías cardiovasculares durante los próximos años debido a los nuevos estilos de vida sedentarios, dieta poco saludable, la inactividad, el consumo de tabaco y alcohol, entre otros. La cirugía convencional mediante el uso de trasplantes autólogos es la principal opción terapéutica. No obstante, puede no existir la posibilidad de dicho tratamiento en ciertos pacientes, especialmente en aquellos de edad avanzada o que presenten algún tipo de patología vascular previa. Por esta razón, la ingeniería tisular es una tecnología prometedora como tratamiento clínico, ya que permite diseñar injertos vasculares de diferentes tamaños capaces de sustituir o reparar las funciones biológicas de los vasos sanguíneos.

Los injertos vasculares de ingeniería de tejidos deberían estar fabricados con un material capaz de tener una alta resistencia mecánica para evitar su rotura y facilitar su manipulación, así como un diseño que pueda sustituir o reparar el tejido del huésped y un tamaño de injerto adecuado para su uso clínico. Actualmente existen una amplia variedad de materiales que son utilizados en el diseño y desarrollo de injertos vasculares de ingeniería de tejidos, los cuales pueden ser categorizados como naturales o sintéticos. En primer lugar, los materiales naturales presentan baja antigenicidad y adecuada biocompatibilidad. Sin embargo, sus características mecánicas, tales como la resistencia mecánica o elasticidad, son inferiores a los materiales sintéticos. Por otro lado, los polímeros sintéticos presentan cualidades biológicas (biocompatibilidad, adhesión y proliferación celular, etc.) inferiores a los naturales. Todas estas características deben ser tenidas en cuenta, ya que son esenciales en el diseño de injertos vasculares de ingeniería tisular. Por esta razón, nuestra hipótesis de la presente tesis doctoral se fundamenta en que la evaluación de las propiedades fisicoquímicas y biológicas de los polímeros permitiría seleccionar el material más eficaz para el diseño de injertos vasculares basados en ingeniería tisular.

La ejecución de los distintos trabajos de investigación desarrollados para tal fin se ha realizado entre varias instituciones. Por un lado, el Centro de Cirugía de Mínima Invasión Jesús Usón (CCMIJU) es una institución dedicada a la investigación y formación quirúrgica. Dicho centro es uno de los Grupos de Investigación incluidos en el Centro de Investigación Biomédica en Red de Enfermedades Cardiovasculares (CIBERCV), dependiente del Instituto de Salud Carlos III, cuyo propósito es contribuir a reducir el impacto de las enfermedades cardiovasculares en nuestro entorno, liderando la investigación, la innovación y la formación en esta disciplina dentro del marco nacional e internacional. Además, el CCMIJU participa en una Red Cooperativa Orientada a conseguir resultados en Salud, concretamente en el área de Terapias Avanzadas (RICORS-TERAV). Esta red pretende promover investigaciones de utilidad para el conjunto de la ciudadanía, coordinando el tejido investigador del Sistema Nacional de Salud, y orientando su actividad investigadora hacia objetivos comunes con resultados transferibles a la población.

Por otro lado, parte de la investigación de la presente tesis se ha llevado a cabo en la "Universidade do Minho", concretamente en el "Centro de Física das Universidades do Minho e do Porto (CF-UM-UP)" y en el "Institute of Science And Innovation for Bio-Sustainability (IB-S)". Una de las líneas de investigación de estas instituciones es el desarrollo de materiales inteligentes y funcionales para aplicaciones biomédicas. Durante la estancia internacional hemos estado involucrados en la elección de los polímeros y en el desarrollo de estructuras desarrollados por ingeniería tisular, así como en el análisis de los resultados obtenidos que quedan recogidos en la presente tesis doctoral.

Objetivos

Una vez introducidos los conceptos generales sobre los que se desarrolla este trabajo, la presente tesis doctoral tiene como objetivo general el análisis y validación de las propiedades fisicoquímicas y biológicas de materiales destinados al diseño de injertos vasculares de ingeniería tisular. A continuación se enumeran los objetivos específicos perseguidos para conseguir este hito.

1. Estudio de los materiales y metodologías mayormente empleados en el diseño de injertos vasculares de ingeniería tisular.
2. Análisis de los desafíos hallados en la implantación de los injertos vasculares de ingeniería tisular.
3. Determinar las propiedades fisicoquímicas y biológicas de un polímero natural y otro sintético seleccionados en el presente trabajo.
4. Evaluar la alteración de las características fisicoquímicas y biológicas de los polímeros utilizados en función de la metodología de ingeniería tisular empleada.
5. Selección de la metodología más eficaz para el diseño de injertos vasculares de ingeniería tisular fundamentada en los resultados obtenidos tras el análisis de los polímeros.

Publicaciones científicas

Los resultados científicos de la presente tesis doctoral están estructurados en dos partes. A continuación, se exponen los distintos artículos científicos que desarrollan cada uno de estos bloques temáticos.

Bloque I) Estado actual de los injertos vasculares de ingeniería tisular.

- **Systematic review of tissue-engineered vascular graft**

  Durán-Rey D, Crisóstomo V, Sánchez-Margallo JA, Sánchez-Margallo FM.

  Front Bioeng Biotechnol. **2021**; 9: 771400.

  DOI: 10.3389/fbioe.2021.771400. PMID: 34805124.

  [Published]

frontiers in Bioengineering and Biotechnology

SYSTEMATIC REVIEW
published: 03 November 2021
doi: 10.3389/fbioe.2021.771400

Systematic Review of Tissue-Engineered Vascular Grafts

David Durán-Rey[1], *Verónica Crisóstomo*[2,3], *Juan A. Sánchez-Margallo*[4] *and Francisco M. Sánchez-Margallo*[3,5]*

[1]*Laparoscopy Unit, Jesús Usón Minimally Invasive Surgery Centre, Cáceres, Spain,* [2]*Cardiovascular Unit, Jesús Usón Minimally Invasive Surgery Centre, Cáceres, Spain,* [3]*Centro de Investigacion Biomédica en Red de Enfermedades Cardiovasculares (CIBERCV), Instituto de Salud Carlos III, Madrid, Spain,* [4]*Bioengineering and Health Technologies Unit, Jesús Usón Minimally Invasive Surgery Centre, Cáceres, Spain,* [5]*Scientific Direction, Jesús Usón Minimally Invasive Surgery Centre, Cáceres, Spain*

Pathologies related to the cardiovascular system are the leading causes of death worldwide. One of the main treatments is conventional surgery with autologous transplants. Although donor grafts are often unavailable, tissue-engineered vascular grafts (TEVGs) show promise for clinical treatments. A systematic review of the recent scientific literature was performed using PubMed (Medline) and Web of Science databases to provide an overview of the state-of-the-art in TEVG development. The use of TEVG in human patients remains quite restricted owing to the presence of vascular stenosis, existence of thrombi, and poor graft patency. A total of 92 original articles involving human patients and animal models were analyzed. A meta-analysis of the influence of the vascular graft diameter on the occurrence of thrombosis and graft patency was performed for the different models analyzed. Although there is no ideal animal model for TEVG research, the murine model is the most extensively used. Hybrid grafting, electrospinning, and cell seeding are currently the most promising technologies. The results showed that there is a tendency for thrombosis and non-patency in small-diameter grafts. TEVGs are under constant development, and research is oriented towards the search for safe devices.

Keywords: tissue-engineered vascular graft, patency, thrombosis, scaffold, animal model, human patient

OPEN ACCESS

Edited by:
Ornella Parolini,
Catholic University of the Sacred Heart, Italy

Reviewed by:
Paul Cahill,
Dublin City University, Ireland
Lynda Veluthenil Thomas,
Sree Chitra Tirunal Institute for Medical Sciences and Technology (SCTIMST), India

****Correspondence:***
Francisco M. Sánchez-Margallo
msanchez@ccmijesususon.com

Specialty section:
This article was submitted to Tissue Engineering and Regenerative Medicine, a section of the journal Frontiers in Bioengineering and Biotechnology

Received: *06 September 2021*
Accepted: *18 October 2021*
Published: *03 November 2021*

Citation:
Durán-Rey D, Crisóstomo V, Sánchez-Margallo JA and Sánchez-Margallo FM (2021) Systematic Review of Tissue-Engineered Vascular Grafts. Front. Bioeng. Biotechnol. 9:771400. doi: 10.3389/fbioe.2021.771400

1 INTRODUCTION

Cardiovascular diseases (CVDs) are the main cause of death globally (World Health Organization, 2020). The narrowing or blockage of blood vessels are disorders that induce reduced blood flow and tissue damage due to poor nutrient provision (Pashneh-Tala et al., 2015). Annual mortality from CVDs is expected to increase to 23.3 million people worldwide by 2030 (Mathers and Loncar, 2006).

A change in lifestyle, including a healthy and balanced diet, could be adequate to prevent CVD. However, surgical and pharmaceutical intervention are often required (Abdulhannan et al., 2012). Endovascular surgeries, including angioplasty, can be used to mitigate these diseases (Pashneh-Tala et al., 2015). However, conventional surgeries using autologous saphenous veins, radial arteries, or internal mammary artery transplants—which create a bypass to restore normal blood flow—are often required (Row et al., 2017). Many studies have been conducted aiming to treat vascular disorders through the use of vascular grafts, and their efficacy in animal models and human patients has been demonstrated.

In certain patients, and especially in the elderly, the use of autologous grafts may not be possible (Mozaffarian et al., 2015). Consequently, new technologies, such as tissue engineering, have begun to be developed. Tissue-engineered vascular grafts (TEVGs) show promise as a clinical treatment (Radke et al., 2018).

Synthetic materials have been studied for the creation of vascular grafts for more than 50 years. In the middle of the last century, vascular grafts were developed using two types of synthetic materials: polytetrafluoroethylene (PTFE, Teflon®) and polyethylene terephthalate (PET, Dacron®). Promising results have been obtained in aorto-iliac replacements and in arteries with medium-sized diameters (6–8 mm). However, these materials have not produced satisfactory results in small-caliber grafts owing to thrombus formation or poor patency rates (Lovett et al., 2007; Pashneh-Tala et al., 2015).

Weinberg and Bell created the first TEVG designed with biosynthetic materials in 1986, created from collagen gel tubes and cultures of vascular cells, such as bovine aortic endothelial cells (EC), smooth muscle cells (SMCs), and fibroblasts from adventitia (Weinberg and Bell, 1986). In the following years, other authors conducted studies using similar materials (Pashneh-Tala et al., 2015). However, one of the problems encountered was that the vascular grafts did not support arterial pressure. Conversely, the use of nondegradable materials may have harmful effects in organisms (L'Heureux et al., 2007). Different vascular graft scaffolds have been developed to correct these effects, wherein animal cells were seeded in partially resorbable polymers (Shum-Tim et al., 1999; Shin'oka et al., 2001). The developed animal models were able to reproduce the different mechanical vascular properties and yielded satisfactory results. However, when human cells were used, vascular grafts did not exhibit adequate mechanical properties for potential applications in humans (Poh et al., 2005).

Ideal TEVGs should be designed with scaffolds that shape the graft with an adhesive matrix mainly consisting of fibrin and vascular cells (Baguneid et al., 2006). In addition, TEVGs should have high strength to prevent rupture and facilitate manipulation, a design capable of replacing the host's tissue, and an adequate graft size for clinical use (Mahara et al., 2015).

Many of the challenges that hampered the development of vascular grafts have been overcome, particularly during the last decade. Nevertheless, there are still many aspects to be improved and problems to be solved to guarantee their safe use. A wide variety of new materials and technologies have been developed to create TEVGs, each providing different properties to these grafts. Therefore, we believe that this systematic review provides an update of the results recently published in the scientific literature, emphasizing the methods, and innovations used in the development of TEVGs. It also summarizes the current results obtained in animal models and human patients and influence of the graft diameter and heparin use on the occurrence of thrombosis and patency in these grafts. Thus, the objective of this work is to provide an overview of the current state-of-the-art in the development of TEVGs to demonstrate the advances and challenges faced over the last decade and present the objectives and clinical applications pursued by the authors.

2 MATERIALS AND METHODS

2.1 Search Strategy

A structured bibliographical search was conducted in the PubMed and Web of Science databases. We used a set of keywords related to TEVGs to identify relevant studies published from September 16, 2010, to September 15, 2020 (see **Supplementary Materials**, full search strategy). This systematic review has been registered on PROSPERO with the registration number CRD42020191561.

2.2 Selection of Articles

A series of inclusion and exclusion criteria were considered to select the articles that best applied for our objectives (see **Supplementary Materials**). In general, articles whose subject was TEVG, written in English, and including surgical procedures and follow-up in animal models or human patients were selected. A flowchart showing the different phases of the systematic review was designed according to the Preferred Reporting Items for Systematic Reviews and Meta-Analysis (PRISMA) statement for reporting systematic reviews and meta-analyses (Moher et al., 2015).

2.3 Statistical Analysis

A meta-analysis of the influence of the vascular graft diameter on thrombosis occurrence and patency was performed for the different models analyzed. For this purpose, the normality of the data distribution was analyzed using the Kolmogorov–Smirnov test. As the distribution of the data was not normal, we used the nonparametric Mann–Whitney U-test for independent samples to compare the data. Additionally, the relationship between qualitative variables of heparin use during surgery and graft patency and the onset of thrombosis was analyzed. The Fisher's exact test was used for this purpose. All statistical analyses were conducted using R (version 4.0.0, R Foundation for Statistical Computing, Vienna, Austria). For all tests, $p < 0.05$ was considered to be statistically significant. Only the models with adequate data for statistical analysis were shown in the graphs.

3 RESULTS

3.1 Selection of Articles

A total of 680 and 838 records were identified in PubMed and Web of Science databases, respectively. Based on the analysis of the title and abstract of each article, 907 records were excluded because: 1) the subject did not comply with the goal of this review (431); 2) they were types of studies that did not meet the inclusion criteria (454); or 3) they were in a language other than English (22). After completely reading these articles, 92 studies were selected, 89 of which used animal models and three were conducted with human patients (**Figure 1**).

3.2 Animal Models and Human Trials for TEVG

Regarding experimental animal models, studies with rodents, ovine, pigs, rabbits, dogs, and baboons were included in this systematic review. In addition, human trials were also analyzed in the review (**Table 1**).

3.3 Place of Implantation

Grafts were implanted in the abdominal aorta, carotid, pulmonary, femoral, and iliac arteries, and the portal, cava,

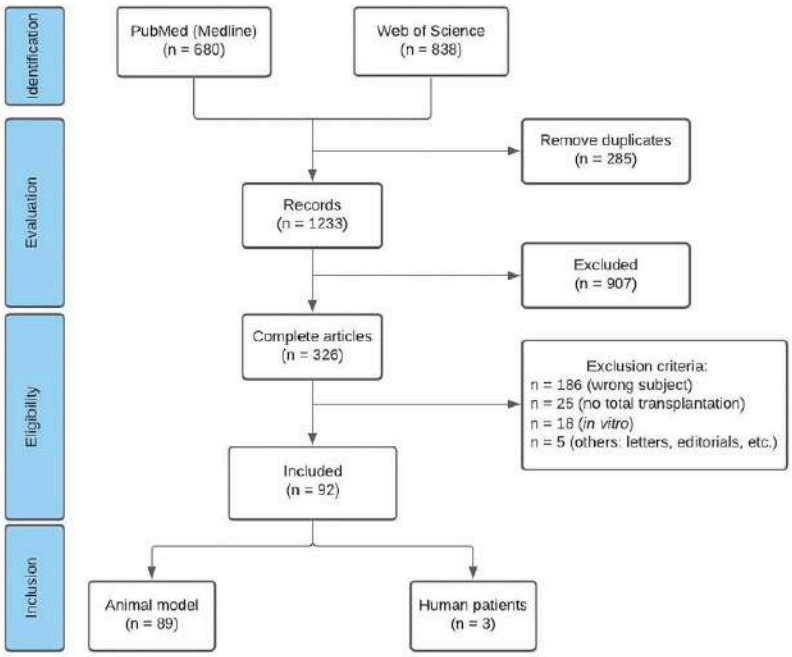

FIGURE 1 | PRISMA flow diagram. Diagram showing the manuscript selection process in accordance with PRISMA guidelines.

and jugular veins. There were some studies where bypass or shunt procedures were performed (Prichard et al., 2011; Koenneker et al., 2012; Tillman et al., 2012; Syedain et al., 2017; Ong et al., 2017a; Valencia-Rivero et al., 2018; Bai et al., 2019; Furukoshi et al., 2019; Itoh et al., 2019).

3.4 Design of TEVG

Four groups were differentiated in this systematic review according to the materials used in the graft design: 1) TEVG created with biodegradable polymers, 2) TEVG developed with natural materials, 3) TEVG created with biodegradable polymers and natural materials or hybrid grafts, and 4) tissue-engineered scaffolds or acellular tissue-engineered grafts (Table 2).

3.5 Statistical Results

Rodents led to a greater occurrence of thrombosis for large-diameter grafts (Figure 2). Conversely, grafts with a large diameter in rodents had good patency (Figure 3). Both porcine and ovine models did not show statistically significant differences in the relationship between the graft diameter and onset of thrombosis (Figure 2) and in the relationship between the graft diameter and patency (Figure 3).

There was a statistically significant correlation between the patency of the vascular graft and the absence of thrombus in murine, ovine, porcine, rabbit, and canine models (Figure 4). There was a correlation between the non-patency of the vascular graft and the onset of thrombosis during surgery in the nonhuman primate model. In the case of human patients, there was a correlation between the nonpatency of the grafts and the occurrences of thrombi.

There was no relationship between the use of heparin and the onset of thrombosis during surgery in the murine and porcine models (Figure 5).

4 DISCUSSION

Conventional surgery with the use of vascular grafts, such as autologous transplants, is a treatment for many CVDs (e.g., atherosclerosis) (Row et al., 2017). However, such autologous vascular grafts are often unavailable (Mozaffarian et al., 2015). Therefore, the development of tissue-engineered vascular grafts (TEVGs) represents an innovative area of research that aims to offer continuous availability. Tissue engineering is a multidisciplinary field combining biomedical engineering, material science, regenerative medicine, and immunology (Best et al., 2018). Although many studies using various materials and methods for the development of TEVGs have been published (Row et al., 2017), some of the defects they entail, such as the occurrences of thrombi, have not been fully corrected yet. In this work, we conducted a comprehensive review of recently

TABLE 1 | Studies with animal models and human patients included in the systematic review.

Animal model/human trials	Number of studies	Percentage of total (%)	References
Rodents	44	46.31	Lovett et al. (2010), Song et al. (2010), Harrington et al. (2011), Hibino et al. (2011), Hwang et al. (2011), Assmann et al. (2012), Quint et al. (2012), De Valence et al. (2013), Conconi et al. (2014), Lee et al. (2014), Tara et al. (2014), Udelsman et al. (2014), Itoh et al. (2015), Tara et al. (2015), Wu et al. (2015), Fukunishi et al. (2016), Gui et al. (2016), Hibino et al. (2016), Jiang et al. (2016), Khosravi et al. (2016), Tondreau et al. (2016), Wang et al. (2016), Yang et al. (2016), Li et al. (2017), Maxfield et al. (2017), Negishi et al. (2017), Best et al. (2018), Lee et al. (2018), Li et al. (2018), Qin et al. (2018), Shafiq et al. (2018), Wu et al. (2018), Xu et al. (2018), Aubin et al. (2019), Bai et al. (2019), Best et al. (2019), Katsimpoulas et al. (2019), Liu et al. (2019), Ran et al. (2019), Shi et al. (2019), Smith et al. (2019), Sologashvili et al. (2019), Yamanami et al. (2019)
Ovine	19	20	Cummings et al. (2012), Koenneker et al. (2012), Tillman et al. (2012), Meier et al. (2014), Stacy et al. (2014), Row et al. (2015), Aper et al. (2016), Fukunishi et al. (2016), Koobatian et al. (2016), Syedain et al. (2016), Fukunishi et al. (2017), Ju et al. (2017), Pepper et al. (2017), Ong et al. (2017a), Madhavan et al. (2018), Valencia-Rivero et al. (2018), Weber et al. (2018), Alessandrino et al. (2019), Wolf et al. (2019)
Pigs	13	13.68	Quint et al. (2011), Mrówczyński et al. (2014), Koens et al. (2015), Mahara et al. (2015), Pellegata et al. (2015), Rothuizen et al. (2016), Dahan et al. (2017), Iacobazzi et al. (2018), Valencia-Rivero et al. (2018), Alessandrino et al. (2019), Itoh et al. (2019), Wang et al. (2019), Yeung et al. (2019)
Rabbits	7	7.37	Zhao et al. (2012), McIlhenny et al. (2015), Hu et al. (2017), Tseng et al. (2017), Jin et al. (2019a), Jin et al. (2019b), Kajbafzadeh et al. (2019)
Dogs	7	7.37	Matsumura et al. (2012), Aytemiz et al. (2013), Matsumura et al. (2013), Isayama et al. (2014), Ma et al. (2017), Furukoshi et al. (2019), Jang et al. (2020)
Human patients	3	3.16	Sugiura et al. (2018), Herrmann et al. (2019), Kirkton et al. (2019)
Baboons	2	2.11	Prichard et al. (2011), Syedain et al. (2017)

published results in the field of TEVG development, both in animal models and for use in humans. Emphasis has been placed on the influence of the graft diameter and the use of heparin on the occurrence of thrombi and patency of the graft.

4.1 Animal Models for TEVG

Six experimental animal models have been included in this review. The ideal animal model should exhibit a cardiovascular anatomy and physiology very similar to that of humans. However, each animal model has a series of peculiarities (Table 3). Rodents were the most commonly used model in the studied literature owing to their low cost. Further, besides being ideal for biocompatibility and cell infiltration studies (Pashneh-Tala et al., 2015), they provide information about the molecular and cellular bases of cardiovascular biology (Lelovas et al., 2014). Furthermore, there are genetically modified strains and immune-deficient rodents that are used to simulate cardiovascular disease in humans (Bergmeister et al., 2019). Nevertheless, cardiovascular physiology, thrombogenicity, and hemostasis mechanisms are different from those in humans (Pashneh-Tala et al., 2015; Bergmeister et al., 2019). It seems that the biocompatibility of rodents allows them to withstand TEVG without the use of heparin to prevent the appearance of thrombosis and to have a good long-term patency. Nevertheless, the use of heparin is advisable to prevent possible thrombus formation (Aslani et al., 2020). The second most used animal model was the ovine model. Unlike rodents, sheep have thrombogenicity mechanisms and fibrinolysis system very similar to humans, as well as endothelialization and neointimal formation of blood vessels (Pashneh-Tala et al., 2015; Bergmeister et al., 2019). However, they have a high tendency of hypercoagulability (Pashneh-Tala et al., 2015). Porcine have a cardiovascular anatomy very similar to that of humans; therefore, there are numerous cardiovascular studies using porcine models in the scientific literature (Lelovas et al., 2014). However, because porcine grow rapidly, they become difficult to handle; thus, some studies have utilized miniature pigs (Mahara et al., 2015; Alessandrino et al., 2019; Itoh et al., 2019; Wang et al., 2019). Extensive heparin has been used in porcine models but there was no evidence for the formation of thrombi during surgery. The immune responses against vascular grafts were very intense and tended to hypercoagulate after surgical intervention (Mulier et al., 2012; Pashneh-Tala et al., 2015). Thus, the use of heparin was fundamental in this animal model. Further, muscular spams are very common in the arteries of pigs and are fragile (Bergmeister et al., 2019). Rabbits present thrombogenicity pathways comparable to other models (Pashneh-Tala et al., 2015), and hemostasis and endothelialization are more similar to that of humans than in the case of rodents. There are some heritable disease models that can be used for certain pathologies, such as hypercholesteremic Watanabe rabbit (Bergmeister et al., 2019). Nevertheless, their vascular physiology is quite different from human physiology (Pashneh-Tala et al., 2015). In the case of the canine model, the main advantages are that the anatomy has been extensively studied and lack of spontaneous endothelialization, which makes their control and monitoring advantageous. However, thrombogenicity presents different mechanisms with respect to the human model (Pashneh-Tala et al., 2015), and have a potent fibrinolytic system (Bergmeister et al., 2019). There are ethical aspects related to a diminished acceptance from an experimental point-of-view. Finally, two studies were conducted with nonhuman primates (Prichard et al., 2011; Syedain et al., 2017). This model has clear similarities with humans in terms of physiology,

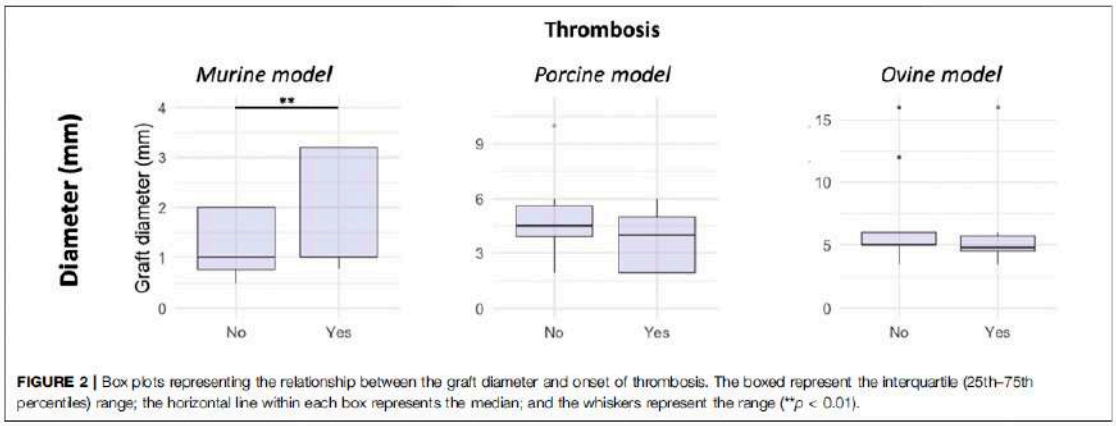

FIGURE 2 | Box plots representing the relationship between the graft diameter and onset of thrombosis. The boxed represent the interquartile (25th–75th percentiles) range; the horizontal line within each box represents the median; and the whiskers represent the range (**$p < 0.01$).

cardiovascular anatomy, and thrombogenicity mechanisms. However, this model is costly and presents ethical considerations regarding its use (Pashneh-Tala et al., 2015).

According to the results found, the ovine and porcine models seem to be appropriate models for TEVGs research. On the one hand, ovine model has an anatomy and hemodynamic mechanism quite similar to human. Further, these animals have a long neck, greatly facilitates surgery. Moreover, porcine is widely used for translational studies due to its strong physiological resemblance to humans. All studies related to new TEVGs should evaluate their biocompatibility, patency, hemodynamic factors, and cell infiltration, among others. As each animal model has a series of advantages and limitations, it is important to know the different characteristics of each animal model to allow their results and possible effects in human patients to be interpreted correctly.

4.2 Human Trials with TEVG

Regarding human patients, this systematic review found three studies conducted in human published in 2018 (Sugiura et al., 2018) and 2019 (Herrmann et al., 2019; Kirkton et al., 2019). This is indicative of the fact that considerable progress has been achieved in the field of TEVGs. However, the use of these vascular grafts in humans remains very restricted owing to certain limitations, such as the presence of stenosis, existence of thrombi, and poor graft patency, among others. Kirkton et al. (2019) developed a vascular graft composed of primary human vascular cells isolated from cadaveric donors and seeded on polyglycolic acid (PGA) scaffolds. Scaffolds were decellularized to remove cellular antigens and were recellularized by vascular cells and noninflammatory host progenitors. Arteriovenous grafts with an internal diameter of 6 mm were implanted in the upper arm in 60 patients with end-stage renal disease to provide access for hemodialysis. The mean follow-up period was 3.8 years. Thromboses or pseudoaneurysms owing to cannulation trauma occurred in 13/60 patients. Herrmann et al. (2019) presented a vascular graft design composed of saphenous veins harvested from multiple organ donors that were cryopreserved, de-endothelialized, and seeded with human, autologous, venous EC from patient vein segments. Fifteen vascular grafts with diameters in the range of 3–6 mm were implanted by coronary artery bypass in 12 patients. The mean survival of patients after surgery was 9.1 ± 1.8 years. At the 6-months follow-up, the vascular graft patency was 80%. It decreased to 50% at 9 months, and at the endpoint, 7/12 patients (8/15 grafts) had graft occlusions or stenosis. Finally, Sugiura et al. (2018) implanted vascular grafts that consisted of woven poly-L-lactide acid (PLLA) or PGA coated with a copolymer sealant solution of poly-L-lactic-co-ε-caprolactone (PLCL) in 25 children. The grafts were seeded with autologous bone marrow mononuclear cells (BM-MNCs). The graft size ranged from 12 to 24 mm. These grafts were implanted as extracardiac total cavopulmonary connections. The mean follow-up period was 11.1 years. There were no lethal complications related to the graft, but a thrombus was detected in one patient, and seven other patients presented asymptomatic stenosis. Asymptomatic complications were diagnosed in the human studies mentioned above (Sugiura et al., 2018; Herrmann et al., 2019; Kirkton et al., 2019). Long-term research is needed to study all the side effects that these TEVGs could produce, thus achieving safe and satisfactory use. The use of TEVGs is still not completely safe in clinical studies due to the high failure rate, such as presence of stenosis, thrombi, or other complications.

4.3 Materials Used in the Design of TEVGs

TEVGs should resemble native blood vessels as closely as possible and have the ability to remodel, grow, self-repair, and respond to the immediate environment (Chlupác et al., 2009). Each article analyzed in this review created its own TEVG, although there were certain materials that were commonly used, such as biodegradable polymers, or biological materials. Notably, some researchers used heparin in the design of TEVGs (Jiang et al., 2016; Koobatian et al., 2016; Hu et al., 2017; Ju et al., 2017; Madhavan et al., 2018; Xu et al., 2018; Jin et al., 2019a; Jin et al., 2019b; Ran et al., 2019; Shi et al., 2019; Smith et al., 2019; Wang et al., 2019). The addition of heparin to materials prevents thrombosis and enhances biocompatibility (Aslani et al., 2020).

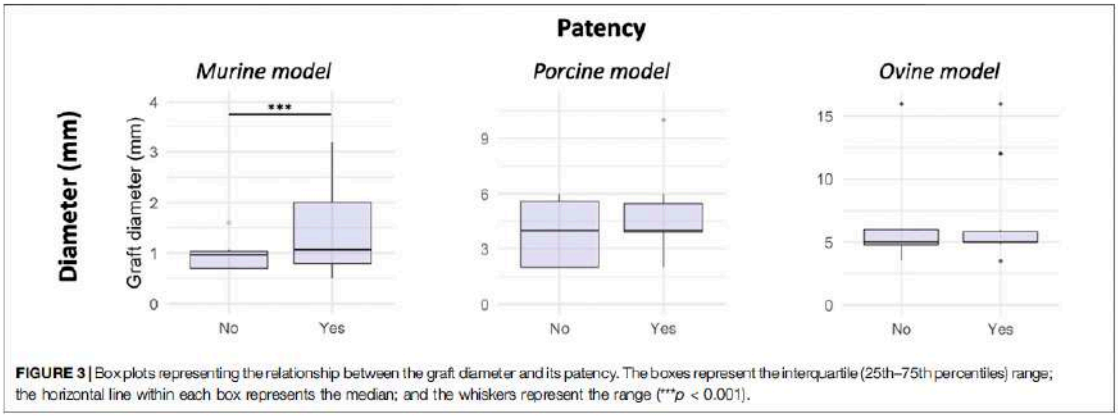

FIGURE 3 | Box plots representing the relationship between the graft diameter and its patency. The boxes represent the interquartile (25th–75th percentiles) range; the horizontal line within each box represents the median; and the whiskers represent the range (***$p < 0.001$).

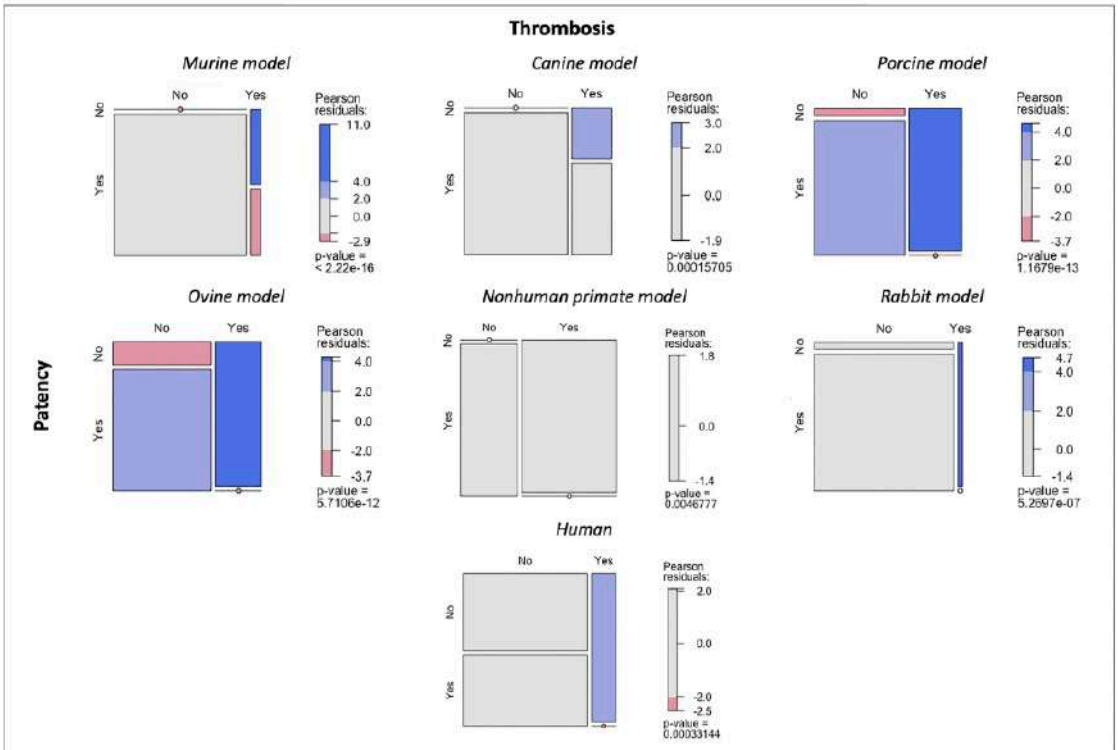

FIGURE 4 | Relationship between graft patency and occurrence of thrombosis. Mosaic plot used to evaluate the association between the graft patency and onset of thrombosis.

The most commonly studied and used polymer is PGA, which has high level of flexibility and lacks of inflammatory response (Pepper et al., 2017; Sugiura et al., 2018; Luo et al., 2020). When seeded with human EC in vascular grafts, PGA can withstand mechanical stress equivalent to the aortic pressure (Chlupác et al., 2009; Mauri et al., 2013). However, PGA should be used in association with other polymers due to short degradation time (6–8 weeks), which is too fast for vascular clinical applications (Leal et al., 2021). On the other hand, PLCL is a copolymer of lactic acid and caprolactone, which presents good

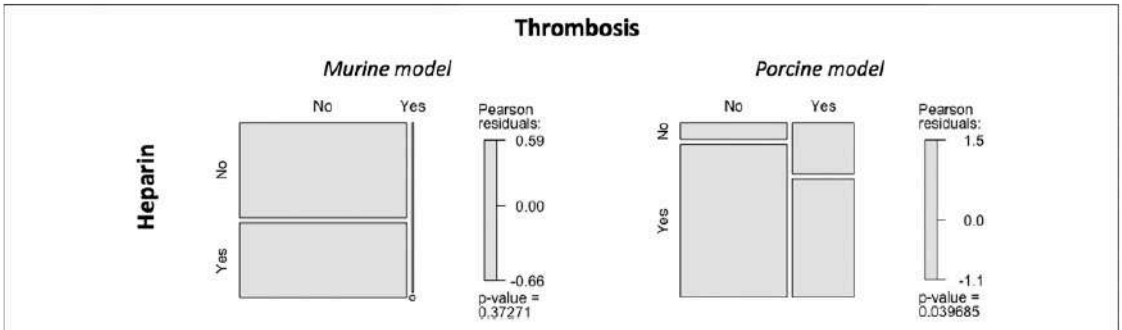

FIGURE 5 | Relationship between the use of heparin and occurrence of thrombosis. Mosaic plot used to evaluate the association between the use of heparin and onset of thrombosis.

TABLE 2 | Materials used in the vascular graft design.

Materials	Number of studies	Percentage of total (%)	References
Biodegradable polymers	11	11.96	Cummings et al. (2012), Harrington et al. (2011), Hibino et al. (2011), Lee et al. (2014), Stacy et al. (2014), Udelsman et al. (2014), Gui et al. (2016), Pepper et al. (2017), Sugiura et al. (2018), Jang et al. (2020), Luo et al. (2020)
Natural materials	17	18.48	Quint et al. (2011), Koenneker et al. (2012), Tillman et al. (2012), Zhao et al. (2012), Meier et al. (2014), Itoh et al. (2015), McIlhenny et al. (2015), Pellegata et al. (2015), Row et al. (2015), Wu et al. (2015), Aper et al. (2016), Rothuizen et al. (2016), Dahan et al. (2017), Ma et al. (2017), Tseng et al. (2017), Iacobazzi et al. (2018), Herrmann et al. (2019), Itoh et al. (2019)
Hybrid grafts	5	5.43	Hu et al. (2017), Ju et al. (2017), Madhavan et al. (2018), Shafiq et al. (2018)
Tissue-engineered scaffolds	59	64.13	Lovett et al. (2010), Song et al. (2010), Hwang et al. (2011), Prichard et al. (2011), Assmann et al. (2012), Matsumura et al. (2012), Quint et al. (2012), Aytemiz et al. (2013), De Valence et al. (2013), Matsumura et al. (2013), Conconi et al. (2014), Isayama et al. (2014), Mrówczyński et al. (2014), Tara et al. (2014), Koens et al. (2015), Mahara et al. (2015), Tara et al. (2015), Fukunishi et al. (2016), Hibino et al. (2016), Jiang et al. (2016), Khosravi et al. (2016), Koobatian et al. (2016), Syedain et al. (2016), Tondreau et al. (2016), Wang et al. (2016), Yang et al. (2016), Fukunishi et al. (2017), Li et al. (2017), Maxfield et al. (2017), Negishi et al. (2017), Ong et al. (2017a), Syedain et al. (2017), Best et al. (2018), Lee et al. (2018), Li et al. (2018), Qin et al. (2018), Valencia-Rivero et al. (2018), Weber et al. (2018), Wu et al. (2018), Xu et al. (2018), Alessandrino et al. (2019), Aubin et al. (2019), Bai et al. (2019), Best et al. (2019), Furukoshi et al. (2019), Jin et al. (2019a), Jin et al. (2019b), Kajbafzadeh et al. (2019), Katsimpoulas et al. (2019), Kirkton et al. (2019), Liu et al. (2019), Ran et al. (2019), Shi et al. (2019), Smith et al. (2019), Sologashvili et al. (2019), Wang et al. (2019), Wolf et al. (2019), Yamanami et al. (2019), Yeung et al. (2019)

biocompatibility and slow degradation (Hu et al., 2017; Pepper et al., 2017). Authors used the combination of PGA with PLCL to increase graft degradation time (Hibino et al., 2011; Lee et al., 2014; Stacy et al., 2014; Hibino et al., 2016; Pepper et al., 2017; Sugiura et al., 2018). Polylactic acid (PLA) is a polymer with a very similar structure and mechanical properties to PGA, but with a longer degradation time (Naito et al., 2011; Ong et al., 2017b). However, PLA exhibits a hydrophobic structure, which interferes in cell adhesion and proliferation (Leal et al., 2021). PLLA is an isomeric form of PLA and is the most studied polymer for cardiovascular tissue engineering applications (Mishra, 2015; Ong et al., 2017b), and the studies showed improved cell viability (Sugiura et al., 2018). Polycaprolactone (PCL) presents mechanical properties that exceed those of natural vessels, such as maximum stress or tensile strength. In addition, PCL has a good biocompatibility and slow biodegradability (Fukunishi et al., 2016; Shafiq et al., 2018). Nevertheless, PCL has hydrophobic characteristics, so needs to be combined with other polymers.

Contrarily, there were TEVGs created from biological materials. Collagen has low antigenicity, high biocompatibility, and enhances cell adhesion and proliferation (Shafiq et al., 2018; Itoh et al., 2019). Further, this material is the main component of the extracellular matrix (ECM) (Ong et al., 2017b). Chitosan is a new material use in TEVG, and provides low toxicity and anticoagulant properties, as well as inhibiting inflammation, and modifying viability chemically (Wu et al., 2015; Fukunishi et al., 2016). Elastin is part of ECM and maintains the elasticity of the blood vessels under blood pressure (Hu et al., 2017). The use of this material prevents intimal hyperplasia in native vessels and provided an organization of the collagen fibers (Leal et al., 2021). Due to the few studies performed with chitosan and elastin, more research should be conducted to provide information on the

TABLE 3 | Summary of the advantages and disadvantages of animal models analyzed.

Animal model	Advantages	Disadvantages
Rodents	Low cost Biocompatibility and cell infiltration studies Genetically modified strains	Cardiovascular physiology Thrombogenicity mechanisms Hemostasis mechanisms
Ovine	Thrombogenicity mechanisms Fibrinolysis system Endothelialization and neointimal formation	Hypercoagulability
Porcine	Cardiovascular anatomy Translational studies	Grow rapidly Hypercoagulability
Rabbits	Thrombogenicity mechanisms Heritable disease models	Vascular physiology
Canine	Anatomy extensively studied Lack of spontaneous endothelialization	Thrombogenicity mechanisms Potent fibrinolytic system Ethical aspects
Nonhuman primates	Physiology Cardiovascular anatomy Thrombogenicity mechanisms	High cost Ethical considerations

effects of these materials in the design of vascular grafts. Another material used relatively frequently is silk fibroin, which is a natural, biodegradable, and biocompatible polymer (Lovett et al., 2010; Aytemiz et al., 2013; Alessandrino et al., 2019; Jin et al., 2019b). This natural proteic material is not immunogenic in humans, favors angiogenesis (Alessandrino et al., 2019), and presents good cell compatibility and hydrophilicity responses (Liu et al., 2019; Jin et al., 2019b). Also, native blood vessels can be decellularized to obtain ECMs (Assmann et al., 2012; Dahan et al., 2017; Bai et al., 2019). These matrices maintain the biological properties of native blood vessels (Simon et al., 2003).

Based on the studies analyzed in this systematic review, it appears that cellular recruitment or endothelialization tended to be used in grafts with biological materials, but mechanical properties were superior for biodegradable polymers. The porosity of biodegradable polymers allows a customized graft design, as well as withstanding different pressures, twisting and stretching. However, they do not seem suitable for cell adhesion and proliferation. On the other hand, natural materials have the capacity for cell adhesion, but have poor mechanical properties. Nevertheless, both endothelialization and mechanical properties are essential for the long-term patency of TEVGs (Wu et al., 2018). For these reasons, a hybrid graft emerged. This graft is a type of TEVG formed by mixing biodegradable polymers and biological materials. An example of this type of hybrid graft was used by Hu et al. (2017) who designed grafts with PLCL, collagen, and elastin. Better results were obtained by the different authors who designed a hybrid graft. The hybrid strategy could be used to create a highly favorable composite material for TEVGs, since these grafts present the advantages of both materials.

4.4 Manufacturing Technology

There are different techniques to produce TEVGs, with electrospinning being the most commonly used method. This technique produces porous and fibrous scaffolds from polymers (Dvir et al., 2010), thereby enhancing the transfer of nutrients and residues through the scaffold. The alignment of the nanofibers allows the scaffold's strength to be increased to promote cell alignment (Woods and Flanagan, 2014). The second most commonly used method is decellularization. Native blood vessels can be decellularized to obtain ECMs. These matrices maintain the biological properties of native blood vessels. Thus, the grafts contain functional proteins capable of promoting cell recruitment. However, the decellularization process can also damage the ECM (Simon et al., 2003), thus negatively affecting the integrity, and mechanical properties of the graft. On the other hand, lyophilization is a physical technique that reduces calcification, and provides a stable graft (Conconi et al., 2014; Bai et al., 2019). Nevertheless, mechanical properties, such as suture strength, are not sufficient for clinical use (Reinhardt et al., 2019). Another technology, known as "biotubes," involves the development of blood vessels by subcutaneous implantation, and is associated with a biological defense mechanism (Rothuizen et al., 2016; Tseng et al., 2017; Furukoshi et al., 2019; Yamanami et al., 2019). Finally, some authors used the innovative 3D bioprinting technique to manufacture TEVGs (Itoh et al., 2015; Itoh et al., 2019; Jang et al., 2020). This technology provides an adequate cell distribution with a high cell density (Leal et al., 2021). However, results showed that 3D bioprinting designs TEVGs with a low mechanical property (Leal et al., 2021). Further, a scaffold may or may not be present in a graft (Campbell and Campbell, 2007), but it would have to be degradable to allow the growth of new tissue from the body itself (Chlupác et al., 2009). There are researchers who designed scaffold-free grafts, wherein tubular tissues were created with 3D bioprinting (Itoh et al., 2015; Itoh et al., 2019).

It should be noted that some studies have designed decellularized vascular grafts with ECs (Koennerker et al., 2012; McIlhenny et al., 2015; Pellegata et al., 2015). This combination avoids the drawbacks of this methodology, obtaining native-like ECM. Nevertheless, research presents electrospinning as the technology most widely used by the authors in the development of TEVGs. The porosity of the scaffold is essential to design a graft in which good cell adhesion and tissue regeneration take place. It is possible to create vascular grafts with conditions very similar to those of a

native vessel due to the great advance of this technology. Electrospinning allows controlling the porosity of the scaffold, providing an excellent cell adhesion and proliferation. However, 3D bioprinting seems to be a promising technology because any 3D organ can be manufactured using a computer software that simulates the structure itself, in addition to selecting the material to be used for printing. Although further studies are needed to ensure the effectiveness of this method.

4.5 Cell Seeding and Cell Types

Cell seeding facilitates cell fixation and infiltration, thus improving graft endothelialization. There are different ways to perform cell seeding, such as static, dynamic, electrostatic, and magnetic techniques. Static or gravitational cell seeding involves direct application of the cell suspension into the scaffold (Ong et al., 2017b; Radke et al., 2018). However, this technique has a series of disadvantages, such as risk of contamination, non-uniform seeding, or the risk of platelet adhesion due to the use of adhesion molecules in the lumen, among others (Radke et al., 2018). The most commonly cell seeding technique was dynamic cell seeding, which enhances seeding efficiency, uniformity and scaffold penetration due to the use of rotational seeding, vacuum seeding, and fluid sheer stress (Ong et al., 2017b; Radke et al., 2018). However, adequate graft porosity is required for optimal utilization of dynamic cell seeding, especially with the use of vacuum pressure that draw cells in through the micropores of the TEVG (Ong et al., 2017b; Radke et al., 2018). The material properties of the TEVG are an important factor for electrostatic cell seeding, which uses a temporary positive charge on the negatively charged graft lumen (Ong et al., 2017b). Finally, magnetic cell seeding use magnetic beads and application of an external magnetic field. This novel technique improves the efficiency of cell seeding due to a better regulation of cellular distribution, in addition to providing faster cell culture (Radke et al., 2018). Nevertheless, beads may cause side effect, so they need to be analyzed to ensure the validity of this technique (Radke et al., 2018). These last two techniques of cell seeding need to be further evaluated to ensure long-term cell retention and other side effects after *in vivo* implantation, in addition to the fact that there are hardly any studies using these cell seedings.

In terms of cell type, mesenchymal stem cells (MSCs) can be obtained from different origins, such as adipose tissue, bone marrow, and umbilical vein blood (Radke et al., 2018). MSCs are a promising cell type for TEVG because improve the patency due to their anti-thrombogenic property, and they can also recruit ECs on site (Hashi et al., 2007; Zhao et al., 2012; Itoh et al., 2015). A wide variety of vascular cells could be obtained with induced pluripotent stem cells (iPSCs) because they could be induced into specific lineages (Radke et al., 2018; Luo et al., 2020), such as SMCs or ECs. Finally, BM-MNCs were the second most commonly used cell type by some of the authors (Hibino et al., 2011; Lee et al., 2014; Stacy et al., 2014; Pepper et al., 2017; Sugiura et al., 2018). BM-MNCs include ECs, MSCs, immune-related cells and hematopoietic stem cells, which main property is their anti-thrombotic effect (Radke et al., 2018). Although various cell types can be used, ECs are the most commonly used cell in the design of TEVGs (Cummings et al., 2012; Koennerker et al., 2012; McIlhenny et al., 2015; Pellegata et al., 2015; Ma et al., 2017), as they provide anticoagulant effects (Ju et al., 2017) and improve endothelialization (Radke et al., 2018). In the study by Ju et al. (2017), the authors compared the effects of EC on a vascular scaffold fabricated by electrospinning of polycaprolactone and type I collagen. The results showed that the control group (scaffold without EC) had no patency owing to the appearance of thrombosis, whereas in the experimental group (scaffold with EC), the graft patency was maintained during the 6-months study.

Nevertheless, cell seeding is currently a challenging field of research because the optimal number of cells for seeding is unknown. Therefore, there is controversy about the need and clinical relevance of cell seeding (Ong et al., 2017b). Furthermore, it has been determined that many of the seeded cells are lost, owing to either cell death or lack of union with other cells (Villalona et al., 2010). For this reason, many researchers have designed cell-free vascular grafts, scaffolds, or acellular vascular grafts. Based on the results, the development of tissue-engineered acellular grafts is a promising technique due to the wide variety of materials that can be employed, both natural materials and biodegradable polymers. These grafts have demonstrated good patency and regeneration potential, biocompatibility, and lack of immunogenicity (Smith et al., 2019). Additionally, TEVG scaffolds provide good mechanical strength and promote cellular proliferation and maturation (Ong et al., 2017b; Yeung et al., 2019). These scaffolds play a fundamental role in functional tissue regeneration because they interact with nearby biomolecule cells, regulating complete tissue regeneration. Also, the addition of vascular endothelial grow factors in the scaffold is very common in order to promote endothelization (Koobatian et al., 2016; Row et al., 2017; Smith et al., 2019).

In addition to all of the above, articles analyzed showed quite similar results in cell-based and cell-free TEVGs, in which the graft was effectively implanted and showed good mechanical and cell proliferation properties. However, cell-free TEVGs may correct some of the problems associated with the use of cells, such as immune rejection, long cell culture times, and avoidance of taking biopsies from patients. As mentioned, cell seeding is currently a challenging field of research, where insufficient cell seeding, damage or lack of cells can lead to the development of thrombosis and have poor patency rates. Cell-free scaffold is favorable for vascular graft design. In contrast to cell seeding, manufacturing techniques are evolving rapidly, and it is becoming easier and safer to design TEVGs.

Although a perfect material and manufacturing technology have not yet been identified, research in this field has become effective from a clinical point-of-view. The studies included in this review achieved to improve vascular grafts in a way that yielded very promising results compared with similar studies conducted previously.

4.6 Challenges of These Studies

Regarding the surgical outcomes, the researchers generally used small-diameter vascular grafts. However, it has been documented that 1) small-diameter TEVGs are especially prone to failure from thrombus adherence and vascular obstruction (Jin et al., 2019a; Jin et al., 2019b), and 2) current vascular grafts have a limited

durability and patency (Iacobazzi et al., 2018). These circumstances seem to be related to poor endothelialization and smooth muscle layer remodeling (Jin et al., 2019b). Some of the strategies used to avoid thrombosis and subsequent graft stenosis and improve patency involve anticoagulant substances during surgery, such as heparin (Siemionow, 2015). However, some researchers did not use heparin during surgery. For this reason, we decided to analyze the relationship between the existence of thrombosis and the patency of the vascular grafts with respect to their diameter, as well as the use of heparin during surgery.

Several studies have been conducted to manufacture small TEVGs to achieve the phenotype of native blood vessels. Results in rodents showed that vascular grafts with larger diameters were patent, and grafts with smaller diameters were occluded. Contrary to expectations, rodents exhibited a greater onset of thrombosis in grafts with larger diameters. Among the analyzed studies, large-diameter vascular grafts had endothelial injury (Quint et al., 2012; Yang et al., 2016) or lack of EC (Assmann et al., 2012; Conconi et al., 2014; Gui et al., 2016; Luo et al., 2020). Therefore, any inappropriate movement may cause trauma to the graft and a blood flow mismatch. A complete endothelial layer plays a critical role in maintaining patency and provides anticoagulant effects (Ju et al., 2017; Wu et al., 2018).

In the porcine model, in contrast, it seems that there is a trend based on which vascular grafts with small diameters leads to thromboses. TEVG is a medical device in contact with the patient's blood. Thus, the formation of thrombi constitutes a common type of failure. For this reason, it is important to use anticoagulants, antiplatelet agents, or both, to avoid the occurrences of thrombi (Jaffer et al., 2015; Siemionow, 2015).

As expected, the results also showed a correlation between the vascular graft patency and the absence of thrombi in mice, ovine, porcine, and canine models. Likewise, the lack of graft patency correlated with the occurrence of thrombi in the nonhuman (baboon) model. Therefore, considering all previous results, it appears that when a small-diameter TEVG is used, there is a tendency for the formation of thrombi and poor vascular graft patency.

Surgical experience and skills, differences in graft diameter from the native vessel, damage or lack of EC, tension in the suture line, damage during surgery, and hemodynamic factors leading to blood flow mismatch are (among others) potential risk factors that could lead to the appearance of thrombi and poor patency of vascular grafts (Pashneh-Tala et al., 2015), especially for small-diameter TEVGs. The surgery must be performed perfectly as any inappropriate movement can cause trauma to the graft. Additionally, a mismatch in the TEVG diameter could cause turbulence in the blood flow, thus triggering a coagulation cascade that can form thrombi.

Good graft porosity, good EC conditions, and the aforementioned recommendations are key factors associated with the prevention of the appearance of thrombosis and the achievement of good patency of vascular grafts.

The three studies on humans included in this review did not indicate the use of heparin. Specifically, 13/60 patients (21.67%) in the study by Kirkton et al. had to be treated for thromboses in the arteriovenous graft (Kirkton et al., 2019), and 1/25 patients (4%) in the study by Sugiura et al. had thrombi in the TEVG (Sugiura et al., 2018). These patients received anticoagulation therapy, such as aspirin or warfarin (Sugiura et al., 2018; Kirkton et al., 2019), which started 2 days after surgery and continued up to 3–6 months. A study by Hibino et al. (2010) on 25 human patients also employed the same anticoagulant therapy during implantation of TEVGs. The TEVG was composed of PGA and PLCL and was seeded with autologous BM-MNCs. The grafts measured between 12 and 24 mm and were implanted in the forms of extracardiac total cavopulmonary connection. After surgery, 24/25 patients (96%) had no evidence of thrombosis for 6 months, and 10/25 patients (40%) did not require long-term medication. This type of anticoagulation therapy has also been used extensively in animal model research. It should be noted that no correlation was found between the use of heparin and the onset of thrombi in the animal model studies investigated in this review. This fact may be attributed to the lack of information regarding the use of heparin during surgery in many of these studies, which made analysis difficult.

When PET or PTFE are used to design artificial vascular grafts, human patients require the long-term use of warfarin and aspirin (Giannico et al., 2006; Nakano et al., 2007; Kim et al., 2008). In contrast, one of the advantages of TEVGs is the fact that they allow antiplatelet or anticoagulation therapy to be skipped owing to the creation of autologous tissue (Hibino et al., 2010). However, the results showed that the use of these therapies to prevent thrombus formation remains relevant. Further, based on the animal models results, there is not yet a TEVG design that presents suitable mechanical and cellular recruitment conditions. Also, the few studies conducted on human studies showed a high percentage of thrombi. The use of TEVGs is not advisable in clinical studies due to tendency for thrombus formation and poor vascular graft patency.

4.7 Blood-Contacting Surfaces in TEVGs

In addition to all of the above factors, as well as the different materials used for TEVG design, there are other factors, such as the topography and architecture of the blood-contacting surface, that have a significant impact on thrombus formation. The topographic gradients of the material surface significantly modify the platelet adhesion and activation (Radke et al., 2018). Those surfaces with a rough topography cause that platelet are less adherent and activated with greater difficulty than smooth one (Hulander et al., 2013). Further, a surface with structured ridges and grooves affects platelet adhesion, which significantly reduces its thrombogenic effect (Radke et al., 2018). Others factors involved in the regulation of platelet adhesion, spreading, and activation are the mechanical properties of the surface that comes into contact with the blood. Stiffer surfaces are more prone to platelet adhesion and spreading (Radke et al., 2018). All of these factors should be taken into account to improve the design of TEVGs. However, articles studied in this systematic review did not include this information in their research, so it was not possible to analyze these data.

Moreover, authors had employed different strategies to produce successful blood-contacting surfaces in TEVGs. One of these strategies is to incorporate anti-thrombotic cells (ECs, MSCs, or BM-MNCs)

and use safe cell seeding (dynamic cell seeding), which have a vital role in avoiding thrombus formation, as previously mentioned. Another strategy was the use of autologous cells, which avoid immune rejection. However, this strategy has a number of disadvantages, such as the need to perform a biopsy, long-term culture period, cells depend on the patient's health, and age, among others (Radke et al., 2018). Finally, the use of heparin was used as strategy to successfully produce blood-contacting surfaces in TEVGs. As already indicated, this anticoagulation molecule regulates platelet activity and enhances biocompatibility (Aslani et al., 2020).

4.8 Futures Perspectives

The field of TEVG research is very extensive, with a wide variety of materials and techniques used in the development of these grafts. TEVGs manufacturing technology advances at an exponential pace, and it is expected that in a few years it will be possible to create vascular grafts with the same characteristics as native ones. In the future, more advanced biomaterial fabrication methods will be developed. These advances will allow the development of scaffolds with complex architecture and topography that could imitate the native ECM of the vessel and provide suitable mechanical properties tailored to clinical needs. In addition, the development of hybrid grafts now largely emulates the native blood vessel due to the combination of natural materials and biodegradable polymers, so the safe clinical use of TEVGs in human patients is getting closer.

Each TEVG analyzed in this systematic review has its own design. However, there are still many aspects that should be taken into account in the future. One of them is that there are a wide variety of animal models, so future research should be oriented according to the objective of the study. As mentioned above, each animal model has a number of limitations. Therefore, it is important to know the different characteristics of each animal model to be able to correctly interpret their results and their possible effects on human patients. In addition, most studies have been performed in young, healthy animals. Nonetheless, the clinical use of these grafts is usually carried out in elderly humans, and these patients often suffer from some type of disease, either renal (TEVGs for hemodialysis) or cardiovascular, in addition to concomitants disorders. Consequently, the design of TEVGs tested in a young and healthy animal model may behave differently in these patients. For this reason, future studies with experimental models with different pathologies should be included.

Substantial variability in TEVG implantation time has been observed, ranging from less than 1 h (Li et al., 2017) to 3 years (Kajbafzadeh et al., 2019). Most articles, however, have follow-up durations in the range between 1 and 6 months. This temporal analysis is very important because in human studies asymptomatic complications were diagnosed. Therefore, long-term research is needed to study all the side effects that these TEVGs could produce, thus achieving subsequent safe and satisfactory use. Additionally, patients generally require the use of vascular grafts immediately. For this reason, studies should be aimed at creating vascular grafts in a rapid and effective way.

TEVGs emerged as alternative replacement vessels for clinical applications. Small-diameter vascular grafts hold promise to overcome the limitations of synthetic grafts. As observed in this review, studies were mainly focused on the development of small-caliber TEVGs, but there is a tendency for thrombus formation and poor vascular graft patency. However, advances in TEVG fabrication technology may address these problems in the near future. Electrospinning showed very encouraging results, developing grafts with good patency and mechanical properties very similar or superior to native vessels. Moreover, it is now possible to 3D print a vascular graft with very satisfactory properties. Although these technologies are promising, the correct use of materials remains a challenge, and mechanical properties and cell recruitment of TEVGs need to be controlled in order to maintain long-term graft patency. All these issues should be further addressed to develop safe TEVGs for clinical applications. Therefore, future studies should be aimed at the development of new materials or combinations of them, as well as testing emerging technologies, and study the cell-material interaction to develop a suitable TEVG.

Finally, it is fundamental that the research should be aimed at designing TEVGs with similar or equal characteristics to the site to be replaced. For this purpose, images of the native vessel should be taken by MRI, computed tomography or any other medical imaging method that allows the dimensions and characteristics of the vessel to be replaced to be analyzed.

4.9 Limitations of the Study

This study has a number of limitations. Research on TEVG has grown exponentially, and a wide variety of results has been obtained. Therefore, because of the high multiplicity in the materials and technologies used in the development of these grafts, considering all studies is challenging. On the other hand, only three studies in human patients were included in the review, so it has not been possible to extract significant results. There is heterogeneity in the protocols and a lack of information in the results obtained from human patients and animal models, which hinders the analysis and interpretation of the data. Finally, the topography, architecture and mechanical properties of the blood-contacting surface could not be analyzed due to lack of data.

4.10 Conclusion

Although there is no ideal animal model for TEVG research, rodent models are the most commonly used animal model. Continuous progress is currently being made in the development of TEVGs, and hybrid grafting, and electrospinning are presented as the most promising technologies. Nevertheless, the major complication arising from the use of TEVGs is the occurrence of thrombosis and the lack of patency, which limits the implementation of TEVGs in clinical applications. These complications seem to be aggravated by the use of small-diameter TEVGs and the lack of anticoagulation therapy. *In vivo* studies are oriented toward the safety of these devices, pursuing a suitable design, and further clinical applications.

DATA AVAILABILITY STATEMENT

The original contributions presented in the study are included in the article/Supplementary Material, further inquiries can be directed to the corresponding author.

AUTHOR CONTRIBUTIONS

DD-R, VC, JAS-M, and FMS-M: Conceptualization, Methodology. DD-R, JAS-M: Investigation, Formal analysis. DD-R, JAS-M: Writing—Original Draft. VC, FMS-M: Writing—Review and Editing. VC, FMS-M: Supervision. FMS-M: Funding acquisition. All authors contributed to the article and approved the submitted version.

FUNDING

This work has been partially funded by the Junta de Extremadura (Spain), the European Social Fund, and the European Regional Development Fund (grant numbers PD18077, TA18023, and GR18199). None of these funding sources had any further role in the study design; in the collection, analysis, and interpretation of data; in the writing of the report; or in the decision to submit.

ACKNOWLEDGMENTS

The authors specially thank Eva Sequeira for her technical support.

SUPPLEMENTARY MATERIAL

The Supplementary Material for this article can be found online at: https://www.frontiersin.org/articles/10.3389/fbioe.2021.771400/full#supplementary-material

REFERENCES

Abdulhannan, P., Russell, D. A., and Homer-Vanniasinkam, S. (2012). Peripheral Arterial Disease: a Literature Review. *Br. Med. Bull.* 104, 21–39. doi:10.1093/bmb/lds027

Alessandrino, A., Chiarini, A., Biagiotti, M., Dal Prà, I., Bassani, G. A., Vincoli, V., et al. (2019). Three-Layered Silk Fibroin Tubular Scaffold for the Repair and Regeneration of Small Caliber Blood Vessels: From Design to *In Vivo* Pilot Tests. *Front. Bioeng. Biotechnol.* 7, 356. doi:10.3389/fbioe.2019.00356

Aper, T., Wilhelmi, M., Gebhardt, C., Hoeffler, K., Benecke, N., Hilfiker, A., et al. (2016). Novel Method for the Generation of Tissue-Engineered Vascular Grafts Based on a Highly Compacted Fibrin Matrix. *Acta Biomater.* 29, 21–32. doi:10.1016/j.actbio.2015.10.012

Aslani, S., Kabiri, M., HosseinZadeh, S., Hanaee-Ahvaz, H., Taherzadeh, E. S., and Soleimani, M. (2020). The Applications of Heparin in Vascular Tissue Engineering. *Microvasc. Res.* 131, 104027. doi:10.1016/j.mvr.2020.104027

Assmann, A., Akhyari, P., Delfs, C., Högel, U., Jacoby, C., Kamiya, H., et al. (2012). Development of a Growing Rat Model for the *In Vivo* Assessment of Engineered Aortic Conduits. *J. Surg. Res.* 176, 367–375. doi:10.1016/j.jss.2011.10.009

Aubin, H., Mas-Moruno, C., Iijima, M., Schütterle, N., Steinbrink, M., Assmann, A., et al. (2016). Customized Interface Biofunctionalization of Decellularized Extracellular Matrix: Toward Enhanced Endothelialization. *Tissue Eng. C: Methods* 22, 496–508. doi:10.1089/ten.TEC.2015.0556

Aytemiz, D., Sakiyama, W., Suzuki, Y., Nakaizumi, N., Tanaka, R., Ogawa, Y., et al. (2013). Small-diameter Silk Vascular Grafts (3 Mm Diameter) with a Double-Raschel Knitted Silk Tube Coated with Silk Fibroin Sponge. *Adv. Healthc. Mater.* 2, 361–368. doi:10.1002/adhm.201200227

Baguneid, M. S., Seifalian, A. M., Salacinski, H. J., Murray, D., Hamilton, G., and Walker, M. G. (2006). Tissue Engineering of Blood Vessels. *Br. J. Surg.* 93, 282–290. doi:10.1002/bjs.5256

Bai, H., Dardik, A., and Xing, Y. (2019). Decellularized Carotid Artery Functions as an Arteriovenous Graft. *J. Surg. Res.* 234, 33–39. doi:10.1016/j.jss.2018.08.008

Bergmeister, H., Hamza, O., Kiss, A., Nagel, F., Pilz, P. M., Plasenzotti, R., et al. (2019). "Animal Models in Cardiovascular Biology," in *Fundamentals of Vascular Biology. Learning Materials in Biosciences.* Editor M. Geiger (Cham: Springer), 271–291. doi:10.1007/978-3-030-12270-6_13

Best, C. A., Szafron, J. M., Rocco, K. A., Zbinden, J., Dean, E. W., Maxfield, M. W., et al. (2019). Differential Outcomes of Venous and Arterial Tissue Engineered Vascular Grafts Highlight the Importance of Coupling Long-Term Implantation Studies with Computational Modeling. *Acta Biomater.* 94, 183–194. doi:10.1016/j.actbio.2019.05.063

Best, C., Fukunishi, T., Drews, J., Khosravi, R., Hor, K., Mahler, N., et al. (2018). Oversized Biodegradable Arterial Grafts Promote Enhanced Neointimal Tissue Formation. *Tissue Eng. A* 24, 1251–1261. doi:10.1089/ten.TEA.2017.0483

Campbell, G., and Campbell, J. (2007). Development of Tissue Engineered Vascular Grafts. *Cpb* 8, 43–50. doi:10.2174/138920107779941426

Chlupáč, J., Filová, E., and Bačáková, L. (2009). Blood Vessel Replacement: 50 Years of Development and Tissue Engineering Paradigms in Vascular Surgery. *Physiol. Res.* 58 (Suppl. 2), S119–S140. doi:10.33549/physiolres.931918

Conconi, M. T., Borgio, L., Di Liddo, R., Sartore, L., Dalzoppo, D., Amistà, P., et al. (2014). Evaluation of Vascular Grafts Based on Polyvinyl Alcohol Cryogels. *Mol. Med. Rep.* 10, 1329–1334. doi:10.3892/mmr.2014.2348

Cummings, L., George, S., Kelm, J., Schmidt, D., Emmert, M. Y., Weber, B., et al. (2011). Tissue-engineered Vascular Graft Remodeling in a Growing Lamb Model: Expression of Matrix Metalloproteinases. *Eur. J. Cardio-Thoracic Surg.* 41, 167–172. doi:10.1016/j.ejcts.2011.02.077

Dahan, N., Sarig, U., Bronshtein, T., Baruch, L., Karram, T., Hoffman, A., et al. (2017). Dynamic Autologous Reendothelialization of Small-Caliber Arterial Extracellular Matrix: A Preclinical Large Animal Study. *Tissue Eng. Part A* 23, 69–79. doi:10.1089/ten.TEA.2016.0126

Dvir, T., Timko, B. P., Kohane, D. S., and Langer, R. (2010). Nanotechnological Strategies for Engineering Complex Tissues. *Nat. Nanotech.* 6, 13–22. doi:10.1038/nnano.2010.246

Fukunishi, T., Best, C. A., Sugiura, T., Opfermann, J., Ong, C. S., Shinoka, T., et al. (2017). Preclinical Study of Patient-specific Cell-free Nanofiber Tissue-Engineered Vascular Grafts Using 3-dimensional Printing in a Sheep Model. *J. Thorac. Cardiovasc. Surg.* 153, 924–932. doi:10.1016/j.jtcvs.2016.10.066

Fukunishi, T., Best, C. A., Sugiura, T., Shoji, T., Yi, T., Udelsman, B., et al. (2016). Tissue-Engineered Small Diameter Arterial Vascular Grafts from Cell-free Nanofiber PCL/Chitosan Scaffolds in a Sheep Model. *PLoS One* 11, e0158555. doi:10.1371/journal.pone.0158555

Furukoshi, M., Tatsumi, E., and Nakayama, Y. (2019). Application of In-Body Tissue Architecture-Induced Biotube Vascular Grafts for Vascular Access: Proof of Concept in a Beagle Dog Model. *J. Vasc. Access.* 21, 314–321. doi:10.1177/1129729819874318

Giannico, S., Hammad, F., Amodeo, A., Michielon, G., Drago, F., Turchetta, A., et al. (2006). Clinical Outcome of 193 Extracardiac Fontan Patients. *J. Am. Coll. Cardiol.* 47, 2065–2073. doi:10.1016/j.jacc.2005.12.065

Gui, L., Dash, B. C., Luo, J., Qin, L., Zhao, L., Yamamoto, K., et al. (2016). Implantable Tissue-Engineered Blood Vessels from Human Induced Pluripotent Stem Cells. *Biomaterials* 102, 120–129. doi:10.1016/j.biomaterials.2016.06.010

Harrington, J. K., Chahboune, H., Criscione, J. M., Li, A. Y., Hibino, N., Yi, T., et al. (2011). Determining the Fate of Seeded Cells in Venous Tissue-engineered Vascular Grafts Using Serial MRI. *FASEB j.* 25, 4150–4161. doi:10.1096/fj.11-185140

Hashi, C. K., Zhu, Y., Yang, G.-Y., Young, W. L., Hsiao, B. S., Wang, K., et al. (2007). Antithrombogenic Property of Bone Marrow Mesenchymal Stem Cells in Nanofibrous Vascular Grafts. *Proc. Natl. Acad. Sci.* 104, 11915–11920. doi:10.1073/pnas.0704581104

Herrmann, F. E. M., Lamm, P., Wellmann, P., Milz, S., Hagl, C., and Juchem, G. (2019). Autologous Endothelialized Vein Allografts in Coronary Artery Bypass Surgery - Long Term Results. *Biomaterials* 212, 87–97. doi:10.1016/j.biomaterials.2019.05.019

Hibino, N., Best, C. A., Engle, A., Ghimbovschi, S., Knoblach, S., Nath, D. S., et al. (2016). Novel Association of miR-451 with the Incidence of TEVG Stenosis in a Murine Model. *Tissue Eng. Part A* 22, 75–82. doi:10.1089/ten.TEA.2014.0664

Hibino, N., McGillicuddy, E., Matsumura, G., Ichihara, Y., Naito, Y., Breuer, C., et al. (2010). Late-term Results of Tissue-Engineered Vascular Grafts in Humans. *J. Thorac. Cardiovasc. Surg.* 139, 431–436. doi:10.1016/j.jtcvs.2009.09.057

Hibino, N., Nalbandian, A., Devine, L., Martinez, R. S., McGillicuddy, E., Yi, T., et al. (2011). Comparison of Human Bone Marrow Mononuclear Cell Isolation Methods for Creating Tissue-Engineered Vascular Grafts: Novel Filter System versus Traditional Density Centrifugation Method. *Tissue Eng. Part C: Methods* 17, 993–998. doi:10.1089/ten.TEC.2011.0110

Hu, Y.-T., Pan, X.-D., Zheng, J., Ma, W.-G., and Sun, L.-Z. (2017). *In Vitro* and *In Vivo* Evaluation of a Small-Caliber Coaxial Electrospun Vascular Graft Loaded with Heparin and VEGF. *Int. J. Surg.* 44, 244–249. doi:10.1016/j.ijsu.2017.06.077

Hulander, M., Lundgren, A., Faxälv, L., Lindahl, T. L., Palmquist, A., Berglin, M., et al. (2013). Gradients in Surface Nanotopography Used to Study Platelet Adhesion and Activation. *Colloids Surf. B: Biointerfaces* 110, 261–269. doi:10.1016/j.colsurfb.2013.04.010

Hwang, S.-J., Kim, S. W., Choo, S. J., Lee, B. W., Im, I.-r., Yun, H. J., et al. (2011). The Decellularized Vascular Allograft as an Experimental Platform for Developing a Biocompatible Small-Diameter Graft Conduit in a Rat Surgical Model. *Yonsei. Med. J.* 52, 227–233. doi:10.3349/ymj.2011.52.2.227

Iacobazzi, D., Swim, M. M., Albertario, A., Caputo, M., and Ghorbel, M. T. (2018). Thymus-Derived Mesenchymal Stem Cells for Tissue Engineering Clinical-Grade Cardiovascular Grafts. *Tissue Eng. Part A* 24, 794–808. doi:10.1089/ten.TEA.2017.0290

Isayama, N., Matsumura, G., Sato, H., Matsuda, S., and Yamazaki, K. (2014). Histological Maturation of Vascular Smooth Muscle Cells in *In Situ* Tissue-Engineered Vasculature. *Biomaterials* 35, 3589–3595. doi:10.1016/j.biomaterials.2014.01.006

Itoh, M., Mukae, Y., Kitsuka, T., Arai, K., Nakamura, A., Uchihashi, K., et al. (2019). Development of an Immunodeficient Pig Model Allowing Long-Term Accommodation of Artificial Human Vascular Tubes. *Nat. Commun.* 10, 2244. doi:10.1038/s41467-019-10107-1

Itoh, M., Nakayama, K., Noguchi, R., Kamohara, K., Furukawa, K., Uchihashi, K., et al. (2015). Scaffold-Free Tubular Tissues Created by a Bio-3D Printer Undergo Remodeling and Endothelialization when Implanted in Rat Aortae. *PLoS One* 10, e0136681. doi:10.1371/journal.pone.0136681

Jaffer, I. H., Fredenburgh, J. C., Hirsh, J., and Weitz, J. I. (2015). Medical Device-Induced Thrombosis: what Causes it and How Can We Prevent it? *J. Thromb. Haemost.* 13 (Suppl. 1), S72–S81. doi:10.1111/jth.12961

Jang, E., Kim, J.-H., Lee, J., Kim, D.-H., and Youn, Y.-N. (2020). Enhanced Biocompatibility of Multi-Layered, 3D Bio-Printed Artificial Vessels Composed of Autologous Mesenchymal Stem Cells. *Polymers* 12, 538. doi:10.3390/polym12030538

Jiang, B., Suen, R., Wang, J.-J., Zhang, Z. J., Wertheim, J. A., Ameer, G. A., et al. (2016). Mechanocompatible Polymer-Extracellular-Matrix Composites for Vascular Tissue Engineering. *Adv. Healthc. Mater.* 5, 1594–1605. doi:10.1002/adhm.201501003

Jin, D., Hu, J., Xia, D., Liu, A. l., Kuang, H., Du, J., et al. (2019a). Evaluation of a Simple Off-The-Shelf Bi-layered Vascular Scaffold Based on poly(L-Lactide-Co-ε-Caprolactone)/silk Fibroin *In Vitro* and *In Vivo*. *Int. J. Nanomedicine* 14, 4261–4276. doi:10.2147/IJN.S205569

Jin, X., Geng, X., Jia, L., Xu, Z., Ye, L., Gu, Y., et al. (2019b). Preparation of Small-Diameter Tissue-Engineered Vascular Grafts Electrospun from Heparin End-Capped PCL and Evaluation in a Rabbit Carotid Artery Replacement Model. *Macromol. Biosci.* 19, 1900114. doi:10.1002/mabi.201900114

Ju, Y. M., Ahn, H., Arenas-Herrera, J., Kim, C., Abolbashari, M., Atala, A., et al. (2017). Electrospun Vascular Scaffold for Cellularized Small Diameter Blood Vessels: A Preclinical Large Animal Study. *Acta Biomater.* 59, 58–67. doi:10.1016/j.actbio.2017.06.027

Kajbafzadeh, A.-M., Khorramirouz, R., Kameli, S. M., Fendereski, K., Daryabari, S. S., Tavangar, S. M., et al. (2019). Three-year Efficacy and Patency Follow-Up of Decellularized Human Internal Mammary Artery as a Novel Vascular Graft in Animal Models. *J. Thorac. Cardiovasc. Surg.* 157, 1494–1502. doi:10.1016/j.jtcvs.2018.08.106

Katsimpoulas, M., Morticelli, L., Gontika, I., Kouvaka, A., Mallis, P., Dipresa, D., et al. (2019). Biocompatibility and Immunogenicity of Decellularized Allogeneic Aorta in the Orthotopic Rat Model. *Tissue Eng. Part A* 25, 399–415. doi:10.1089/ten.TEA.2018.0037

Khosravi, R., Best, C. A., Allen, R. A., Stowell, C. E. T., Onwuka, E., Zhuang, J. J., et al. (2016). Long-Term Functional Efficacy of a Novel Electrospun Poly(Glycerol Sebacate)-Based Arterial Graft in Mice. *Ann. Biomed. Eng.* 44, 2402–2416. doi:10.1007/s10439-015-1545-7

Kim, S.-J., Kim, W.-H., Lim, H.-G., and Lee, J.-Y. (2008). Outcome of 200 Patients after an Extracardiac Fontan Procedure. *J. Thorac. Cardiovasc. Surg.* 136, 108–116. doi:10.1016/j.jtcvs.2007.12.032

Kirkton, R. D., Santiago-Maysonet, M., Lawson, J. H., Tente, W. E., Dahl, S. L. M., Niklason, L. E., et al. (2019). Bioengineered Human Acellular Vessels Recellularize and Evolve into Living Blood Vessels after Human Implantation. *Sci. Transl. Med.* 11, eaau6934. doi:10.1126/scitranslmed.aau6934

Koenneker, S., Teebken, O. E., Bonehie, M., Pflaum, M., Jockenhoevel, S., Haverich, A., et al. (2010). A Biological Alternative to Alloplastic Grafts in Dialysis Therapy: Evaluation of an Autologised Bioartificial Haemodialysis Shunt Vessel in a Sheep Model. *Eur. J. Vasc. Endovascular Surg.* 40, 810–816. doi:10.1016/j.ejvs.2010.04.023

Koens, M. J. W., Krasznai, A. G., Hanssen, A. E. J., Hendriks, T., Praster, R., Daamen, W. F., et al. (2015). Vascular Replacement Using a Layered Elastin-Collagen Vascular Graft in a Porcine Model: One Week Patency versus One Month Occlusion. *Organogenesis* 11, 105–121. doi:10.1080/15476278.2015.1038448

Koobatian, M. T., Row, S., Smith, R. J., Jr, Koenigsknecht, C., Andreadis, S. T., and Swartz, D. D. (2016). Successful Endothelialization and Remodeling of a Cell-free Small-Diameter Arterial Graft in a Large Animal Model. *Biomaterials* 76, 344–358. doi:10.1016/j.biomaterials.2015.10.020

L'Heureux, N., Dusserre, N., Marini, A., Garrido, S., de la Fuente, L., and McAllister, T. (2007). Technology Insight: the Evolution of Tissue-Engineered Vascular Grafts-From Research to Clinical Practice. *Nat. Rev. Cardiol.* 4, 389–395. doi:10.1038/ncpcardio0930

Leal, B. B. J., Wakabayashi, N., Oyama, K., Kamiya, H., Braghirolli, D. I., and Pranke, P. (2021). Vascular Tissue Engineering: Polymers and Methodologies for Small Caliber Vascular Grafts. *Front. Cardiovasc. Med.* 7, 592361. doi:10.3389/fcvm.2020.592361

Lee, K.-W., Gade, P. S., Dong, L., Zhang, Z., Aral, A. M., Gao, J., et al. (2018). A Biodegradable Synthetic Graft for Small Arteries Matches the Performance of Autologous Vein in Rat Carotid Arteries. *Biomaterials* 181, 67–80. doi:10.1016/j.biomaterials.2018.07.037

Lee, Y.-U., Yi, T., Tara, S., Lee, A. Y., Hibino, N., Shinoka, T., et al. (2014). Implantation of Inferior Vena Cava Interposition Graft in Mouse Model. *J. Vis. Exp.* 4, 51632. doi:10.3791/51632

Lelovas, P. P., Kostomitsopoulos, N. G., and Xanthos, T. T. (2014). A Comparative Anatomic and Physiologic Overview of the Porcine Heart. *J. Am. Assoc. Lab. Anim. Sci.* 53, 432–438.

Li, W., Chen, J., Xu, P., Zhu, M., Wu, Y., Wang, Z., et al. (2018). Long-term Evaluation of Vascular Grafts with Circumferentially Aligned Microfibers in a Rat Abdominal Aorta Replacement Model. *J. Biomed. Mater. Res.* 106, 2596–2604. doi:10.1002/jbm.b.34076

Li, X., Xu, J., Nicolescu, C. T., Marinelli, J. T., and Tien, J. (2017). Generation, Endothelialization, and Microsurgical Suture Anastomosis of Strong 1-Mm-Diameter Collagen Tubes. *Tissue Eng. Part A* 23, 335–344. doi:10.1089/ten.TEA.2016.0339

Liu, J., Qin, Y., Wu, Y., Sun, Z., Li, B., Jing, H., et al. (2019). The Surrounding Tissue Contributes to Smooth Muscle Cell's Regeneration and Vascularization of Small Diameter Vascular Grafts. *Biomater. Sci.* 7, 914–925. doi:10.1039/c8bm01277f

Lovett, M., Cannizzaro, C., Daheron, L., Messmer, B., Vunjak-Novakovic, G., and Kaplan, D. L. (2007). Silk Fibroin Microtubes for Blood Vessel Engineering. *Biomaterials* 28, 5271–5279. doi:10.1016/j.biomaterials.2007.08.008

Lovett, M., Eng, G., Kluge, J., Cannizzaro, C., Vunjak-Novakovic, G., and Kaplan, D. L. (2010). Tubular Silk Scaffolds for Small Diameter Vascular Grafts. *Organogenesis* 6, 217–224. doi:10.4161/org.6.4.13407

Luo, J., Qin, L., Zhao, L., Gui, L., Ellis, M. W., Huang, Y., et al. (2020). Tissue-Engineered Vascular Grafts with Advanced Mechanical Strength from Human iPSCs. *Cel. Stem Cel.* 26, 251–261.e8. doi:10.1016/j.stem.2019.12.012

Ma, X., He, Z., Li, L., Liu, G., Li, Q., Yang, D., et al. (2017). Development and *In Vivo* Validation of Tissue-Engineered, Small-Diameter Vascular Grafts from

Decellularized Aortae of Fetal Pigs and Canine Vascular Endothelial Cells. *J. Cardiothorac. Surg.* 12, 101. doi:10.1186/s13019-017-0661-x

Madhavan, K., Elliot, W., Tan, Y., Monnet, E., and Tan, W. (2018). Performance of Marrow Stromal Cell-Seeded Small-Caliber Multilayered Vascular Graft in a Senescent Sheep Model. *Biomed. Mater.* 13, 055004. doi:10.1088/1748-605X/aac7a6

Mahara, A., Somekawa, S., Kobayashi, N., Hirano, Y., Kimura, Y., Fujisato, T., et al. (2015). Tissue-engineered Acellular Small Diameter Long-Bypass Grafts with Neointima-Inducing Activity. *Biomaterials* 58, 54–62. doi:10.1016/j.biomaterials.2015.04.031

Mathers, C. D., and Loncar, D. (2006). Projections of Global Mortality and burden of Disease from 2002 to 2030. *Plos Med.* 3, e442. doi:10.1371/journal.pmed.0030442

Matsumura, G., Isayama, N., Matsuda, S., Taki, K., Sakamoto, Y., Ikada, Y., et al. (2013). Long-term Results of Cell-free Biodegradable Scaffolds for *In Situ* Tissue Engineering of Pulmonary Artery in a Canine Model. *Biomaterials* 34, 6422–6428. doi:10.1016/j.biomaterials.2013.05.037

Matsumura, G., Nitta, N., Matsuda, S., Sakamoto, Y., Isayama, N., Yamazaki, K., et al. (2012). Long-term Results of Cell-free Biodegradable Scaffolds for *In Situ* Tissue-Engineering Vasculature: in a Canine Inferior Vena Cava Model. *PLoS One* 7, e35760. doi:10.1371/journal.pone.0035760

Mauri, A., Zeisberger, S. M., Hoerstrup, S. P., and Mazza, E. (2013). Analysis of the Uniaxial and Multiaxial Mechanical Response of a Tissue-Engineered Vascular Graft. *Tissue Eng. Part A* 19, 583–592. doi:10.1089/ten.tea.2012.0075

Maxfield, M. W., Stacy, M. R., Kurobe, H., Tara, S., Yi, T., Cleary, M. A., et al. (2017). Novel Application and Serial Evaluation of Tissue-Engineered portal Vein Grafts in a Murine Model. *Regenerative Med.* 12, 929–938. doi:10.2217/rme-2017-0021

McIlhenny, S., Zhang, P., Tulenko, T., Comeau, J., Fernandez, S., Policha, A., et al. (2015). eNOS Transfection of Adipose-Derived Stem Cells Yields Bioactive Nitric Oxide Production and Improved Results in Vascular Tissue Engineering. *J. Tissue Eng. Regen. Med.* 9, 1277–1285. doi:10.1002/term.1645

Meier, L. A., Syedain, Z. H., Lahti, M. T., Johnson, S. S., Chen, M. H., Hebbel, R. P., et al. (2014). Blood Outgrowth Endothelial Cells Alter Remodeling of Completely Biological Engineered Grafts Implanted into the Sheep Femoral Artery. *J. Cardiovasc. Trans. Res.* 7, 242–249. doi:10.1007/s12265-013-9539-z

Mishra, M. (2015). *Encyclopedia of Biomedical Polymers and Polymeric Biomaterials*. 1er ed. US: Taylor & Francis.

Moher, D., Shamseer, L., Shamseer, L., Clarke, M., Ghersi, D., Liberati, A., et al. (2015). Preferred Reporting Items for Systematic Review and Meta-Analysis Protocols (PRISMA-P) 2015 Statement. *Syst. Rev.* 4, 1. doi:10.1186/2046-4053-4-1

Mozaffarian, D., Benjamin, E. J., Go, A. S., Arnett, D. K., Blaha, M. J., Cushman, M., et al. (2015). Heart Disease and Stroke Statistics-2015 Update. *Circulation* 131, e29–322. doi:10.1161/CIR.0000000000000152

Mrówczyński, W., Mugnai, D., de Valence, S., Tille, J.-C., Khabiri, E., Cikirikcioglu, M., et al. (2014). Porcine Carotid Artery Replacement with Biodegradable Electrospun Poly-E-Caprolactone Vascular Prosthesis. *J. Vasc. Surg.* 59, 210–219. doi:10.1016/j.jvs.2013.03.004

Mulier, K. E., Greenberg, J. G., and Beilman, G. J. (2012). Hypercoagulability in Porcine Hemorrhagic Shock Is Present Early after Trauma and Resuscitation. *J. Surg. Res.* 174, e31–e35. doi:10.1016/j.jss.2011.10.005

Naito, Y., Shinoka, T., Duncan, D., Hibino, N., Solomon, D., Cleary, M., et al. (2011). Vascular Tissue Engineering: towards the Next Generation Vascular Grafts. *Adv. Drug Deliv. Rev.* 63, 312–323. doi:10.1016/j.addr.2011.03.001

Nakano, T., Kado, H., Tachibana, T., Hinokiyama, K., Shiose, A., Kajimoto, M., et al. (2007). Excellent Midterm Outcome of Extracardiac Conduit Total Cavopulmonary Connection: Results of 126 Cases. *Ann. Thorac. Surg.* 84, 1619–1626. doi:10.1016/j.athoracsur.2007.05.074

Negishi, J., Hashimoto, Y., Yamashita, A., Zhang, Y., Kimura, T., Kishida, A., et al. (2017). Evaluation of Small-Diameter Vascular Grafts Reconstructed from Decellularized Aorta Sheets. *J. Biomed. Mater. Res.* 105, 1293–1298. doi:10.1002/jbm.a.36017

Ong, C. S., Fukunishi, T., Liu, R. H., Nelson, K., Zhang, H., Wieczorek, E., et al. (2017a). Bilateral Arteriovenous Shunts as a Method for Evaluating Tissue-Engineered Vascular Grafts in Large Animal Models. *Tissue Eng. Part C: Methods* 23, 728–735. doi:10.1089/ten.TEC.2017.0217

Ong, C. S., Zhou, X., Huang, C. Y., Fukunishi, T., Zhang, H., and Hibino, N. (2017b). Tissue Engineered Vascular Grafts: Current State of the Field. *Expert Rev. Med. Devices* 14, 383–392. doi:10.1080/17434440.2017.1324293

Pashneh-Tala, S., MacNeil, S., and Claeyssens, F. (2016). The Tissue-Engineered Vascular Graft-Past, Present, and Future. *Tissue Eng. B: Rev.* 22, 68–100. doi:10.1089/ten.teb.2015.0100

Pellegata, A. F., Dominioni, T., Ballo, F., Maestroni, S., Asnaghi, M. A., Zerbini, G., et al. (2015). Arterial Decellularized Scaffolds Produced Using an Innovative Automatic System. *Cells Tissues Organs* 200, 363–373. doi:10.1159/000439082

Pepper, V. K., Clark, E. S., Best, C. A., Onwuka, E. A., Sugiura, T., Heuer, E. D., et al. (2017). Intravascular Ultrasound Characterization of a Tissue-Engineered Vascular Graft in an Ovine Model. *J. Cardiovasc. Trans. Res.* 10, 128–138. doi:10.1007/s12265-016-9725-x

Poh, M., Boyer, M., Solan, A., Dahl, S. L., Pedrotty, D., Banik, S. S., et al. (2005). Blood Vessels Engineered from Human Cells. *The Lancet* 365, 2122–2124. doi:10.1016/S0140-6736(05)66735-9

Prichard, H. L., Manson, R. J., DiBernardo, L., Niklason, L. E., Lawson, J. H., and Dahl, S. L. M. (2011). An Early Study on the Mechanisms that Allow Tissue-Engineered Vascular Grafts to Resist Intimal Hyperplasia. *J. Cardiovasc. Trans. Res.* 4, 674–682. doi:10.1007/s12265-011-9306-y

Qin, K., Wu, Y., Pan, Y., Wang, K., Kong, D., and Zhao, Q. (2018). Implantation of Electrospun Vascular Grafts with Optimized Structure in a Rat Model. *J. Vis. Exp.* 136, 57340. doi:10.3791/57340

Quint, C., Arief, M., Muto, A., Dardik, A., and Niklason, L. E. (2012). Allogeneic Human Tissue-Engineered Blood Vessel. *J. Vasc. Surg.* 55, 790–798. doi:10.1016/j.jvs.2011.07.098

Quint, C., Kondo, Y., Manson, R. J., Lawson, J. H., Dardik, A., and Niklason, L. E. (2011). Decellularized Tissue-Engineered Blood Vessel as an Arterial Conduit. *Proc. Natl. Acad. Sci.* 108, 9214–9219. doi:10.1073/pnas.1019506108

Radke, D., Jia, W., Sharma, D., Fena, K., Wang, G., Goldman, J., et al. (2018). Tissue Engineering at the Blood-Contacting Surface: A Review of Challenges and Strategies in Vascular Graft Development. *Adv. Healthc. Mater.* 7, 1701461. doi:10.1002/adhm.201701461

Ran, X., Ye, Z., Fu, M., Wang, Q., Wu, H., Lin, S., et al. (2019). Design, Preparation, and Performance of a Novel Bilayer Tissue-Engineered Small-Diameter Vascular Graft. *Macromol. Biosci.* 19, 1800189. doi:10.1002/mabi.201800189

Reinhardt, J. W., Rosado, J. d. D. R., Barker, J. C., Lee, Y.-U., Best, C. A., Yi, T., et al. (2019). Early Natural History of Neotissue Formation in Tissue-Engineered Vascular Grafts in a Murine Model. *Regenerative Med.* 14, 389–408. doi:10.2217/rme-2018-0133

Rothuizen, T. C., Damanik, F. F. R., Lavrijsen, T., Visser, M. J. T., Hamming, J. F., Lalai, R. A., et al. (2016). Development and Evaluation of *In Vivo* Tissue Engineered Blood Vessels in a Porcine Model. *Biomaterials* 75, 82–90. doi:10.1016/j.biomaterials.2015.10.023

Row, S., Peng, H., Schlaich, E. M., Koenigsknecht, C., Andreadis, S. T., and Swartz, D. D. (2015). Arterial Grafts Exhibiting Unprecedented Cellular Infiltration and Remodeling *In Vivo*: the Role of Cells in the Vascular wall. *Biomaterials* 50, 115–126. doi:10.1016/j.biomaterials.2015.01.045

Row, S., Santandreu, A., Swartz, D. D., and Andreadis, S. T. (2017). Cell-free Vascular Grafts: Recent Developments and Clinical Potential. *Technology* 05, 13–20. doi:10.1142/S2339547817400015

Shafiq, M., Zhang, Q., Zhi, D., Wang, K., Kong, D., Kim, D.-H., et al. (2018). *In Situ* Blood Vessel Regeneration Using SP (Substance P) and SDF (Stromal Cell-Derived Factor)-1α Peptide Eluting Vascular Grafts. *Atvb* 38, e117–e134. doi:10.1161/ATVBAHA.118.310934

Shi, J., Chen, S., Wang, L., Zhang, X., Gao, J., Jiang, L., et al. (2019). Rapid Endothelialization and Controlled Smooth Muscle Regeneration by Electrospun Heparin-loaded Polycaprolactone/gelatin Hybrid Vascular Grafts. *J. Biomed. Mater. Res.* 107, 2040–2049. doi:10.1002/jbm.b.34295

Shin'oka, T., Imai, Y., and Ikada, Y. (2001). Transplantation of a Tissue-Engineered Pulmonary Artery. *N. Engl. J. Med.* 344, 532–533. doi:10.1056/NEJM200102153440717

Shum-Tim, D., Stock, U., Hrkach, J., Shinoka, T., Lien, J., Moses, M. A., et al. (1999). Tissue Engineering of Autologous Aorta Using a New Biodegradable Polymer. *Ann. Thorac. Surg.* 68, 2298–2304. doi:10.1016/s0003-4975(99)01055-3

Siemionow, M. Z. (2015). *Plastic and Reconstructive Surgery. Experimental Models and Research Designs*. University of Illinois, Chicago, USA: Springer.

Simon, P., Kasimir, M. T., Seebacher, G., Weigel, G., Ullrich, R., Salzer-Muhar, U., et al. (2003). Early Failure of the Tissue Engineered Porcine Heart Valve SYNERGRAFT in Pediatric Patients. *Eur. J. Cardio-Thoracic Surg.* 23, 1002–1006. doi:10.1016/s1010-7940(03)00094-0

Smith, R. J., Yi, T., Nasiri, B., Breuer, C. K., and Andreadis, S. T. (2019). Implantation of VEGF-functionalized Cell-free Vascular Grafts: Regenerative and Immunological Response. *FASEB j.* 33, 5089–5100. doi:10.1096/fj.201801856R

Sologashvili, T., Saat, S. A., Tille, J.-C., De Valence, S., Mugnai, D., Giliberto, J. P., et al. (2019). Effect of Implantation Site on Outcome of Tissue-Engineered Vascular Grafts. *Eur. J. Pharmaceutics Biopharmaceutics* 139, 272–278. doi:10.1016/j.ejpb.2019.04.012

Song, L., Wang, L., Shah, P. K., Chaux, A., and Sharifi, B. G. (2010). Bioengineered Vascular Graft Grown in the Mouse Peritoneal Cavity. *J. Vasc. Surg.* 52, 994–1002. doi:10.1016/j.jvs.2010.05.015

Stacy, M. R., Naito, Y., Maxfield, M. W., Kurobe, H., Tara, S., Chan, C., et al. (2014). Targeted Imaging of Matrix Metalloproteinase Activity in the Evaluation of Remodeling Tissue-Engineered Vascular Grafts Implanted in a Growing Lamb Model. *J. Thorac. Cardiovasc. Surg.* 148, 2227–2233. doi:10.1016/j.jtcvs.2014.05.037

Sugiura, T., Matsumura, G., Miyamoto, S., Miyachi, H., Breuer, C. K., and Shinoka, T. (2018). Tissue-Engineered Vascular Grafts in Children with Congenital Heart Disease: Intermediate Term Follow-Up. *Semin. Thorac. Cardiovasc. Surg.* 30, 175–179. doi:10.1053/j.semtcvs.2018.02.002

Syedain, Z. H., Graham, M. L., Dunn, T. B., O'Brien, T., Johnson, S. L., Schumacher, R. J., et al. (2017). A Completely Biological "Off-The-Shelf" Arteriovenous Graft that Recellularizes in Baboons. *Sci. Transl. Med.* 9, eaan4209. doi:10.1126/scitranslmed.aan4209

Syedain, Z., Reimer, J., Lahti, M., Berry, J., Johnson, S., Bianco, R., et al. (2016). Tissue Engineering of Acellular Vascular Grafts Capable of Somatic Growth in Young Lambs. *Nat. Commun.* 7, 12951. doi:10.1038/ncomms12951

Tara, S., Kurobe, H., de Dios Ruiz Rosado, J., Best, C. A., Shoji, T., Mahler, N., et al. (2015). Cilostazol, Not Aspirin, Prevents Stenosis of Bioresorbable Vascular Grafts in a Venous Model. *Arterioscler. Thromb. Vasc. Biol.* 35, 2003–2010. doi:10.1161/ATVBAHA.115.306027

Tara, S., Kurobe, H., Rocco, K. A., Maxfield, M. W., Best, C. A., Yi, T., et al. (2014). Well-organized Neointima of Large-Pore Poly(l-Lactic Acid) Vascular Graft Coated with Poly(l-Lactic-Co-ε-Caprolactone) Prevents Calcific Deposition Compared to Small-Pore Electrospun Poly(l-Lactic Acid) Graft in a Mouse Aortic Implantation Model. *Atherosclerosis* 237, 684–691. doi:10.1016/j.atherosclerosis.2014.09.030

Tillman, B. W., Yazdani, S. K., Neff, L. P., Corriere, M. A., Christ, G. J., Soker, S., et al. (2012). Bioengineered Vascular Access Maintains Structural Integrity in Response to Arteriovenous Flow and Repeated Needle Puncture. *J. Vasc. Surg.* 56, 783–793. doi:10.1016/j.jvs.2012.02.030

Tondreau, M. Y., Laterreur, V., Vallières, K., Gauvin, R., Bourget, J.-M., Tremblay, C., et al. (2016). In VivoRemodeling of Fibroblast-Derived Vascular Scaffolds Implanted for 6 Months in Rats. *Biomed. Res. Int.* 2016, 1–12. doi:10.1155/2016/3762484

Tseng, Y. C., Roan, J. N., Ho, Y. C., Lin, C. C., and Yeh, M. L. (2017). An *In Vivo* Study on Endothelialized Vascular Grafts Produced by Autologous Biotubes and Adipose Stem Cells (ADSCs). *J. Mater. Sci. Mater. Med.* 28, 166. doi:10.1007/s10856-017-5986-4

Udelsman, B. V., Khosravi, R., Miller, K. S., Dean, E. W., Bersi, M. R., Rocco, K., et al. (2014). Characterization of Evolving Biomechanical Properties of Tissue Engineered Vascular Grafts in the Arterial Circulation. *J. Biomech.* 47, 2070–2079. doi:10.1016/j.jbiomech.2014.03.011

Valence, S. d., Tille, J.-C., Chaabane, C., Gurny, R., Bochaton-Piallat, M.-L., Walpoth, B. H., et al. (2013). Plasma Treatment for Improving Cell Biocompatibility of a Biodegradable Polymer Scaffold for Vascular Graft Applications. *Eur. J. Pharmaceutics Biopharmaceutics* 85, 78–86. doi:10.1016/j.ejpb.2013.06.012

Valencia Rivero, K. T., Jaramillo Escobar, J., Galvis Forero, S. D., Miranda Saldaña, M. C., López Panqueva, R. d. P., Sandoval Reyes, N. F., et al. (2018). New Regenerative Vascular Grafts for Hemodialysis Access: Evaluation of a Preclinical Animal Model. *J. Invest. Surg.* 31, 192–200. doi:10.1080/08941939.2017.1303100

Villalona, G. A., Udelsman, B., Duncan, D. R., McGillicuddy, E., Sawh-Martinez, R. F., Hibino, N., et al. (2010). Cell-Seeding Techniques in Vascular Tissue Engineering. *Tissue Eng. Part B: Rev.* 16, 341–350. doi:10.1089/ten.TEB.2009.0527

Wang, T., Dong, N., Yan, H., Wong, S. Y., Zhao, W., Xu, K., et al. (2019). Regeneration of a Neoartery through a Completely Autologous Acellular Conduit in a Minipig Model: a Pilot Study. *J. Transl. Med.* 17, 24. doi:10.1186/s12967-018-1763-5

Wang, Z., Zheng, W., Wu, Y., Wang, J., Zhang, X., Wang, K., et al. (2016). Differences in the Performance of PCL-Based Vascular Grafts as Abdominal Aorta Substitutes in Healthy and Diabetic Rats. *Biomater. Sci.* 4, 1485–1492. doi:10.1039/c6bm00178e

Weber, C., Reinhardt, S., Eghbalzadeh, K., Wacker, M., Guschlbauer, M., Maul, A., et al. (2018). Patency and *In Vivo* Compatibility of Bacterial Nanocellulose Grafts as Small-Diameter Vascular Substitute. *J. Vasc. Surg.* 68, 177S–187S. doi:10.1016/j.jvs.2017.09.038

Weinberg, C. B., and Bell, E. (1986). A Blood Vessel Model Constructed from Collagen and Cultured Vascular Cells. *Science* 231, 397–400. doi:10.1126/science.2934816

Wolf, F., Paefgen, V., Winz, O., Mertens, M., Koch, S., Gross-Weege, N., et al. (2019). MR and PET-CT Monitoring of Tissue-Engineered Vascular Grafts in the Ovine Carotid Artery. *Biomaterials* 216, 119228. doi:10.1016/j.biomaterials.2019.119228

Woods, I., and Flanagan, T. C. (2014). Electrospinning of Biomimetic Scaffolds for Tissue-Engineered Vascular Grafts: Threading the Path. *Expert Rev. Cardiovasc. Ther.* 12, 815–832. doi:10.1586/14779072.2014.925397

World Health Organization (2020). Cardiovascular Diseases (CVDs). Fact Sheet. https://www.who.int/news-room/fact-sheets/detail/cardiovascular-diseases-(cvds (Accessed May 20, 2020).

Wu, Y., Li, L., Chen, W., Zeng, W., Zeng, L., Wen, C., et al. (2015). Maintaining Moderate Platelet Aggregation and Improving Metabolism of Endothelial Progenitor Cells Increase the Patency Rate of Tissue-Engineered Blood Vessels. *Tissue Eng. Part A* 21, 2001–2012. doi:10.1089/ten.TEA.2015.0013

Wu, Y., Qin, Y., Wang, Z., Wang, J., Zhang, C., Li, C., et al. (2018). The Regeneration of Macro-Porous Electrospun Poly(ε-Caprolactone) Vascular Graft during Long-Termin Situimplantation. *J. Biomed. Mater. Res.* 106, 1618–1627. doi:10.1002/jbm.b.33967

Xu, Z., Gu, Y., Li, J., Feng, Z., Guo, L., Tong, Z., et al. (2018). Vascular Remodeling Process of Heparin-Conjugated Poly(ε-Caprolactone) Scaffold in a Rat Abdominal Aorta Replacement Model. *J. Vasc. Res.* 55, 338–349. doi:10.1159/000494509

Yamanami, M., Kanda, K., Kawasaki, T., Kami, D., Watanabe, T., Gojo, S., et al. (2019). Development of Xenogeneic Decellularized Biotubes for Off-the-shelf Applications. *Artif. Organs* 43, 773–779. doi:10.1111/aor.13432

Yang, X., Wei, J., Lei, D., Liu, Y., and Wu, W. (2016). Appropriate Density of PCL Nano-Fiber Sheath Promoted Muscular Remodeling of PGS/PCL Grafts in Arterial Circulation. *Biomaterials* 88, 34–47. doi:10.1016/j.biomaterials.2016.02.026

Yeung, E., Inoue, T., Matsushita, H., Opfermann, J., Mass, P., Aslan, S., et al. (2020). *In Vivo* implantation of 3-dimensional Printed Customized Branched Tissue Engineered Vascular Graft in a Porcine Model. *J. Thorac. Cardiovasc. Surg.* 159, 1971–1981. doi:10.1016/j.jtcvs.2019.09.138

Zhao, J., Liu, L., Wei, J., Ma, D., Geng, W., Yan, X., et al. (2012). A Novel Strategy to Engineer Small-Diameter Vascular Grafts from Marrow-Derived Mesenchymal Stem Cells. *Artif. Organs* 36, 93–101. doi:10.1111/j.1525-1594.2011.01231.x

Conflict of Interest: The authors declare that the research was conducted in the absence of any commercial or financial relationships that could be construed as a potential conflict of interest.

Publisher's Note: All claims expressed in this article are solely those of the authors and do not necessarily represent those of their affiliated organizations, or those of the publisher, the editors and the reviewers. Any product that may be evaluated in this article, or claim that may be made by its manufacturer, is not guaranteed or endorsed by the publisher.

Bloque II) Análisis fisicoquímicos y biológicos de materiales destinados al desarrollo de injertos vasculares de ingeniería tisular.

- **Development of silk fibroin scaffolds for vascular repair**

  Durán-Rey D, Brito-Pereira R, Ribeiro C, Ribeiro S, Sánchez-Margallo JA, Crisóstomo V, Irastorza I, Silván U, Lanceros-Méndez S, Sánchez-Margallo FM.

  Biomacromolecules. **2023**; 24(3): 1121-1130.

  DOI: 10.1021/acs.biomac.2c01124. PMID: 36754364.

  [Published]

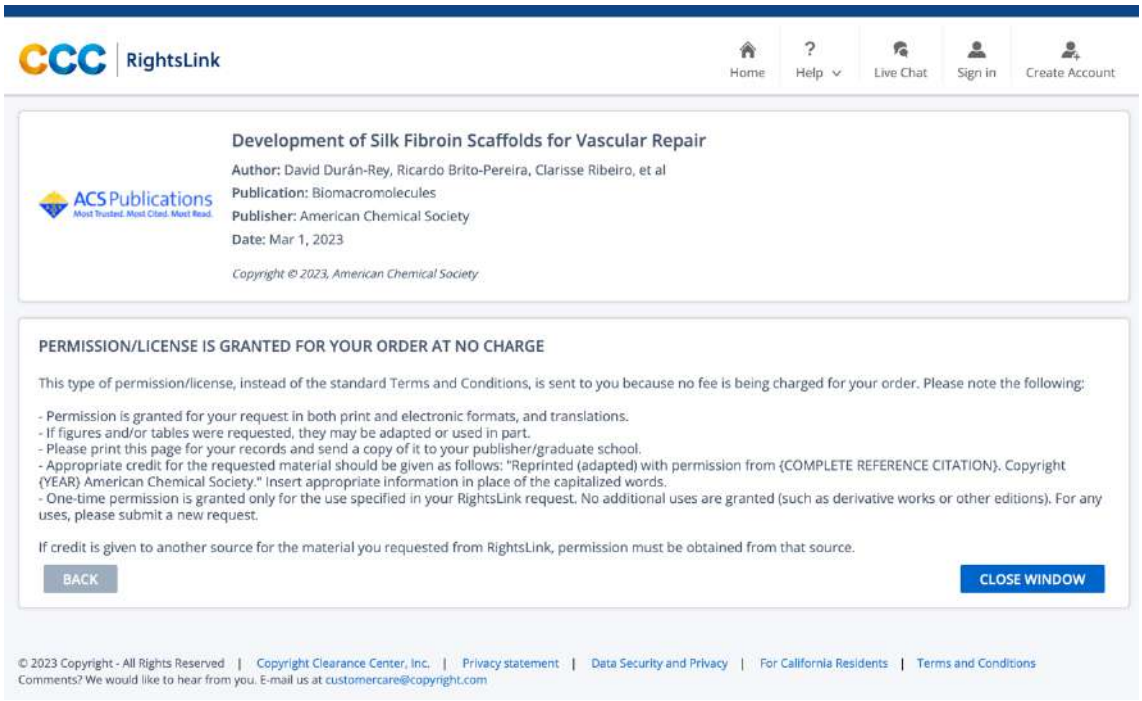

BioMACROMOLECULES

pubs.acs.org/Biomac Article

Development of Silk Fibroin Scaffolds for Vascular Repair

David Durán-Rey, Ricardo Brito-Pereira, Clarisse Ribeiro, Sylvie Ribeiro, Juan A. Sánchez-Margallo, Verónica Crisóstomo, Igor Irastorza, Unai Silván, Senentxu Lanceros-Méndez, and Francisco M. Sánchez-Margallo*

Cite This: *Biomacromolecules* 2023, 24, 1121−1130 Read Online

ACCESS | Metrics & More | Article Recommendations

ABSTRACT: Silk fibroin (SF) is a biocompatible natural protein with excellent mechanical characteristics. SF-based biomaterials can be structured using a number of techniques, allowing the tuning of materials for specific biomedical applications. In this study, SF films, porous membranes, and electrospun membranes were produced using solvent-casting, salt-leaching, and electrospinning methodologies, respectively. SF-based materials were subjected to physicochemical and biological characterizations to determine their suitability for tissue regeneration applications. Mechanical analysis showed stress−strain curves of brittle materials in films and porous membranes, while electrospun membranes featured stress−strain curves typical of ductile materials. All samples showed similar chemical composition, melting transition, hydrophobic behavior, and low cytotoxicity levels, regardless of their architecture. Finally, all of the SF-based materials promote the proliferation of human umbilical vein endothelial cells (HUVECs). These findings demonstrate the different relationship between HUVEC behavior and the SF sample's topography, which can be taken advantage of for the design of vascular implants.

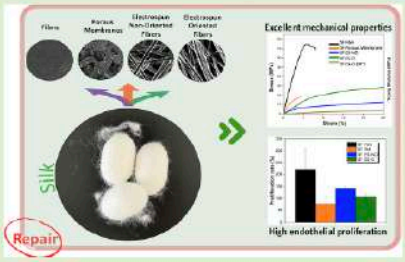

1. INTRODUCTION

Tissue engineering (TE) aims to develop structures or scaffolds to regenerate damaged organs or tissues.[1,2] Currently, there are a wide variety of materials that can be used in TE, including synthetic and natural polymers. Polyglycolic acid, poly-L-lactide acid, or polycaprolactones are examples of synthetic polymers with mechanical properties adequate for their use in TE applications such as vascular, intestine, bone, and liver grafts, among others.[3,4] Regarding natural polymers with potential for TE applications, collagen, chitosan, and elastin are among the most studied ones. In general terms, these materials are characterized by good biocompatibility and low antigenicity and allow good cellular infiltration, but show poor mechanical properties.[2−4]

A natural polymer with strong potential in the TE field is silk fibroin (SF). This protein is obtained from the cocoons of the *Bombyx mori* silkworm. SF is biocompatible, not immunogenic in humans,[5,6] and presents piezoelectric properties.[7] Different silk fibroin structures have been observed, among which silk I and silk II are the dominant ones.[2] Silk I is a metastable structure made from hydrophobic polar groups (α-helix), while silk II is formed by β-sheets.[2] Also, SF presents a crystalline dimorphism between crystalline units of silk I and II,[8] the piezoelectric activity of the SF being related to the lack of a center of symmetry. Further, the C−O−N−H dipoles of α-helix and β-sheets are oriented along the longitudinal direction of the fibers in electrospun SF samples. When a stress is applied in the thickness direction, dipole movements are generated, resulting in an electric polarization of the fiber.[9,10] Therefore, the alignment of the polymer chains and the dipole orientation within the fibers provide good electroactive properties to SF.[11]

Materials with piezoelectric properties have been employed in biomedical applications in order to imitate the biophysical cues characteristic of tissues such as skin, bone, and tendon.[12,13] Consequently, SF has been applied in a wide variety of areas in the scope of TE, including vascular grafts as it favors angiogenesis,[3,5] bone tissue regeneration where it promotes osteogenic differentiation,[2] and skin tissue regeneration due to its ability to promote keratinocyte and fibroblast attachment,[14] among others.

Electric fields are known to modulate the phenotype of vascular endothelial cells[15] and promote neovessel formation in vivo.[16] Furthermore, electric fields can regulate the vascular

Received: September 16, 2022
Revised: January 5, 2023
Published: February 8, 2023

https://doi.org/10.1021/acs.biomac.2c01124
Biomacromolecules 2023, 24, 1121−1130

endothelial permeability, an important parameter of tissue regeneration and wound healing.[17,18] In this way, SF has a demonstrated ability to induce tissue regeneration, including endothelial tissue, which helps to prevent the thrombosis development during vascular grafting.[19]

SF-based biomaterials can be engineered in different ways, such as solvent-casting, particle-leaching, or electrospinning processing, among others, that result in structures such as flat and porous films and electrospun membranes. However, each of these structured materials displays different morphological, mechanical, and biological characteristics depending on its architecture and the methodology employed for its preparation. These factors are essential for determining the potential of the structured materials for TE applications and, thus, should be thoroughly evaluated.[2,20]

Previous studies have shown that the above-mentioned material characteristics are important factors in the development of structures intended for cardiovascular repair.[3] In the present work, SF constructs with different morphologies have been obtained for cardiovascular repair applications. Therefore, films, porous membranes, and electrospun membranes with random and parallel fiber orientations were prepared using solvent-casting, salt-leaching, and electrospinning methodologies, respectively. All of these structured materials were characterized using physicochemical methods, contact angle measurements, cytotoxicity assessment, cell proliferation, and degradation testing in order to establish their applicability in TE.

2. EXPERIMENTAL SECTION

2.1. Materials. Cocoons of *Bombyx mori* silkworm were provided by APPACDM from Castelo Branco, Portugal. Calcium chloride ($CaCl_2$), sodium chloride (NaCl), sodium carbonate (Na_2CO_3), and formic acid (FA), were acquired from Sigma-Aldrich. Distilled water was prepared in our laboratory. All chemicals and materials were used as received.

2.2. Silk Fibroin Solution Preparation. The cocoons from *Bombyx mori* were first cleaned and then cut into pieces of 1 cm^2 before being boiled at 80 °C in 0.05 wt % Na_2CO_3 water solution for 60 min in a silk to water ratio (w/v) of 1:40 (i.e., 40 mL of aqueous Na_2CO_3 solution for each 1 g of silk). After that, the resultant solid fibers of SF were cleaned and rinsed with abundant distilled water, squeezed out to remove water, and dried overnight (JP Selecta oven, Model 2000208). Once the SF fibers were totally dried, they were dissolved in a 0.17 M solution of FA/$CaCl_2$ in a 10:1 v/w ratio (10 mL of FA per each gram of SF). The solution was then centrifuged at 7500 rpm for 10 min in order to remove residues and impurities. The silk solution was placed in an airing chamber at room temperature for 24 h to evaporate the FA. Progressive washing with a distilled water bath was used in the resulting material to remove the $CaCl_2$. The next step was drying overnight at room temperature. In a last step, SF was dissolved in FA in a 10:1 v/w FA:SF ratio to obtain an SF/FA solution suitable for further sample processing.

2.3. Sample Preparation. Different processing techniques and corresponding post-treatments were used to obtain different SF-based structures with tailored architectures and physicochemical properties.

2.3.1. Film Preparation. The SF/FA solution was homogeneously dissolved using a magnetic stirrer. Subsequently, the solution was placed in a Petri dish, which was left at room temperature for 24 h to remove the solvent. The obtained films had a thickness of ~40/60 μm.

2.3.2. Porous Membrane Preparation. The salt-leaching method was used to prepare the porous membranes (PM). Sifted NaCl particles with an average diameter of ~90 μm were added in a 10:3 w/w (SF/salt) ratio to the previously prepared SF/FA solution. Energetic stirring was used for 1 h to obtain a homogeneous mixture containing dispersed NaCl and dissolved SF. The resulting solution was poured over glass Petri dishes, placed in an airing chamber at room temperature, and dried until complete solvent evaporation. NaCl was then removed from the SF/NaCl samples by washing in a distilled water bath at room temperature. Several water changes were applied until the solution showed constant values of electrical conductivity, indicative that NaCl was completely eliminated. The obtained PM were finally dried for 24 h in an airing chamber.

2.3.3. Electrospun Randomly Oriented and Oriented Fiber Mats. The SF solution was collected in a 10 mL single-use syringe and placed in a syringe pump (New Era NE-1000) at a 0.5 mL h^{-1} flow rate. A blunt steel needle was placed in the syringe, which had an inner diameter of 500 μm, and electrospinning was performed at 15 kV with a high voltage power supply (Glassman PS/FC30P04). A grounded 20 × 15 cm rotating drum collector at a speed of 120 rpm was used to obtain the resulting SF electrospun randomly oriented (ES-NO) membranes. The collector was placed 15 cm from the needle. To obtain electrospun oriented (ES-O) membranes, a grounded rotating drum collector was used rotating at 1500 rpm.

2.4. Sample Characterization. *2.4.1. Physicochemical Characterization.* Cross-section and surface images of the silk fibroin membranes were obtained by scanning electron microscopy (SEM) using a JEOL JSM-7000F instrument. The images were also used to evaluate the average pore size and fiber diameter distributions by image analysis (ImageJ software).[21]

Sample porosity was obtained with a pycnometer by the liquid displacement method. The pycnometer was filled with ethanol, weighed, and labeled as W_1. The sample with a weight labeled W_s was immersed in the ethanol, and after the sample was saturated, the volume of the pycnometer was filled by adding additional ethanol. The system was then weighed and labeled as W_2. The sample was finally taken out of the pycnometer; the weight of the system with ethanol was labeled W_3, and the porosity of the sample was calculated as the average of three values using eq 1:[22]

$$\varepsilon = \frac{W_2 - W_3 - W_s}{W_1 - W_3} \quad (1)$$

Ethanol was used as the displacement liquid as it is a nonsolvent for SF membranes, and it can penetrate the pores without inducing sample degradation, shrinking, or swelling. The values of the porosity for the different samples were calculated as the average ± standard deviation of 5 replicates of each type of sample.

A Data Physics OCA20 instrument was used to perform the water contact angle assays with ultrapure water, following the static sessile drop method. A water drop was placed on the surface of the sample, and the contact angle was measured with SCA20 software. The average contact angle and the corresponding standard deviation were obtained after measuring at six different positions for each sample and for three different samples.

For porosity and contact angle assays, the statistical analysis was performed using GraphPad by Dotmatics, and the results were analyzed statistically using the t test. Differences are considered statistically significant when the p-value < 0.05.

Stress–strain mechanical measurements in the tensile mode were performed. A Shimadzu AD-IS universal testing system with a load cell of 50 N was used for the assays at a stretching rate of 1 mm min^{-1} in samples cut in 15 mm long and 10 mm wide rectangles. Average sample thicknesses for the films, PM, ES-NO membranes, and ES-O membranes samples were ~106.3, ~274.7, ~103, and ~110 μm, respectively, measured using a Fischer Dualscope MPOR instrument. ES-O SF membranes were stretched along and at an angle of 90° regarding the direction of the fibers [ES-O (90°)]. The measurements of each membrane were performed in triplicate.

Infrared measurements (FTIR) were carried out with an Agilent 4300 apparatus (from 4000 to 650 cm^{-1}, after 64 scans with a resolution of 4 cm^{-1}) in the attenuated total reflectance mode (ATR).

The deconvolution of the FTIR spectral region corresponding to amide I was performed with OriginPro 8.1 software (OriginLab, Northampton, MA), to obtain the relative content of the secondary

https://doi.org/10.1021/acs.biomac.2c01124
Biomacromolecules 2023, 24, 1121−1130

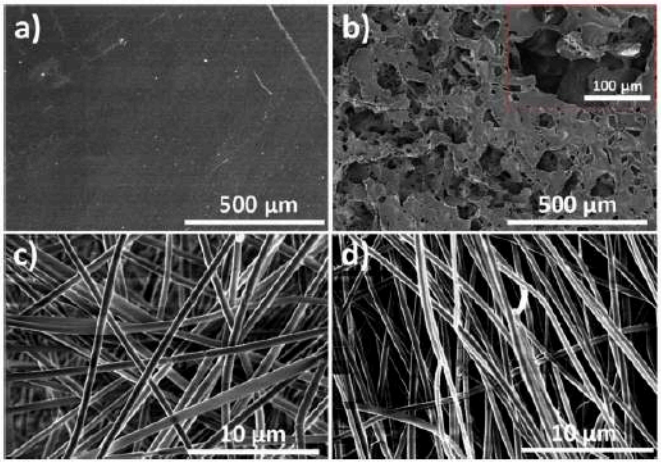

Figure 1. SEM images of the silk fibroin membranes: (a) film, (b) porous membrane (inset: magnification of a pore microstructure), (c) electrospun randomly oriented fibers (ES-NO), and (d) electrospun oriented fibers (ES-O).

structures present in each sample. This region was fitted by a linear baseline correction and 15 points with the Savitzky–Golay method.[23] The number of components and peak positions identified by the second derivative were the starting parameters for curve fitting iteratively (R^2 > 0.999) with a Gaussian function using the Levenberg–Marquardt algorithm.[23] Curve fitting was carried out based on the same set of parameters for all samples in order to achieve comparable secondary structure assignment. The contribution of each component to the amide I band was obtained from the relative area of the bands by integrating the area and normalizing to the total area of amide I.

Differential scanning calorimetry (DSC) studies were carried out in a Mettler Toledo DSC822e setup at a heating rate of 10 °C min^{-1}. Small pieces of the samples were cut and placed into 40 μL aluminum pans.

2.4.2. Cytotoxicity Assay. Indirect cytotoxicity of the different SF samples was evaluated using the ISO 10993-5 standard method. Samples were first cut into 1.5 cm^2 pieces and sterilized under ultraviolet (UV) illumination for 1 h on both sides. Samples were then washed with sterile phosphate-buffered saline solution (PBS, pH 7.4) and incubated for 24 h in DMEM in a 24-well tissue culture plate.

Simultaneously, L929 adipose cells were cultured at 37 °C with 5% CO_2 using Dulbecco's modified Eagle's medium (DMEM, Biochrom), containing 4.5 g L^{-1} glucose, 10% fetal bovine serum (FBS, Biochrom), and 1% (v/v) penicillin/streptomycin solution (P/S, Biochrom), seeded in a 96-well tissue culture plate (5 × 104 cell mL^{-1}), and were incubated for 24 h to ensure the cell attachment. The cell culture medium was then removed and replaced with 100 μL of the culture medium in which materials were incubated. As negative and positive controls, fresh DMEM and dimethyl sulfoxide (DMSO) at 20% were used, respectively. Subsequently, cells in the 96-well culture plate were incubated for 72 h, after which (3-(4,5-dimethylthiazol-2-yl)-5-(3-carboxymethoxyphenyl)-2-(4-sulfophenyl)-2*H*-tetrazolium) (MTS, Promega) was used to quantify the cell metabolic activity of the cells in each well. Briefly, the cell culture medium was removed; new medium with the MTS solution (in a 1:5 ratio) was added, and it was incubated for 2 h. Then, a spectrophotometric plate reader (Biotech Synergy HT) at 490 nm was allowed to obtain the optical density. Cell viability was obtained according to eq 2[24] and was presented as the average and standard deviation of four replicates.

$$\text{cell viability (\%)} = \frac{\text{absorbance of sample}}{\text{negative control absorbance}} \times 100 \quad (2)$$

2.4.3. Degradation Assays. The degradation of the SF samples was obtained by measuring the weight loss in PBS at pH 7.4. Samples were cut in 1 cm^2 and placed in 12-well tissue culture polystyrene plates, which were in contact with air or immersed in 3 mL of PBS at 37 °C. The variations of pH and ion concentration were avoided by exchanging the PBS weekly. Each sample was weighted using a Sartorius Cubis II Micro Lab balance and compared with the initial weight at weeks 1, 2, and 4. For this purpose, at the different time points, the samples were washed with distilled water and placed in an oven (JP Selecta, model 2000208) at 37 °C for 6 h for drying prior to weighing.

2.5. Cell Culture Assays. *In vitro* assays were carried out in circular SF samples (films, PM, ES-NO, and ES-O) with a diameter of 13 mm. The samples were sterilized by washing 5 times in PBS 1× solution for 5 min each and then by exposing to UV light for 2 h (1 h each side). Finally, the samples were placed in 24-well cell culture plates.

HUVECs (human umbilical vein endothelial cells) were grown in a 75 cm^2 cell-culture flask and cultured with endothelial cell growth medium (Pan Biotech). Incubation took place at 37 °C in humidified air containing a 5% CO_2 atmosphere. The cell culture medium was changed every 2 days, and cells were detached with Accutase (GRisp) when they reached 80–90% confluence.

For cell proliferation assays, HUVECs were seeded on the samples at a density of 7500 cells cm^{-2}. The drop method was used in order to allow cell attachment to the different samples. The plates containing the cells seeded on the samples were incubated at 37 °C in a saturated humidity atmosphere (95% air and 5% CO_2). The samples were analyzed by cell viability at specific times.

The evaluation of the cell viability of HUVECs on the developed materials was analyzed by the MTS assay, carried out after 1 and 4 days. At these times, the cell/films were transferred to new wells, and new medium containing MTS solution (1:5 proportion) was added. The plate was incubated at 37 °C for 3 h, and the absorbance was measured at 490 nm (Biotech Synergy HT, microplate reader). The experimental data were obtained from four replicates for each sample and are provided as mean ± standard deviation. All data were analyzed with GraphPad by Dotmatics and statistically analyzed using the *t* test. Differences were considered statistically significant when the *p*-value < 0.05.

3. RESULTS AND DISCUSSION

3.1. Physicochemical Characterization. The morphology of the SF membranes was determined by SEM imaging

https://doi.org/10.1021/acs.biomac.2c01124
Biomacromolecules 2023, 24, 1121−1130

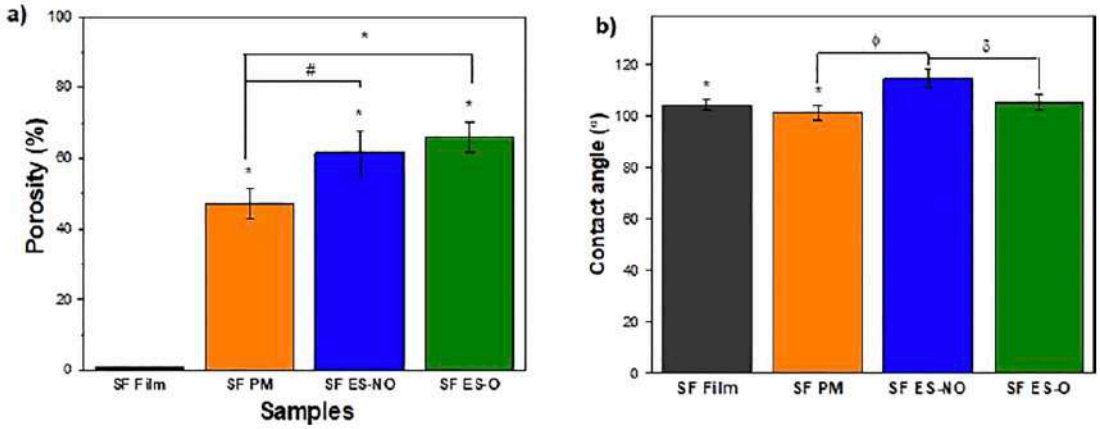

Figure 2. (a) Porosity of the silk fibroin (SF) films, porous membranes (PM), randomly oriented electrospun membranes (ES-NO), and oriented electrospun membranes (ES-O). Data are expressed as the mean ± standard deviation with $n = 5$. $^{*}p < 0.0001$ vs SF film, $^{\#}p < 0.003$, and $^{*}p < 0.0001$. (b) Respective contact angle. Data are expressed as the mean ± standard deviation with $n = 6$. $^{*}p < 0.0001$ vs SF ES-NO, $^{\phi}p < 0.05$, and $^{\delta}p < 0.0004$.

(Figure 1). Bulk films prepared using the solvent casting method showed a compact and smooth surface with no apparent fractures or voids (Figure 1a). This specific morphology is attributable to the solvent evaporation conditions during the processing of the films. In order to ensure slow solvent evaporation and, therefore, avoid Marangoni instabilities, the solution used for the preparation of the SF films should have a high solvent content, and the solvent should be evaporated at room temperature,[25] as rapid solvent evaporation leads to the development of Marangoni instabilities, which results in a rougher air surface of the film.[26]

The salt-leaching method was used to manufacture porous SF membranes. For that, NaCl particles were added to the SF mixture, resulting in porous scaffolds with an approximate pore size of 90 μm (Figure 1b and corresponding magnification in the inset). It is worth noting that the salt-leaching method provides a means to control the pore size of the membranes by varying the size of the NaCl particles. Nevertheless, structures with a network of regular interconnected pores are difficult to obtain with this methodology due the variations in the dispersion of the NaCl particles. In addition, this technique results in irregular and nonreproducible morphologies.[27,28]

Finally, fiber-based SF membranes were produced by electrospinning. ES-NO and ES-O membranes present a smooth fiber surface, as well as cylindrical random and oriented fibers (Figure 1c,d). Topographical characterization reveals an average fiber diameter of 467 ± 45 and 448.1 ± 37 nm for ES-NO and ES-O, respectively. The difference in fiber size between ES-NO and ES-O is caused by the stretching during their collection in the rotating drum.[22,29]

The degree of porosity is above 45% in all samples, independently of the processing method and sample morphology, except for the compact films (Figure 2a). The degree of porosity of porous, ES-NO, and ES-O membranes was 47.2 ± 4.11, 61.7 ± 6.18, and 66.1 ± 4.29%, respectively. The lower porosity values of the ES-NO samples with respect to the oriented ones can be explained by the tighter packing of the randomly distributed fibers (Figure 1).[30] Note that porosity, morphology, and fiber diameter can be further tuned depending on the specific processing parameters, methodology, and natural variations of silk fibroin.[27,30−32]

The wettability of the samples was determined by water contact angle assays. SF is a natural polymer whose surface wettability varies depending on the topography, surface chemistry, and surface energy.[33] Furthermore, surface wettability is an essential parameter for cell adhesion and proliferation.[34,35] Surfaces are considered hydrophobic when the water contact angle is above 90° and hydrophilic if the contact angle is below that value.[36]

The obtained water contact angle values were around 105° in SF membranes (Figure 2b). However, scaffold structuring had some impact on surface wettability. Films and porous, ES-NO, and ES-O membranes showed an average contact angle value of 104.58 ± 1.94, 101.45 ± 2.92, 114.87 ± 3.34, and 105.52 ± 2.77°, respectively. The SF PM presented a slightly lower contact angle value than the other SF constructs due to their relatively large pore size, which allows liquid percolation into the pores. On the other hand, electrospun membranes, in particular ES-NO membranes, display higher surface roughness than films, which is a parameter that strongly affects surface wettability.[37] Nevertheless, variations in terms of compactness, composition, and crystallinity, as well as surface roughness, are factors that explain the variations in wettability, once surface chemistry is the same for all developed structures.[22,37]

The mechanical properties of SF membranes are a key parameter to be considered in order to obtain safe and durable biomedical components. Consequently, stress−strain measurements were performed in all SF samples. The mechanical characteristics of the developed samples are mainly determined by their morphology and internal structure. In general, the characteristic stress−strain mechanical curves of SF feature a linear elastic regime followed by a plastic regime after yielding.[38] Materials can show a behavior with differentiated elastic and plastic zones, or present little or no plastic deformation, and are named ductile and brittle materials, respectively. The Young's modulus was calculated by applying Hooke's law in the linear regime of the curves.[39]

The prepared SF scaffolds presented different stress−strain mechanical responses depending on their morphology (Figure

https://doi.org/10.1021/acs.biomac.2c01124
Biomacromolecules 2023, 24, 1121−1130

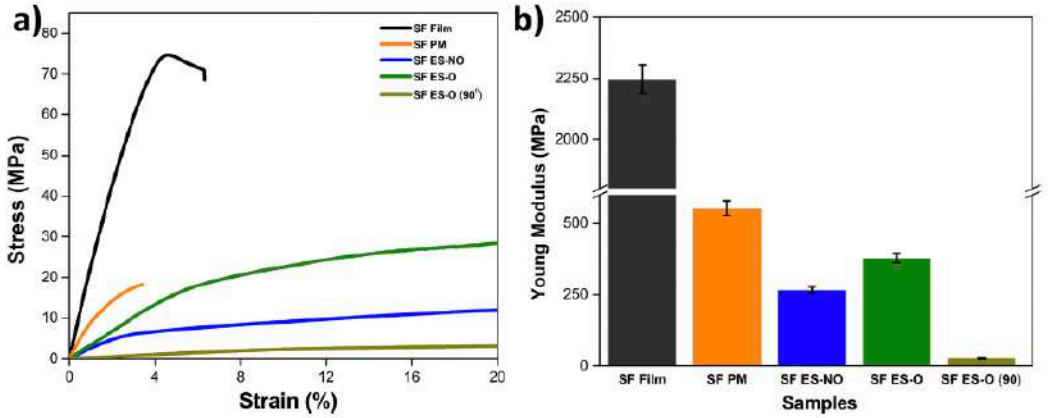

Figure 3. (a) Stress−strain mechanical curves up to 20% of strain. (b) Young's moduli mean value and standard deviation for silk fibroin (SF) film, porous membrane (PM), randomly oriented electrospun membranes (ES-NO), oriented electrospun membranes (ES-O), and 90° ES-O.

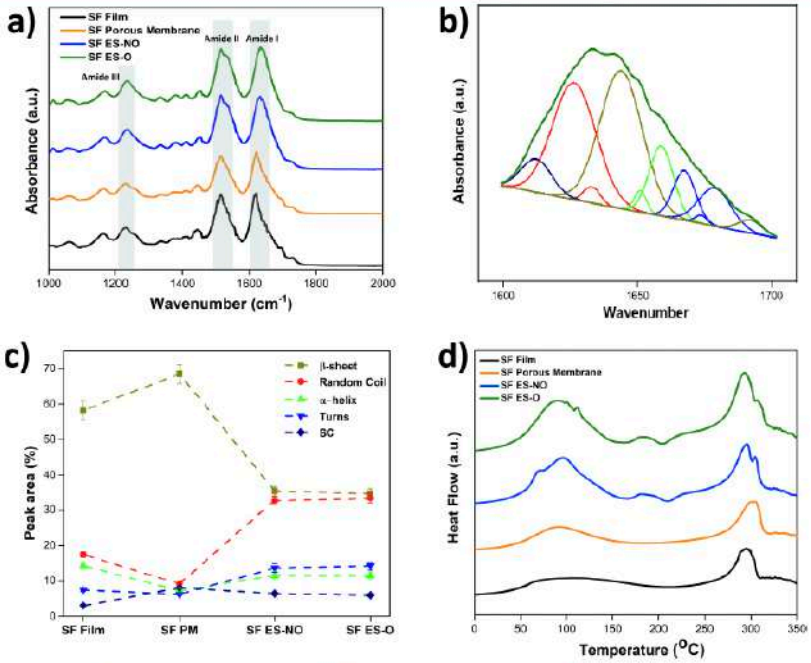

Figure 4. (a) Representative FTIR spectra of the silk fibroin (SF) film, porous membrane (PM), electrospun randomly oriented membranes (ES-NO), and electrospun oriented membranes (ES-O). (b) Representative amide I deconvolution spectrum for electrospun oriented membranes (ES-O). (c) Area fraction of the distinct components resolved in this spectral region. β-sheet (green olive), random coils (red), α-helix (light green), turns (blue), and side chains SC (navy blue) are the various contributions to the amide I structure. (d) Representative DSC thermograms of the silk fibroin (SF) film, porous membrane (PM), electrospun randomly oriented membranes (ES-NO), and electrospun oriented membranes (ES-O).

3). Further, there were relevant differences in their Young's moduli. The films feature the highest Young's modulus of 2246.71 ± 58.32 MPa, followed by PM with 553 ± 26.17 MPa. The Young's modulus value in SF films is determined by the intrinsic characteristics of the material due to their compact morphology. Films showed an initial elastic deformation followed by a very short plastic deformation until the final rupture, while SF PM did not show plastic deformation. In other words, films and PM feature stress−strain curves typical of brittle materials due to the ternary configuration of SF structures. This material mainly consists of nonordered amorphous regions (random coils), and a hydrogen-bond network of β-structured crystallites (β-sheets). Random coils provide flexibility and are responsible for the elasticity, while β-

https://doi.org/10.1021/acs.biomac.2c01124
Biomacromolecules 2023, 24, 1121−1130

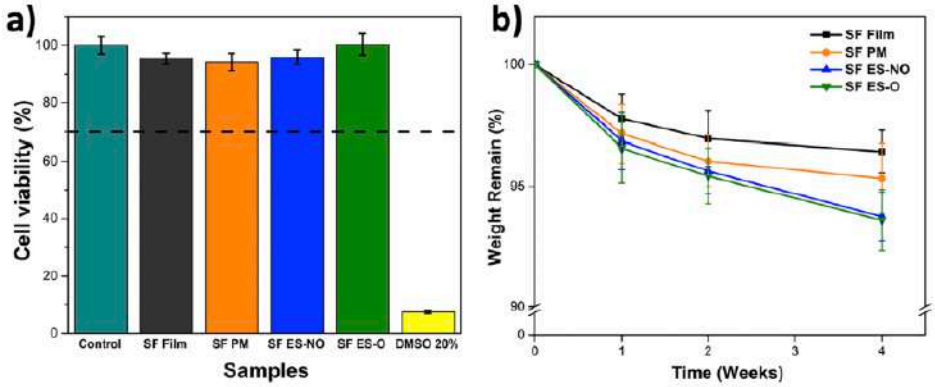

Figure 5. (a) Cytotoxicity of SF-based materials, silk fibroin (SF) film, porous membrane (PM), electrospun randomly oriented membranes (ES-NO), and electrospun oriented membranes (ES-O), determined by extraction with culture media, negative control, and positive control [dimethyl sulfoxide (DMSO) at 20%]. L929 cells were incubated with the media for 72 h, after which the relative metabolic activity was measured ($n = 4 \pm$ standard deviation). (b) Degradation assay of SF films, PM, and ES-NO at 1, 2, and 4 weeks.

sheets are related to the strength and rigidity of the material.[40] Slow evaporation of the solvent was used during sample preparation in order to improve polymer chain organization, which results in a highly crystallized structure.[41] Consequently, SF structures with high β-sheet and low random coil content were the result of the solvent casting process.[25] Therefore, the accumulated structural force is maintained by the random coils at the beginning of the deformation, which causes the entangled chains to unwind, and results in the elastic regime of the films and PM. Since the amorphous regions are completely unfolded, β-sheet nodes support the deformation and endure the stress until their breakage.[25]

On the other hand, electrospun membranes feature the lowest Young's moduli when compared with films and PM. For the electrospun samples, the highest value of the effective Young's modulus, 378.49 ± 17.23 MPa, was obtained for the electrospun membranes when stretched along the fiber direction [ES-O (0°)], and the lowest for the ES-O samples when deformed perpendicular to the fiber orientation (90°), which presented Young's modulus values of 26.71 ± 1.88 MPa. On the other hand, ES-NO samples present an intermediate Young modulus of 265.63 ± 12.11 MPa independently of the deformation direction.

In fact, it has been shown that the elastic modulus of electrospun membranes strongly depends on the relative orientation between the fibers and the stretching direction, which decreases when the angle between fiber orientation and strain direction increases.[42−45] This is due to fiber reorientation and pore collapse as fibers are constricted in the direction of the applied stress.[44] All electrospun SF membranes are characterized by stress−strain curves typical of a ductile material. This mechanical behavior can be explained by the variation of the structure of the sample (compaction) before fiber deformation. The SF electrospun membranes are characterized by an increase in random structures and a decrease in β-sheets due to the fast solvent evaporation rates during the electrospinning process.[25] In the same way, results showed that yield strain and stress of ES-O (0°) are larger than those of ES-NO and ES-O (90°), as the force is applied along the fibers in the case of ES-O (0°), while in ES-NO and ES-O (90°), the applied stress initial effect is the reorientation of the fibers along the stretching direction.[43] The electrospinning technology causes the SF to have a ductile behavior, increasing its plastic regime. It is also worth noting that SF exhibits superior mechanical properties when compared to other natural materials, such as elastin, resilin, or wool, among others.[2,46]

FTIR spectra (Figure 4a) of different SF membranes showed no relevant differences among them, indicating that the processing methods did not induce chemical changes in SF. Amide I (which corresponds to C=O stretching) and II (N—H in-plane bending) bands with peaks at 1645 and 1537 cm^{-1} are evidenced in the spectra of all samples. The bands identifying amide III (—N and N—H functionalities) at around 1235 cm^{-1} are less apparent in ES-O and ES-NO SF morphologies, which might be related to variations of the secondary structure or to an increase of the proportion of random coils to β-sheet conformations.[21] This change can be attributed to the slower process of solvent evaporation during the casting process of SF films and PM, which results in improved polymer chain organization and as a consequence the formation of a highly crystallized structure.[25]

The secondary structure of SF was studied trough an analysis of the amide I region at 1700−1580 cm^{-1}. This region corresponds to the most prominent vibrational bands of the protein backbone, being related with the C=O stretching vibration, CCN deformation, out of phase CN stretching vibration, and NH in-plane bending.[47] The amide I deconvolution was applied to determine the relative amount of secondary structures, by fitting (hidden) peaks from the original spectra (Figure 4b, as an example). The disclosed structures are β-sheets (1703−1697 and 1628−1615 cm^{-1}), random coils (1655−1628 cm^{-1}), α-helices (1662−1656 cm^{-1}), turns (1696−1663 cm^{-1}), and side chains (1615−1605 cm^{-1}).[48,49] Hidden bands corresponding to the five structures appear in all samples after peak fitting (Figure 4c).

β-sheet conformation is the most abundant in all morphologies, comprising more than 60% of the total amide I peak area in films and PM and nearly 35% in ES-O and ES-NO. As indicated before, this demonstrated that the differences in the rate of the solvent evaporation process play an essential role in the crystalline conformation of the different morphologies. The formic acid used as solvent for the preparation of the different samples leads to strong interactions

https://doi.org/10.1021/acs.biomac.2c01124
Biomacromolecules 2023, 24, 1121−1130

with SF due to its polar character. Thus, SF self-interactions are weakened, and therefore, the SF secondary structure unpacks to random coils. Further, the removal of formic acid induces the crystallization into β-sheets.[49]

As expected, the random coil conformation presents an inverse behavior regarding the presence of β-sheets, being less represented in the PM ~9.15% and increasing in the O-ES ~33.52%.[49]

Regarding the slight differences in β-sheet conformation between SF films and PM, the presence of salt leads to an increase in the β-sheet content with respect to the SF films, which is ascribed to the interaction of the salt with SF, due to the ionic character of the former.[50]

Figure 4d shows the DSC thermograms of the different samples in the range from 0 to 350 °C. Since no preheating was carried out, the firsts endothermic peaks around 85 °C are due to the solvent that remains trapped within the membrane structures. SF ES-NO and ES-O are characterized by an endothermic peak around 280 °C due to the degradation of the crystalline SF structures, in particular the side chains group amino acid residues and the cleavage of peptide bonds.[22,25] SF Films also present an endothermic peak near 280 °C, proving that the physical structure does not significantly affect the thermal properties of the material.[51] On the other hand, the SF PM display an endothermic peak around 300 °C (an increase of 20 °C compared with the other samples), which is attributed to the formation of β-sheet conformations during the continuous diffusion process of the salt particles in ultrapure water.

3.2. Degradation Assays. To test whether SF material architecture affects the material degradation rate, the mass loss was analyzed over time when incubated in PBS at 37 °C. The results show that SF in the form of electrospun fiber membranes has a higher rate of degradation than SF films and SF PM. Furthermore, SF films have a lower rate of degradation than SF PM (Figure 5b). The greater or lesser weight loss of the different samples strongly depends on their surface area, related to the morphology and microstructure. Electrospun SF membranes consist of porous structures composed of fibers with large surface areas. On the other hand, SF films display no porosity, with PBS therefore just contacting the external part of the sample, which ultimately results in a slower degradation. Finally, SF PM represent an intermediate situation. Additionally, previous studies have demonstrated that the degradation rate increases when the contact angle decreases.[52,53]

Although degradation varies among the membranes, results show a degradation of approximately 5% after 4 weeks in all structures. Research on rats implanted with SF scaffolds demonstrated their complete degradation after one year.[54] The degradation time of the SF-based structured materials in vivo is difficult to predict, as it varies depending on the scaffold architecture, implantation site, and the type and concentration of enzymes.[47]

3.3. Cytotoxicity Assessment. Low cytotoxicity is key for the applicability of materials in TE.[55] For this reason, L929 cells derived from adipose tissue were used to determine the effect of SF-based materials on cell survival (Figure 5a). In the scope of the ISO standard 10993-5, if the values of cell viability are higher than 70%, the material is considered to be noncytotoxic. It is shown that, independently of their architecture, in indirect contact, all studied materials displayed cell viability values close to 100%. This result is consistent with previous studies that proved the good biocompatibility of SF-based materials.[47]

3.4. Cell Proliferation. The cell proliferation of HUVECs on the different SF samples was evaluated through MTS assay (Figure 6).

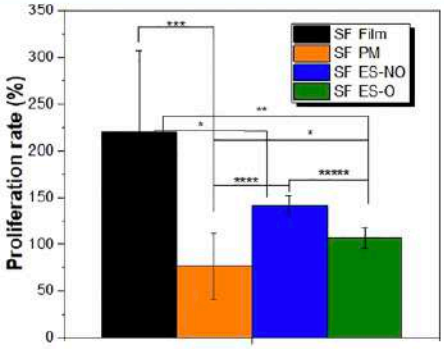

Figure 6. Proliferation rate determined by the MTS assay on HUVECs seeded on the SF samples after 4 days. The proliferation rate was calculated regarding the cells growing on the material after 24 h of cell adhesion. Results are reported as mean ± standard deviation with $n = 4$. *$p < 0.05$, **$p < 0.003$, ***$p \leq 0.0007$, ****$p \leq 0.0002$ and *****$p \leq 0.0001$.

HUVECs proliferate when cultured on all of the different samples, with the higher proliferation observed on SF films and the lowest on the SF PM. Since the wettability of all of the SF samples is similar, the difference observed can be assigned to the surface topography. Regarding electrospun fibers, HUVECs proliferate faster on randomly distributed ones as compared to on the oriented ones. Previous studies with a terpolymer based on hexyl methacrylate (HMA), methyl methacrylate (MMA), and methacrylic acid (MAA) demonstrated that electrospun membranes can significantly improve the proliferation of endothelial cells, especially the samples with a random fiber distribution.[56]

These findings show the response of HUVECs on different SF topographies, which is suitable for the design of vascular implants.

4. CONCLUSIONS

Silk fibroin is a biocompatible natural protein with excellent mechanical properties and low immunogenicity in humans, and is consequently widely used for TE applications. However, depending on the processing methods used for the preparation of SF scaffolds and on the resulting architecture, the material displays different physicochemical and biological properties. In the present work, SF films, PM, and electrospun membranes were designed, produced, and subjected to physicochemical characterization, cytotoxicity estimation, and degradation analysis. Films and PM are characterized by high β-sheet and low random coil content due to the slow evaporation of the solvent, presenting stress−strain curves of brittle materials. In scaffolds generated by electrospinning, an increase in random structures and a decrease in β-sheets of SF were observed, resulting in a stress−strain mechanical response typical of ductile materials. Independently of the processing method and sample morphology, there were no relevant chemical differences among them, with the observed amide I (C═O

https://doi.org/10.1021/acs.biomac.2c01124
Biomacromolecules 2023, 24, 1121−1130

stretching), II (N—H in-plane bending), and III (—N and N—H functionalities) bands. On the other hand, SF electrospun membranes and films showed similar endothermic peaks around 280 °C, proving that the physical structure does not significantly affect the thermal properties of the material. However, SF PM showed a slightly higher endothermic peak around 300 °C, likely due to an increased formation of β-sheet conformations during the diffusion process of the salt particles in ultrapure water. In relation to surface wettability, all SF membranes presented a hydrophobic behavior, as electrospun membranes are slightly more hydrophobic probably due to their surface roughness. Cytotoxicity and degradation rate are key factors to determine the applicability of materials intended for tissue engineering. All SF scaffolds showed low cytotoxicity regardless of their architecture, demonstrating that SF is well suited for TE applications. Finally, degradation rate depends on the design and morphology of the SF structure. With respect to cell proliferation, all of the produced SF samples promote the HUVECs proliferation, which is higher on the films and randomly oriented electrospun membranes. The results confirm that SF is a suitable candidate to be explored for cardiovascular applications, based on its intrinsic characteristics and the possible morphological variations.

AUTHOR INFORMATION

Corresponding Author

Francisco M. Sánchez-Margallo – *Jesús Usón Minimally Invasive Surgery Centre, Cáceres 10004, Spain; Centro de Investigación Biomédica en Red de Enfermedades Cardiovasculares (CIBERCV) and RICORS-TERAV Network, Instituto de Salud Carlos III, Madrid 28029, Spain*; Email: msanchez@ccmijesususon.com

Authors

David Durán-Rey – *Jesús Usón Minimally Invasive Surgery Centre, Cáceres 10004, Spain*; orcid.org/0000-0002-2106-3524

Ricardo Brito-Pereira – *CMEMS-UMinho, University of Minho, 4800-058 Guimarães, Portugal; LABBELS-Associate Laboratory, 4710-057 Braga/Guimarães, Portugal; CF—UM-UP—Physics Centre of Minho and Porto Universities and LaPMET—Laboratory of Physics for Materials and Emergent Technologies, University of Minho, 4710-057 Braga, Portugal; IB-S, Institute of Science and Innovation for Bio-Sustainability, Universidade do Minho, 4710-057 Braga, Portugal*

Clarisse Ribeiro – *CF—UM-UP—Physics Centre of Minho and Porto Universities and LaPMET—Laboratory of Physics for Materials and Emergent Technologies, University of Minho, 4710-057 Braga, Portugal*; orcid.org/0000-0002-9120-4847

Sylvie Ribeiro – *CF—UM-UP—Physics Centre of Minho and Porto Universities and LaPMET—Laboratory of Physics for Materials and Emergent Technologies, University of Minho, 4710-057 Braga, Portugal*

Juan A. Sánchez-Margallo – *Jesús Usón Minimally Invasive Surgery Centre, Cáceres 10004, Spain; RICORS-TERAV Network, Instituto de Salud Carlos III, Madrid 28029, Spain*

Verónica Crisóstomo – *Jesús Usón Minimally Invasive Surgery Centre, Cáceres 10004, Spain; Centro de Investigación Biomédica en Red de Enfermedades Cardiovasculares (CIBERCV) and RICORS-TERAV Network, Instituto de Salud Carlos III, Madrid 28029, Spain*

Igor Irastorza – *CF—UM-UP—Physics Centre of Minho and Porto Universities and LaPMET—Laboratory of Physics for Materials and Emergent Technologies, University of Minho, 4710-057 Braga, Portugal; Cell Biology and Histology Department, Faculty of Medicine, Leioa 48940, Spain*

Unai Silván – *BCMaterials, Basque Center for Materials, Applications and Nanostructures, Leioa 48940, Spain; Ikerbasque, Basque Foundation for Science, Bilbao 48009, Spain*

Senentxu Lanceros-Méndez – *CF—UM-UP—Physics Centre of Minho and Porto Universities and LaPMET—Laboratory of Physics for Materials and Emergent Technologies, University of Minho, 4710-057 Braga, Portugal; BCMaterials, Basque Center for Materials, Applications and Nanostructures, Leioa 48940, Spain; Ikerbasque, Basque Foundation for Science, Bilbao 48009, Spain*; orcid.org/0000-0001-6791-7620

Complete contact information is available at: https://pubs.acs.org/10.1021/acs.biomac.2c01124

Author Contributions

D.D.-R., R.B.-P.: Conceptualization, Writing—Original Draft, and Methodology. C.R., S.R., I.I., U.S.: Writing—Cell culture assays. D.D.-R., R.B.-P., C.R., S.R., J.A.S.-M.: Investigation, Formal analysis. V.C., U.S., S.L.-M., F.M.S.-M.: Writing—Review and Editing. S.L.-M., F.M.S.-M.: Supervision and Funding acquisition. The manuscript was written through contributions of all authors. All authors have given approval to the final version of the manuscript.

Funding

Work has been partially funded by the Junta de Extremadura (Spain), the Spanish Ministry of Science and Innovation, the European Social Fund, the European Regional Development Fund, and the European Next Generation Funds (Grant Numbers PD18077, TA18023, and GR21201). The authors thank the Portuguese Foundation for Science and Technology (FCT) for financial support under grants SFRH/BD/140698/2018 (R.B.-P.) and 2020.04163.CEECIND (C.R.). The authors acknowledge funding by Spanish State Research Agency (AEI) and the European Regional Development Fund (ERFD) through the project PID2019-106099RB-C43/AEI/10.13039/501100011033 and from the Basque Government Industry and Education Departments under the ELKARTEK and PIBA programs, respectively. None of these funding sources had any further role in the study design; in the collection, analysis, and interpretation of data; in the writing of the report; or in the decision to submit.

Notes

The authors declare no competing financial interest.

REFERENCES

(1) Motamedi, A. S.; Mirzadeh, H.; Hajiesmaeilbaigi, F.; Bagheri-Khoulenjani, S.; Shokrgozar, M. A. Piezoelectric electrospun nanocomposite comprising Au NPs/PVDF for nerve tissue engineering. *J. Biomed. Mater. Res., Part A* **2017**, *105*, 1984−1993.

(2) Sun, W.; Gregory, D. A.; Tomeh, M. A.; Zhao, X. Silk Fibroin as a Functional Biomaterial for Tissue Engineering. *Int. J. Mol. Sci.* **2021**, *22*, 1499.

(3) Durán-Rey, D.; Crisóstomo, V.; Sánchez-Margallo, J. A.; Sánchez-Margallo, F. M. Systematic Review of Tissue-Engineered Vascular Grafts. *Front. Bioeng. Biotechnol.* **2021**, *9*, 771400.

(4) Ong, C. S.; Zhou, X.; Huang, C. Y.; Fukunishi, T.; Zhang, H.; Hibino, N. Tissue Engineered Vascular Grafts: Current State of the Field. *Expert Rev. Med. Devices* **2017**, *14*, 383−392.
(5) Alessandrino, A.; Chiarini, A.; Biagiotti, M.; Dal Prà, I.; Bassani, G. A.; Vincoli, V.; Settembrini, P.; Pierimarchi, P.; Freddi, G.; Armato, U. Three-Layered Silk Fibroin Tubular Scaffold for the Repair and Regeneration of Small Caliber Blood Vessels: From Design to In Vivo Pilot Tests. *Front. Bioeng. Biotechnol.* 2019, *7*, 356.
(6) Jin, X.; Geng, X.; Jia, L.; Xu, Z.; Ye, L.; Gu, Y.; Zhang, A. Y.; Feng, Z. G. Preparation of Small-Diameter Tissue-Engineered Vascular Grafts Electrospun from Heparin End-Capped PCL and Evaluation in a Rabbit Carotid Artery Replacement Model. *Macromol. Biosci.* **2019**, *19*, No. e1900114.
(7) Wen, D. L.; Sun, D. H.; Huang, P.; Huang, W.; Su, M.; Wang, Y.; Han, M. D.; Kim, B.; Brugger, J.; Zhang, H. X.; Zhang, X. S. Recent progress in silk fibroin-based flexible electronics. *Microsyst. Nanoeng.* **2021**, *7*, 35.
(8) Lotz, B.; Cesari, F. C. The chemical structure and the crystalline structures of Bombyx mori silk fibroin. *Biochimie* 1979, *61*, 205−214.
(9) Fukada, E. Piezoelectric properties of organic polymers. *Ann. N.Y. Acad. Sci.* **1974**, *238*, 7−25.
(10) Fukada, E. Piezoelectricity of biopolymers. *Biorheology* **1995**, *32*, 593−609.
(11) Sencadas, V.; Garvey, C.; Mudie, S.; Kirkensgaard, J. J. K.; Gouadec, G.; Hauser, S. Electroactive properties of electrospun silk fibroin for energy harvesting applications. *Nano Energy* **2019**, *66*, 104106.
(12) Liu, Z.; Wan, X.; Wang, Z. L.; Li, L. Electroactive Biomaterials and Systems for Cell Fate Determination and Tissue Regeneration: Design and Applications. *Adv. Mater.* **2021**, *33*, 2007429.
(13) Petty, A. J.; Keate, R. L.; Jiang, B.; Ameer, G. A.; Rivnay, J. Conducting Polymers for Tissue Regeneration in Vivo. *Chem. Mater.* **2020**, *32*, 4095−4115.
(14) Zhang, X.; Reagan, M. R.; Kaplan, D. L. Electrospun silk biomaterial scaffolds for regenerative medicine. *Adv. Drug Delivery Rev.* **2009**, *61*, 988−1006.
(15) Ribeiro, C.; Sencadas, V.; Correia, D. M.; Lanceros-Méndez, S. Piezoelectric polymers as biomaterials for tissue engineering applications. *Colloids Surf., B* **2015**, *136*, 46−55.
(16) Chen, Y.; Ye, L.; Guan, L.; Fan, P.; Liu, R.; Liu, H.; Chen, J.; Zhu, Y.; Wei, X.; Liu, Y.; Bai, H. Physiological electric field works via the VEGF receptor to stimulate neovessel formation of vascular endothelial cells in a 3D environment. *Biol. Open* **2018**, *7*, bio035204.
(17) Bai, H.; Forrester, J. V.; Zhao, M. DC electric stimulation upregulates angiogenic factors in endothelial cells through activation of VEGF receptors. *Cytokine* **2011**, *55*, 110−115.
(18) Mohana Sundaram, P.; Rangharajan, K. K.; Akbari, E.; Hadick, T. J.; Song, J. W.; Prakash, S. Direct current electric field regulates endothelial permeability under physiologically relevant fluid forces in a microfluidic vessel bifurcation model. *Lab Chip* **2021**, *21*, 319−330.
(19) Alessandrino, A.; Chiarini, A.; Biagiotti, M.; Dal Prà, I.; Bassani, G. A.; Vincoli, V.; Settembrini, P.; Pierimarchi, P.; Freddi, G.; Armato, U. Three-Layered Silk Fibroin Tubular Scaffold for the Repair and Regeneration of Small Caliber Blood Vessels: From Design to in vivo Pilot Tests. *Front. Bioeng. Biotechnol.* 2019, *7*, 356.
(20) Khorshidi, S.; Solouk, A.; Mirzadeh, H.; Mazinani, S.; Lagaron, J. M.; Sharifi, S.; Ramakrishna, S.; Hadjizadeh, A.; Doillon, C. J. A review of key challenges of electrospun scaffolds for tissue-engineering applications. *J. Tissue Eng. Regener. Med.* **2016**, *10* (4), 715.
(21) Brito-Pereira, R.; Correia, D. M.; Ribeiro, C.; Francesko, A.; Etxebarria, I.; Pérez-Álvarez, L.; Vilas, J. L.; Martins, P.; Lanceros-Méndez, S. Silk fibroin-magnetic hybrid composite electrospun fibers for tissue engineering applications. *Composites, Part B* **2018**, *141*, 70−75.
(22) Brito-Pereira, R.; Macedo, A. S.; Ribeiro, C.; Cardoso, V. F.; Lanceros-Méndez, S. Natural based reusable materials for microfluidic substrates: The silk road towards sustainable portable analytical systems. *Appl. Mater. Today* **2022**, *28*, 101507.
(23) Yang, H.; Yang, S.; Kong, J.; Dong, A.; Yu, S. Obtaining information about protein secondary structures in aqueous solution using Fourier transform IR spectroscopy. *Nat. Protoc.* 2015, *10*, 382−396.
(24) Fernandes, M. M.; Correia, D. M.; Ribeiro, C.; Castro, N.; Correia, V.; Lanceros-Mendez, S. Bioinspired Three-Dimensional Magnetoactive Scaffolds for Bone Tissue Engineering. *ACS Appl. Mater. Interfaces* **2019**, *11*, 45265−45275.
(25) Reizabal, A.; Brito-Pereira, R.; Fernandes, M. M.; Castro, N.; Correia, V.; Ribeiro, C.; Costa, C. M.; Perez, L.; Vilas, J. L.; Lanceros-Méndez, S. Silk fibroin magnetoactive nanocomposite films and membranes for dynamic bone tissue engineering strategies. *Materialia* 2020, *12*, 100709.
(26) Strawhecker, K. E.; Kumar, S. K.; Douglas, J. F.; Karim, A. The critical role of solvent evaporation on the roughness of spin-cast polymer films. *Macromolecules (Washington, DC, U. S.)* **2001**, *34*, 4669−4672.
(27) Ribeiro, C.; Costa, C. M.; Correia, D. M.; Nunes-Pereira, J.; Oliveira, J.; Martins, P.; Gonçalves, R.; Cardoso, V. F.; Lanceros-Méndez, S. Electroactive poly(vinylidene fluoride)-based structures for advanced applications. *Nat. Protoc.* 2018, *13*, 681−704.
(28) Cardoso, V. F.; Lopes, A. C.; Botelho, G.; Lanceros-Méndez, S. Poly(vinylidene fluoride-trifluoroethylene) porous films: Tailoring microstructure and physical properties by solvent casting strategies. *Soft Mater.* 2015, *13*, 243−253.
(29) Ishii, Y.; Sakai, H.; Murata, H. A new electrospinning method to control the number and a diameter of uniaxially aligned polymer fibers. *Mater. Lett.* 2008, *62*, 3370−3372.
(30) Pereira, R. F. P.; Gonçalves, H. M. R.; Correia, D. M.; Costa, C. M.; Silva, M. M.; Lanceros-Méndez, S.; Bermudez, V. Z. Plasma-treated Bombyx mori cocoon separators for high-performance and sustainable lithium-ion batteries. *Mater. Today Sustain.* 2020, *9*, 100041.
(31) Ribeiro, C.; Sencadas, V.; Ribelles, J. L. G.; Lanceros-Méndez, S. Influence of Processing Conditions on Polymorphism and Nanofiber Morphology of Electroactive Poly(vinylidene fluoride) Electrospun Membranes. *Soft Mater.* **2010**, *8*, 274−287.
(32) Bhardwaj, N.; Kundu, S. C. Electrospinning: a fascinating fiber fabrication technique. *Biotechnol. Adv.* 2010, *28*, 325−347.
(33) Tian, D.; Song, Y.; Jiang, L. Patterning of controllable surface wettability for printing techniques. *Chem. Soc. Rev.* 2013, *42*, 5184−5209.
(34) Kitsara, M.; Blanquer, A.; Murillo, G.; Humblot, V.; Vieira, S. B.; Nogués, C.; Ibáñez, E.; Esteve, J.; Barrios, L. Permanently hydrophilic, piezoelectric PVDF nanofibrous scaffolds promoting unaided electromechanical stimulation on osteoblasts. *Nanoscale* 2019, *11*, 8906−8917.
(35) Razafiarison, T.; Holenstein, C. N.; Stauber, T.; Jovic, M.; Vertudes, E.; Loparic, M.; Kawecki, M.; Bernard, L.; Silvan, U.; Snedeker, J. G. Biomaterial surface energy-driven ligand assembly strongly regulates stem cell mechanosensitivity and fate on very soft substrates. *Proc. Natl. Acad. Sci. U. S. A.* 2018, *115*, 4631−4636.
(36) Otitoju, T. A.; Ahmad, A. L.; Ooi, B. S. Superhydrophilic (superwetting) surfaces: A review on fabrication and application. *J. Ind. Eng. Chem. (Amsterdam, Neth.)* **2017**, *47*, 19−40.
(37) Szewczyk, P. K.; Ura, D. P.; Metwally, S.; Knapczyk-Korczak, J.; Gajek, M.; Marzec, M. M.; Bernasik, A.; Stachewicz, U. (2018). Roughness and Fiber Fraction Dominated Wetting of Electrospun Fiber-Based Porous Meshes. *Polymers (Basel, Switz.)* 2019, *11*, 34.
(38) Brito-Pereira, R.; Ribeiro, C.; Lanceros-Méndez, S.; Cardoso, V. F. Biodegradable Polymer-Based microfluidic membranes for sustainable point-of-care devices. *Chem. Eng. J. (Amsterdam, Neth.)* 2022, *448*, 137639.
(39) Brito-Pereira, R.; Macedo, A. S.; Tubio, C. R.; Lanceros-Méndez, S.; Cardoso, V. F. Fluorinated Polymer Membranes as Advanced Substrates for Portable Analytical Systems and Their Proof of Concept for Colorimetric Bioassays. *ACS Appl. Mater. Interfaces* 2021, *13*, 18065−18076.

https://doi.org/10.1021/acs.biomac.2c01124
Biomacromolecules 2023, 24, 1121−1130

(40) He, Y.-X.; Zhang, N.-N.; Li, W.-F.; Jia, N.; Chen, B.-C.; Zhou, K.; Zhang, J.; Chen, Y.; Zhou, C.-Z. N-Terminal domain of Bombyx mori fibroin mediates the assembly of silk in response to pH decrease. *J. Mol. Biol.* **2012**, *418*, 197−207.
(41) Um, I. C.; Kweon, H. Y.; Lee, K. G.; Park, Y. H. The role of formic acid in solution stability and crystallization of silk protein polymer. *Int. J. Biol. Macromol.* **2003**, *33*, 203−213.
(42) Wu, H. J.; Hu, M. H.; Tuan-Mu, H. Y.; Hu, J. J. Preparation of aligned poly(glycerol sebacate) fibrous membranes for anisotropic tissue engineering. *Mater. Sci. Eng., C* **2019**, *100*, 30−37.
(43) Maciel, M. M.; Ribeiro, S.; Ribeiro, C.; Francesko, A.; Maceiras, A.; Vilas, J. L.; Lanceros-Méndez, S. Relation between fiber orientation and mechanical properties of nano-engineered poly-(vinylidene fluoride) electrospun composite fiber mats. *Composites, Part B* **2018**, *139*, 146−154.
(44) Heo, S. J.; Nerurkar, N. L.; Baker, B. M.; Shin, J. W.; Elliott, D. M.; Mauck, R. L. Fiber Stretch and Reorientation Modulates Mesenchymal Stem Cell Morphology and Fibrous Gene Expression on Oriented Nanofibrous Microenvironments. *Ann. Biomed. Eng.* **2011**, *39*, 2780−2790.
(45) Wang, H. W.; Zhou, H. W.; Gui, L. L.; Ji, H. W.; Zhang, X. C. Analysis of effect of fiber orientation on Young's modulus for unidirectional fiber reinforced composites. *Composites, Part B* **2014**, *56*, 733−739.
(46) Huang, W.; Ling, S.; Li, C.; Omenetto, F. G.; Kaplan, D. L. Silkworm silk-based materials and devices generated using bionano-technology. *Chem. Soc. Rev.* **2018**, *47*, 6486−6504.
(47) Kundu, B.; Rajkhowa, R.; Kundu, S. C.; Wang, X. Silk fibroin biomaterials for tissue regenerations. *Adv. Drug Delivery Rev.* **2013**, *65*, 457−470.
(48) Rabotyagova, O. S.; Cebe, P.; Kaplan, D. L. Role of polyalanine domains in beta-sheet formation in spider silk block copolymers. *Macromol. Biosci.* **2010**, *10*, 49−59.
(49) Reizabal, A.; Correia, D. M.; Costa, C. M.; Perez-Alvarez, L.; Vilas-Vilela, J. L.; Lanceros-Méndez, S. Silk Fibroin Bending Actuators as an Approach Toward Natural Polymer Based Active Materials. *ACS Appl. Mater. Interfaces* **2019**, *11*, 30197−30206.
(50) Reizabal, A.; Gonçalves, R.; Fidalgo-Marijuan, A.; Costa, C. M.; Pérez, L.; Vilas, J. L.; Lanceros-Méndez, S. Tailoring silk fibroin separator membranes pore size for improving performance of lithium ion batteries. *J. Membr. Sci.* **2020**, *598*, 117678.
(51) Cebe, P.; Partlow, B. J.; Kaplan, D. L.; Wurm, A.; Zhuravlev, E.; Schick, C. Silk I and Silk II studied by fast scanning calorimetry. *Acta Biomater.* **2017**, *55*, 323−332.
(52) Cai, B.; Gu, H.; Wang, F.; Printon, K.; Gu, Z.; Hu, X. Ultrasound regulated flexible protein materials: Fabrication, structure and physical-biological properties. *Ultrason. Sonochem.* **2021**, *79*, 105800.
(53) Baran, E. T.; Tuzlakoğlu, K.; Mano, J. F.; Reis, R. L. Enzymatic degradation behavior and cytocompatibility of silk fibroin-starch-chitosan conjugate membranes. *Mater. Sci. Eng., C* **2012**, *32*, 1314−1322.
(54) Wang, Y.; Rudym, D. D.; Walsh, A.; Abrahamsen, L.; Kim, H. J.; Kim, H. S.; Kirker-Head, C.; Kaplan, D. L. In vivo degradation of three-dimensional silk fibroin scaffolds. *Biomaterials* **2008**, *29*, 3415−3428.
(55) Adan, A.; Kiraz, Y.; Baran, Y. Cell Proliferation and Cytotoxicity Assays. *Curr. Pharm. Biotechnol.* **2016**, *17*, 1213−1221.
(56) Veleva, A. N.; Heath, D. E.; Johnson, J. K.; Nam, J.; Patterson, C.; Lannutti, J. J.; Cooper, S. L. Interactions between endothelial cells and electrospun methacrylic terpolymer fibers for engineered vascular replacements. *J. Biomed. Mater. Res., Part A* **2009**, *91*, 1131−1139.

https://doi.org/10.1021/acs.biomac.2c01124
Biomacromolecules 2023, 24, 1121−1130

- **Development and evaluation of different electroactive poly(vinylidene fluoride) architectures for endothelial cell culture**

  Durán-Rey D, Brito-Pereira R, Ribeiro C, Ribeiro S, Sánchez-Margallo JA, Crisóstomo V, Irastorza I, Silván U, Lanceros-Méndez S, Sánchez-Margallo FM.

  Front Bioeng Biotechnol. **2022**; 10:1044667.

  DOI: 10.3389/fbioe.2022.1044667. PMID: 36338140.

  [Published]

frontiers | Frontiers in Bioengineering and Biotechnology

TYPE Original Research
PUBLISHED 19 October 2022
DOI 10.3389/fbioe.2022.1044667

OPEN ACCESS

EDITED BY
Roman Surmenev,
Tomsk Polytechnic University, Russia

REVIEWED BY
Vladimir Botvin,
Tomsk Polytechnic University, Russia
Alexandra Pershina,
Siberian State Medical University, Russia
Abdulkarim Amirov,
Immanuel Kant Baltic Federal University, Russia

*CORRESPONDENCE
Francisco M. Sánchez-Margallo,
msanchez@ccmijesususon.com

SPECIALTY SECTION
This article was submitted to Biomaterials, a section of the journal Frontiers in Bioengineering and Biotechnology

RECEIVED 14 September 2022
ACCEPTED 07 October 2022
PUBLISHED 19 October 2022

CITATION
Durán-Rey D, Brito-Pereira R, Ribeiro C, Ribeiro S, Sánchez-Margallo JA, Crisóstomo V, Irastorza I, Silván U, Lanceros-Méndez S and Sánchez-Margallo FM (2022), Development and evaluation of different electroactive poly(vinylidene fluoride) architectures for endothelial cell culture.
Front. Bioeng. Biotechnol. 10:1044667.
doi: 10.3389/fbioe.2022.1044667

Development and evaluation of different electroactive poly(vinylidene fluoride) architectures for endothelial cell culture

David Durán-Rey[1], Ricardo Brito-Pereira[2,3,4,5], Clarisse Ribeiro[4,6], Sylvie Ribeiro[4,6], Juan A. Sánchez-Margallo[1,8], Verónica Crisóstomo[1,7,8], Igor Irastorza[4,9], Unai Silván[10,11], Senentxu Lanceros-Méndez[10,11] and Francisco M. Sánchez-Margallo[1,7,8]*

[1]Jesús Usón Minimally Invasive Surgery Centre, Cáceres, Spain, [2]CMEMS-UMinho, University of Minho, Guimarães, Portugal, [3]LABBELS-Associate Laboratory, Braga/Guimarães, Portugal, [4]CF-UM-UP, Physics Centre of Minho and Porto Universities, University of Minho—Campus de Gualtar, Braga, Portugal, [5]IB-S Institute of Science and Innovation for Bio-Sustainability, University of Minho, Campus de Gualtar, Braga, Portugal, [6]LaPMET—Laboratory of Physics for Materials and Emergent Technologies, University of Minho, Braga, Portugal, [7]Centro de Investigación Biomédica en Red de Enfermedades Cardiovasculares (CIBERCV), Instituto de Salud Carlos III, Madrid, Spain, [8]RICORS-TERAV Network, Instituto de Salud Carlos III, Madrid, Spain, [9]Cell Biology and Histology Department, Faculty of Medicine, Leioa, Spain, [10]BCMaterials, Basque Center for Materials, Applications and Nanostructures, UPV/EHU Science Park, Leioa, Spain, [11]Ikerbasque, Basque Foundation for Science, Bilbao, Spain

Tissue engineering (TE) aims to develop structures that improve or even replace the biological functions of tissues and organs. Mechanical properties, physical-chemical characteristics, biocompatibility, and biological performance of the materials are essential factors for their applicability in TE. Poly(vinylidene fluoride) (PVDF) is a thermoplastic polymer that exhibits good mechanical properties, high biocompatibility and excellent thermal properties. However, PVDF structuring, and the corresponding processing methods used for its preparation are known to significantly influence these characteristics.

In this study, doctor blade, salt-leaching, and electrospinning processing methods were used to produce PVDF-based structures in the form of films, porous membranes, and fiber scaffolds, respectively. These PVDF scaffolds were subjected to a variety of characterizations and analyses, including physicochemical analysis, contact angle measurement, cytotoxicity assessment and cell proliferation.

All prepared PVDF scaffolds are characterized by a mechanical response typical of ductile materials. PVDF films displayed mostly vibration modes for the a-phase, while the remaining PVDF samples were characterized by a higher content of electroactive β-phase due the low temperature solvent evaporation during processing. No significant variations have been observed between the different PVDF membranes with respect to the melting transition. In addition, all analysed PVDF samples present a hydrophobic behavior. On the other hand,

cytotoxicity assays confirm that cell viability is maintained independently of the architecture and processing method. Finally, all the PVDF samples promote human umbilical vein endothelial cells (HUVECs) proliferation, being higher on the PVDF film and electrospun randomly-oriented membranes. These findings demonstrated the importance of PVDF topography on HUVEC behavior, which can be used for the design of vascular implants.

KEYWORDS

PVDF, films, membranes, electrospinning, tissue engineering, scaffolds

1 Introduction

Properties of the extracellular matrix (ECM) such as porosity, stiffness and architecture strongly affect cell behavior. Therefore, there is a need to control these parameters in scaffolds and materials intended for tissue engineering (TE) applications (Khorshidi et al., 2015). A large number of materials have been proposed for the repair of different tissues or organs, such as cardiac (Weinberger et al., 2017), gastrointestinal (Penkala and Kim, 2007), vascular (Durán-Rey et al., 2021), nerve (Motamedi et al., 2017a), and bone tissues (Fernandes et al., 2019). Characteristics, such as their mechanical properties, biocompatibility and physicochemical characteristics, together with the biological performance of the scaffolds, are essential to ensure an optimal cell response.

Active and smart materials are increasingly being implemented for advanced tissue regeneration strategies, being piezoelectric materials of particular interest, as they can generate an electrical potential in response to an applied stress or mechanical deformation (Motamedi et al., 2017b; Li et al., 2019; Mokhtari et al., 2021). Considering that electric stimulation has shown great promise for the development of materials for TE by mimicking the dynamic electroactive microenvironment of specific cells and tissues (Balint et al., 2013), the development of scaffolds that combine piezoelectric properties and topographical cues known to induce specific cellular responses are of particular interest.

Poly(vinylidene fluoride) (PVDF) ($-CH_2-CF_2-$) is a thermoplastic polymer which is widely used in biomedical applications (Ahmed et al., 2014; Fernandes et al., 2019). This synthetic material shows a number of properties that makes it an ideal piezoelectric candidate for TE applications, including high biocompatibility and good mechanical performance (Motamedi et al., 2017a; Haddadi et al., 2018; Mokhtari et al., 2021). In addition, the piezoelectric response of PVDF and copolymers is the highest among polymer materials (Motamedi et al., 2017b; Li et al., 2019; Mokhtari et al., 2021).

A wide variety of structured scaffolds based on PVDF have been developed so far. One of the most widely used methodologies for the manufacturing of PVDF-based films on rigid or flexible large-area surfaces, is doctor blade (Ribeiro et al., 2018), which renders flat films of homogenous thickness. This PVDF architecture is the most used in sensor and actuator applications (Seminara et al., 2011). On the other hand, porous PVDF structures, such as porous membranes, can be produced by salt-leaching or phase separation methods (Ribeiro et al., 2018), among others. These structures have been proposed as candidates for the repair of a number of tissues, including as vessels, bones, and muscles (Ribeiro et al., 2018). Finally, PVDF scaffolds using electrospinning technology are composed of nano- or microfibers with controlled orientation (Maciel et al., 2017). The effect of such ECM-like topographies has shown to have a great impact on cell behavior, and this structuring approach has been consequently widely proposed for biomedical TE applications (Li et al., 2019; Mokhtari et al., 2021).

The physicochemical and biological characteristics of PVDF scaffolds strongly depend on their architecture and preparation methodology. In addition, studies have identified that these factors are important for the development of structured scaffolds for cardiovascular system repair (Durán-Rey et al., 2021).

Endothelial cells are important constituents of the blood vessels playing a critical role in the cardiovascular homeostasis (Sun et al., 2020). Furthermore, when the biomaterial is implanted, the interaction between the material and the endothelium, that is the cellular membrane formed by endothelial cells that line the inside of the heart and blood vessels, is a key factor that determines the outcome (Hauser et al., 2017). In most of the studies, this interaction has been investigated with human umbilical vein endothelial cells (HUVECs), that represent a widely used source of the endothelial cells for *in vitro* studies (Kocherova et al., 2019). Previous studies have demonstrated the importance of surface electric charges and of the piezoelectric activity of biomaterials on the adhesion of endothelial cells and on their function (Bouaziz et al., 1997; Hitscherich et al., 2016).

In this context, PVDF-based structures have been developed by doctor blade, salt-leaching, and electrospinning methodologies to generate films, porous membranes, and electrospun scaffolds with random and oriented architectures, in order to tune their physicochemical properties and biocompatibility with HUVECs.

2 Materials and methods

2.1 Materials

Poly(vinylidene fluoride), PVDF, 10/10 powder was obtained from *Solvay* (Brussels, Belgium). N,N-dimethylformamide (DMF) and absolute ethanol were obtained from *Merck* and Sodium Chloride (NaCl) was obtained from *Sigma*. All reagents and solvents were used as received.

2.2 Sample preparation

Several processing techniques and post-treatment protocols were employed to produce the different PVDF based structures.

2.2.1 PVDF solution preparation

First, a 10 wt% solution of PVDF powder was dissolved in DMF under magnetic stirring. A slight heating at 30°C was applied during the first 30 min of dissolution to speed up the process and the solution was then allowed to cool under magnetic stirring until a homogeneous and transparent solution was obtained, which took no more than 3 h. The polymer concentration was defined in order to obtain a solution compatible with the processing techniques and conditions in order to obtain the membranes (Ribeiro et al., 2018).

2.2.2 Films preparation

The PVDF solution was homogeneously distributed by doctor blade method (~450 µm spacer) over clean glass substrates. The samples were then placed in an oven (JP Selecta, Model 2000208) for 10 min at a temperature of 210°C for polymer melting and complete removal of the solvent. Next, films were removed from the oven and allowed to cool at room temperature. Samples with an average thickness of ~24.53 µm were obtained.

2.2.3 Porous membrane preparation

Porous membranes were prepared by a salt-leaching method. NaCl particles with an approximate size of 2 µm were added to the PVDF solution in a proportion of 10:3 (w: w) PVDF:salt. After a 1 h of energetic stirring, a homogeneous mixture was obtained. The resulting solution containing the dispersed NaCl was poured over glass Petri dishes and the solvent was evaporated at room temperature. The PVDF/NaCl membranes were then washed by distilled water bath at room temperature until the washing solution showed constant electrical conductivity values indicating the completely removal of the NaCl. Finally, the obtained porous membranes were placed in an airing chamber and dried for 24 h. Samples with an average thickness of ~252.67 µm were obtained.

2.2.4 Electrospun fiber mats

The PVDF solution was transferred to 10 ml disposable syringes fitted with a blunt steel needle with an inner diameter of 500 µm and placed in a syringe pump (*New Era NE-1000*). Electrospinning was conducted using a high voltage power supply (*Glassman PS/FC30P04*) set at 15 kV and the syringe was pumped with a flow rate of 0.5 ml h^{-1}. The resulting randomly oriented electrospun PVDF 10/10 membranes were collected on a grounded 20 × 15 cm static plate collector placed 15 cm from the needle. The processed membranes are identified in the following as ES-NO membranes.

Oriented PVDF membranes were obtained after a process similar to the one described above, except for the use of a grounded rotating drum collector, which was set at a speed of 1,500 rpm. The processed membranes are identified as ES-O membranes. Samples with an average thickness of ~137.5 µm and ~26.53 µm were obtained for the randomly oriented and oriented samples, respectively.

2.3 Sample characterization

2.3.1 Physicochemical characterization

Scanning electron microscope (SEM) JEOL JSM-7000F was used to obtain the surface and cross section morphologies of the PVDF membranes. From these images, the pore size and fiber diameter distributions were determined using the software ImageJ (Brito-Pereira et al., 2018).

Pycnometer was used to measure the porosity of the samples by liquid displacement. The pycnometer was filled with ethanol, the weight was measured and labelled as W_1. The sample, which weight was (W_S), was immersed in ethanol. Once the sample was saturated, additional ethanol was added to completely fill the volume of the pycnometer, and the system was weighed (W_2). Finally, the sample was taken out of the pycnometer. W_3 was the weight of the system with ethanol. The porosity of the sample was obtained as the average of three values according to Eq. 1 (Brito-Pereira et al., 2022):

$$\varepsilon = \frac{W_2 - W_3 - W_S}{W_1 - W_3} \quad (1)$$

Absolute ethanol is a non-solvent for PVDF, so it was used as displacement liquid since it can penetrate the pores without inducing swelling, shrinking or sample degradation.

The wettability of the samples was evaluated with an OCA20 instrument by the static sessile drop method with ultrapure water. For that, a water drop was placed onto the surface of the samples and the SCA20 software was used to measure the contact angle. The mean contact angle and standard deviation were calculated from the measurement at six different positions for each sample.

The different PVDF structures were subjected to stress-stress measurements using a *Shimadzu AD-IS* universal testing set up with a load cell of 50 N. The dimensions of the samples were 15 mm long and 10 mm wide. Average sample thickness for the samples, as measured using a Fischer Dualscope MPOR were ~24.53 μm (films), ~252.67 μm (porous membranes), ~137.5 μm (electrospun randomly oriented scaffolds), and ~26.53 μm (electrospun oriented scaffolds). Samples were stretched at a rate of 5 mm/min^{-1} for films and 1 mm/min^{-1} for the remaining scaffolds. Three samples of each structure of PVDF were used to perform the measurements, and the ES-O PVDF membranes were stretched along and in 90° regarding the direction of the fibers [ES-O (90°)].

Infrared measurements (FTIR) and differential scanning calorimetry (DSC) were also performed to evaluate polymer phase and thermal behaviour and degree of crystallinity, respectively. FTIR was performed using a Jasco FT/IR 4100 (Agilent 4300) system in attenuated total reflectance mode (ATR) from 4000 to 650 cm^{-1}. A resolution of 4 cm^{-1} was used to obtain FTIR spectra after 64 scans. The 763 and 840 cm^{-1} absorption bands are attributed to α and β phases of PVDF, respectively (Martins et al., 2014). The β phase content of the produced samples was calculated according Eq. 2.

$$F(\beta) = \frac{A_\beta}{\left(K_\beta / K_\alpha\right) A_\alpha + A_\beta} \times 100 \quad (2)$$

where, F(β) is the β phase content; A_α and A_β the absorbance at 763 and 840 cm^{-1} respectively; K_α and K_β the adsorption coefficients at the respective wavenumber, with values of 6.1 × 10^4 and 7.7 × 10^4 cm^2 mol^{-1}, respectively (Martins et al., 2014).

Differential scanning calorimetry (DSC) studies were performed in a Mettler Toledo DSC822e apparatus using a heating rate of 10°C.min^{-1}. The samples were cut into small pieces and placed into 40 μL aluminum pans. Through the obtained thermograms, the degree of crystallinity (χc) was determined by Eq. 3 (Maciel et al., 2017):

$$\mathcal{X}_c\,(\%) = \frac{\Delta H_f}{x\Delta H_\alpha + y\Delta H_\beta} \times 100 \quad (3)$$

where, according to FTIR-ATR measurements, x and y are the fraction of α and β phases of PVDF, respectively. ΔH_f is the melting enthalpy of the samples and ΔH_α (93.04 J g^{-1}) and ΔH_β (103.4 J g^{-1}) are the melting enthalpies of the α and β phases of a 100% crystalline sample of PVDF (Benz and Euler, 2003).

2.3.2 Cytotoxicity assay

The ISO 10993-5 standard test was used to evaluate the indirect cytotoxicity of the different samples. For this purpose, L929 adipose cells were cultured in 75 cm^2 cell culture flask in a humidified environment at 37°C with 5% CO_2, using Dulbecco's modified Eagle's medium (DMEM, Biochrom), with 4.5 g.L^{-1} glucose, 10% fetal bovine serum (FBS, Biochrom) and 1% (v/v) penicillin/streptomycin solution (P/S, Biochrom).

Before the assay, the samples were cut in 1.5 cm^2 and sterilized using ultraviolet radiation for 1 h on each side. After that, samples were washed with sterile phosphate-buffered saline solution (PBS, pH 7.4).

After sterilization, samples were incubated in DMEM in a 24-well tissue culture plate for 24 h. Simultaneously, 5 × 10^4 cell/mL cells were seeded in a 96-well plate and allowed to adhere for 24 h. After that, the culture medium in the 96-well culture plate was removed and replaced with 100 μL of the culture medium, which was in contact with the PVDF samples. As positive control dimethylsulfoxide (DMSO) at 20% and a negative control (fresh DMEM) were used. After 72 h (3-(4,5-dimethylthiazol-2-yl)-5-(3-carboxymethoxyphenyl)-2-(4-sulfophenyl)-2H-tetrazolium) (MTS, Promega) was used to quantify cell survival. Briefly, the culture medium was replaced with fresh medium containing MTS solution in a 1:5 ratio and cells were incubated for 2 h. After that, a spectrophotometric plate reader (Biotech Synergy HT) at 490 nm was used to measure the optical density. The cell viability was calculated according to Eq. 4 (Fernandes et al., 2019):

$$cell\ viability\ (\%) = \frac{absorbance\ of\ sample}{negative\ control\ absorbance} x100 \quad (4)$$

2.4 Cell culture assays

For the *in vitro* assays, PVDF samples (films, porous membrane, ES-NO and ES-O) were cut into circular shapes with 13 mm of diameter. For sterilization, the samples were washed 5 times in PBS 1x solution for 5 min each. Subsequently, the samples were exposed to ultraviolet (UV) light for 2 h (1 h each side). Finally, 24-well cell culture plates were used to place the samples.

Human Umbilical Vein Endothelial Cells (HUVEC's cells, ATCC) were grown in 75 cm^2 cell-culture flask and cultured with endothelial cell growth medium (*Pan Biotech*). A humidified air containing 5% CO_2 atmosphere was used to incubate the flask at 37°C. The culture medium was changed every 2 days. Accutase (*Grisp*) was used to detach the cells when they reached 80%–90% confluence.

For proliferation tests, HUVEC's cells were seeded on the different samples at a density of 7,500 cells. cm^{-2}. The drop method was used to allow the cell attachment on the different samples. Samples were incubated at 37°C in a saturated humidity atmosphere containing 95% air and 5% CO_2. After selected times, cell viability and immunofluorescence microscopy were used to analyse the samples.

For the proliferation assays, the MTS assay was used to evaluate the cell viability of HUVEC's on the different materials. This method can be used as indirect assay to

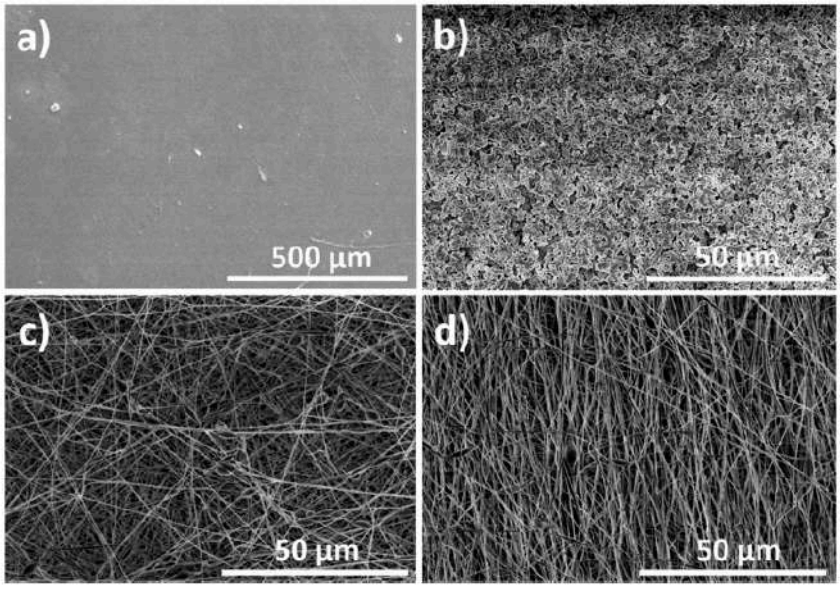

FIGURE 1
Representative SEM images of the processed PVDF structures, namely: **(A)** films, **(B)** porous scaffold, **(C)** electrospun randomly-oriented fibers, and **(D)** electrospun oriented fibers.

evaluate cell proliferation, according to the increase of cell viability. The MTS assay was carried out after 1 and 4 days. At these time points, the cell/films were transferred to new wells and fresh medium containing MTS solution (1:5 proportion of medium) was added. The plate was incubated at 37°C for 3 h. Finally, a microplate reader (*Biotech Synergy HT*) was used to measure the absorbance at 490 nm. Experimental data were obtained from four replicates of each sample. Results were expressed as mean ± standard deviation. All quantitative data were analyzed using GraphPad by Dotmatics. The results were analyzed statistically using the *t*-test. Differences were considered statistically significant when p-value < 0.01.

After 4 days, fluorescent labelling was used to staining the actin and nucleus of the cells in the different samples. For that, the medium from each well was removed, the samples were washed with PBS 1x and fixed with 4% formaldehyde for 10 min at 37°C in a 5% CO_2 incubator. After fixation, PBS 1x (three times) was used to wash the samples, and they were permeabilized with 0.1% Triton X-100 for 10 min at room temperature. After that, all samples were incubated for 45 min at room temperature in 0.1 µg ml^{-1} of Phalloidin–Tetramethylrhodamine B isothiocyanate (TRITC, *Sigma-Aldrich*). Then, 1 µg ml^{-1} of DAPI (*Sigma-Aldrich*) was used to incubate the samples for 5 min. Afterwards, the samples were washed again with distilled water (two times). Finally, fluorescence microscopy (Olympus BX51 Microscope) was used to visualise the samples.

3 Results and discussion

3.1 Physicochemical characterization

In order to verify the morphology of the PVDF membranes after processing, representative SEM images of the PVDF membranes were obtained (Figure 1). From these images, the main pore size and fiber diameter distributions were determined using the image analysis software ImageJ.

The images reveal the different characteristics of each PVDF-based structure. First, PVDF films produced by doctor blade lack porosity, while PVDF membranes prepared by salt-leaching method are characterized by pores of approximately 2 µm. It is to notice that the used methodology allows the control of the pore size by tuning the size of the NaCl particles added to the mixture. However, structures manufactured with salt-leaching do not present an interconnected network of pores, and frequently show irregular and non-reproducible architectures (Cardoso et al., 2015; Ribeiro et al., 2018). Finally, fibrous PVDF scaffolds with randomly distributed (ES-NO) and oriented fibers (ES-O) produced by electrospinning contained average fiber widths of 634.7 ± 31 and 598.1 ± 27 nm, respectively. These

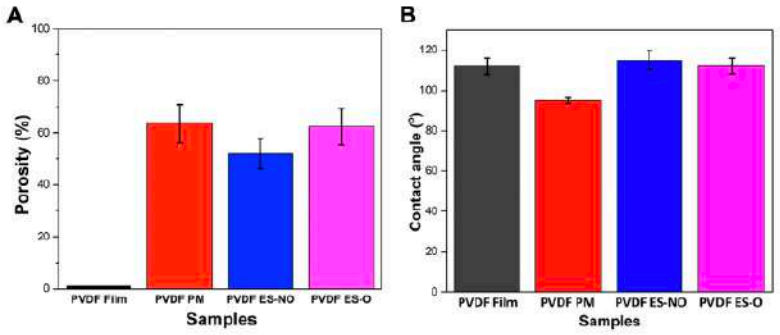

FIGURE 2
(A) Porosimetry results of the PVDF film, porous membrane (PM), electrospun randomly-oriented membranes (ES-NO) and electrospun oriented membranes (ES-O). **(B)** Representative contact angle of the PVDF film, PM, ES-NO and ES-O.

results are consistent with previously published data of PVDF electrospun scaffolds (Brito-Pereira et al., 2021). The fact that ES-O scaffolds had a smaller average fiber diameter than ES-NO scaffolds can be attributed to the stretching of the oriented fibers during their collection in the rotating drum (Ribeiro et al., 2010).

Independently of the processing method and porous membrane architecture, the mean degree of porosity was above 50% (Figure 2A). Porosity values of 63.51% ± 7.45%, 51.9% ± 5.8%, and 62.3% ± 6.89% were calculated for porous membranes, ES-NO, and ES-O scaffolds, respectively. Nevertheless, the degree of porosity, as well as pore structure and fiber widths, can be further tune according to the selected processing parameters and methodology (Bhardwaj and Kundu, 2010; Ribeiro et al., 2010; Ribeiro et al., 2018).

Wettability is a key parameter affecting cell adhesion, proliferation and differentiation (Razafiarison et al., 2018; Kitsara et al., 2019). The water contact angle of the processed films, porous scaffolds, ES-NO and ES-O membranes were 111.98 ± 4.12°, 94.99 ± 1.43°, 115.01 ± 4.68°, and 112.19 ± 3.90°, respectively (Figure 2B). Note that hydrophobic surfaces show water contact angles higher than 90°, while values below 90° correspond to hydrophilic surfaces. In turn, materials with water contact angle values above 150° and below 10° are termed superhydrophobic and superhydrophilic, respectively (Otitoju et al., 2017). Therefore, all PVDF membranes showed a hydrophobic behavior, though slight differences in the surface wettability are observed depending on the topography of the membranes. Electrospun membranes show a more hydrophobic behavior than other membrane structures (Ahmed et al., 2014; Szewczyk et al., 2018). In particular, PVDF porous membranes show a relatively large pore size, which causes the liquid to percolate into the pores and, therefore, slightly lowers the contact angle value (Szewczyk et al., 2018).

The mechanical properties of biomaterials for TE applications are particularly relevant for the development of safe and durable solutions. Although the PVDF structures are composed of the same material, their mechanical stability varies depending on the geometry and manufacturing methodology. Therefore, stress-strain measurements were performed in all PVDF samples. PVDF is a thermoplastic elastomer which characteristic stress-strain mechanical response (Figure 3) feature a first linear elastic regime, where the structure returns to its original shape when stress ceases, followed by a plastic regime after yielding, where the material does not recover its original shape, undergoing permanent deformation. Finally, the rupture stress-strain is reached if the sample is stretched further. On the other hand, materials can be divided mainly into ductile, which have a typical elastic and plastic zone that is perfectly differentiated, and brittle materials, which typically present little or no plastic deformation. Hooke's law is applied to calculate the Young's modulus from the linear regime of the curves (Brito-Pereira et al., 2021).

All analyzed PVDF structures feature stress-strain curves characteristic of ductile materials (Figure 3A). However, there are significant differences in the Young's moduli and in the mechanical properties of the materials depending on the architecture of the structures (Figure 3B).

PVDF films are stiff with a flat and dense morphology and characterized by a Young's modulus higher than the PVDF porous membranes (Cardoso et al., 2015), being 279.22 ± 13.27 and 83.01 ± 2.52 MPa, respectively. On the other hand, mechanical analysis of films and porous membranes showed a maximum elongation of approximately 24% and 18%, respectively, which correspond to their rupture stress-strain. Films have generally higher stress-strain values than porous membranes, as the mechanical response of the latter is first determined by the deformation of the porous structure.

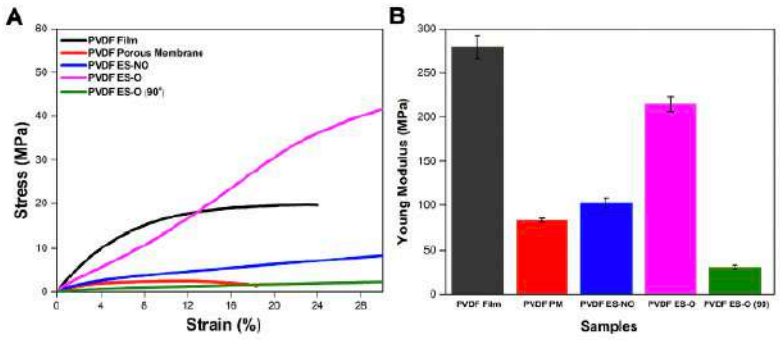

FIGURE 3
(A) Stress-strain curves up to 28% of strain for the PVDF film, porous membrane (PM), electrospun randomly-oriented membranes (ES-NO), electrospun oriented membranes (ES-O) and 90° electrospun oriented membranes [ES-O (90°)]. **(B)** Young's modulus with mean and standard deviation.

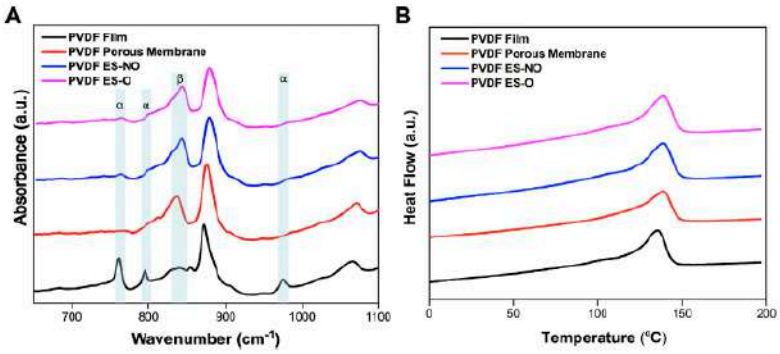

FIGURE 4
(A) Representative FTIR spectra of PVDF film, porous scaffold, electrospun randomly-oriented membranes (ES-NO) and electrospun oriented membranes (ES-O). **(B)** Representative DSC thermograms of the PVDF film, porous membrane, ES-NO and ES-O.

Furthermore, stress-strain values of porous membranes have a higher variability due to the random distribution of the pores (Cardoso et al., 2015).

Regarding the electrospun membranes, samples deformed along the main fiber direction (ES-O (0°)) showed a higher value of the effective Young's modulus (214.77 ± 8.64 MPa), followed by ES-NO (102.73 ± 5.39 MPa) and ES-O (90°) (31.16 ± 2.26 MPa), respectively. These results are consistent with previous studies, where the Young's modulus decreases with increasing angle between fiber orientation and strain direction (Heo et al., 2011; Wang et al., 2014; Maciel et al., 2017). This is due to fiber reorientation and collapsing of pores as fibers are recruited toward the direction of applied strain (Heo et al., 2011). On the contrary, electrospun membranes showed an elongation larger than 28%. Previous studies indicated that the elongation at break of electrospun PVDF membranes could reach 142%, displaying good ductility (Cai et al., 2019). In fact, ES-O (0°) showed a yield strain and stress larger than ES-NO and ES-O (90°). This is because the stress is applied mostly along the fiber direction in the case of ES-O (0°), while in ES-NO and ES-O (90°) the stress is first devoted to the reorientation of the fibers along the stretching direction (Maciel et al., 2017). In this way, the mechanical properties of the material are dependent on the orientation of the fibers and, therefore, can be adjusted to the specific biomedical application.

Further, FTIR analysis show that the processing method used to generate PVDF structures has a great influence on the crystalline phase of the scaffolds (Figure 4A). PVDF films

TABLE 1 β-Phase content, melting temperature and degree of crystallinity of the produced PVDF samples, as obtained from FTIR and DSC respectively.

	β phase content	T_m (°C)	X_c (%)
PVDF Film	6.3 ± 0.1	135.7 ± 3.5	49.1 ± 2.1
PVDF PM	99.0 ± 0.8	138.8 ± 4.0	38.7 ± 1.4
PVDF ES-NO	90.0 ± 1.8	138.7 ± 4.1	51.3 ± 3.6
PVDF ES-O	88.9 ± 1.6	138.9 ± 3.7	50.4 ± 2.5

processed at high temperatures display higher content of *a*-phase (762, 796 and 975 cm^{-1}), as the processing temperature is one of the key factors determining the crystalline structure of the polymer (Ribeiro et al., 2010). On the other hand, when processed at room temperature, structured PVDF (porous, ES-NO and ES-O) are characterized by having a higher content of electroactive *β*-phase (840 cm^{-1}). Table 1 summarizes the electroactive *β*-phase content of the different samples, calculated after Eq. 2, showing that the samples processed at room temperatures show an electroactive *β*-phase content above 88%, whereas for the films obtained after high temperature processing it is reduced below 7%.

DSC measurements were performed in all membranes (Figure 4B) and just slight variation are observed in the melting transition (T_M), which occurs at 135.7 ± 3.5°C for PVDF films and 138.8 ± 4.0°C for the remaining membranes. The different is fully attributed to the crystallization conditions: whereas the films are processes from the melt, the membranes are the final result of a solvent evaporation process. The melting enthalpy obtained from the area underneath the melting peak of each thermogram, and the degree of crystallinity were calculated after Eq. 3, resulting in 49.1% ± 2.1% for films, 38.7% ± 1.4% for porous membranes, 51.3% ± 3.6% for randomly oriented fibers and 50.4% ± 2.5% for oriented fibers (Table 1).

It can be concluded that the degree of crystallinity slight differs for all different membranes with a mean value between 40% and 55%, which is typical for PVDF membranes and that the decrease of the β phase content of the films does not induces significant changes the degree of crystallinity (Ribeiro et al., 2010). Thus, the variations of the mechanical properties are just attributed to the different morphological features of the PVDF membranes and not in differences in the degree of crystallinity, which agrees with the literature (Brito-Pereira et al., 2021).

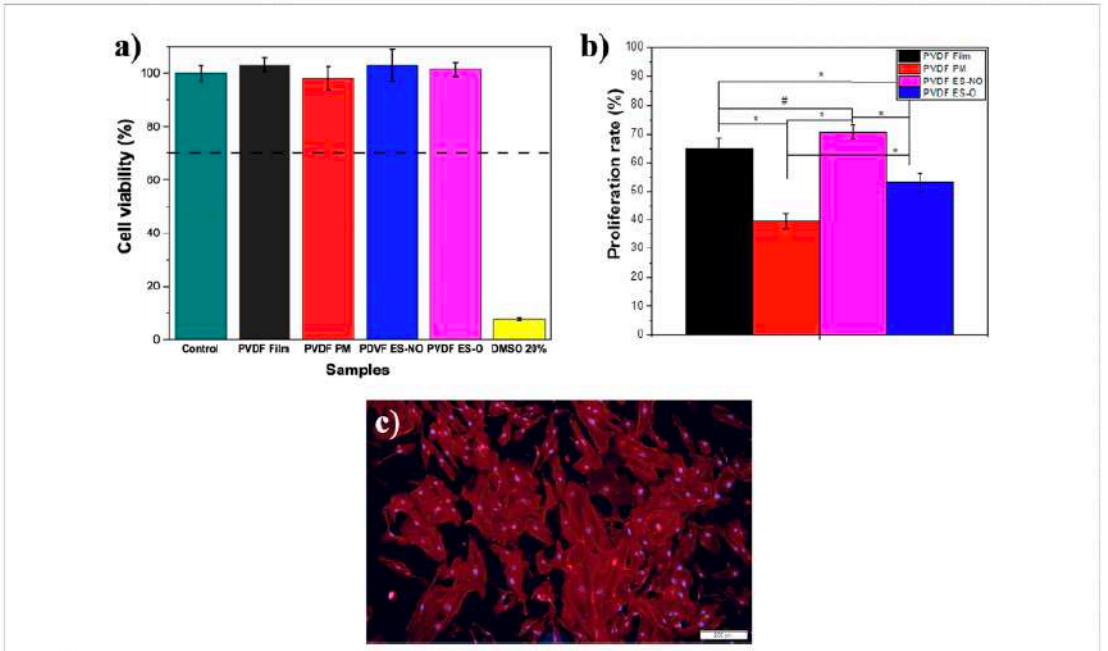

FIGURE 5
(A) Cell viability of control L929 cells, in contact with the extraction media of PVDF films, porous membrane (PM), electrospun randomly-oriented membranes (ES-NO), and electrospun oriented membranes (ES-O) (relative metabolic activity was presented as the percentage of the negative control with $n = 4 \pm$ standard deviation). **(B)** Proliferation rate determined using the MTS assay on HUVEC's cells seeded on the different PVDF samples after 4 days. The proliferation rate was calculated regarding the cells growing on the material after 24 h of cell adhesion. Results are expressed as mean ± standard deviation, $n = 4$. #$p < 0.002$ and *$p < 0.0001$. **(C)** HUVEC's cells after 4 days of cell culture on PVDF films.

3.2 Cytotoxicity assay

Low cytotoxicity is essential for biomaterials for TE applications. PVDF has been used as a scaffold for different TE applications (Motamedi et al., 2017a; Ribeiro et al., 2018b; Fernandes et al., 2019). Nevertheless, since different processing techniques were used and in order to prove that they did not affect the toxicity of the produced samples, an indirect cytotoxicity assay was carried out. For this reason, analysis of indirect toxicity using L929 adipose cells was used to assess the cytotoxicity of all generated structures (Figure 5A). According to the ISO 10993-5, when the cell viability suffers a reduction larger than 30%, the samples are considered cytotoxic. All PVDF morphologies showed cell viability values close to 100%, independently of their architecture and processing conditions, which is in concordance with previous studies (Ribeiro et al., 2018c).

3.3 Cell proliferation

HUVEC cell viability after incubation with extraction media, and proliferation after seeding on the different PVDF samples were evaluated through MTS assay (Figure 5B).

None of the generated PVDF scaffolds did show toxicity in indirect culture conditions (Figure 5A). In addition, when seeded on the structured materials HUVEC cells did proliferate, being the highest proliferation ratios observed in cells seeded on PVDF films and ES-NO membranes.

Fiber diameter and porosity affect cell adhesion, ingrowth and proliferation, and for that reason, these are parameters must be carefully considered for the production of materials for tissue engineering applications. Previous studies have demonstrated an increase in the initial attachment of endothelial cells on fibers with lower fiber diameters (Bergmeister et al., 2013). In our experiments, scaffolds of PVDF randomly and oriented fibers display similar fiber diameter and porosity, so the differences observed on HUVECs proliferation are most likely caused by fiber orientation. Nevertheless, the specific response to fibrous topographies has been shown to be highly affected by the composition of the fibers and environmental factors (Veleva et al., 2009; Cui et al., 2017; Yu et al., 2020).

In order to evaluate the cytoskeleton morphology of the cells and to verify cell viability, immunofluorescence tests were also performed in the films (Figure 5C). It is shown that all PVDF samples promote the formation of HUVEC monolayers composed of well-spread cells.

Overall, it is demonstrated that the electroactive PVDF based scaffolds with different morphologies can be used for HUVECs cell culture, allowing the further design of vascular implants.

4 Conclusion

PVDF is a thermoplastic electroactive polymer which is widely used in TE applications. It has been shown that, when structured, PVDF displays different characteristics depending on the architecture of the scaffold and processing methodology. Thus, PVDF has been processed in the form films, porous and electrospun membranes. It is shown that all PVDF membranes feature stress-strain curves typical of a ductile material. However, films and porous membranes present a maximum elongation of approximately 24% and 18%, respectively, while electrospun membranes show an elongation greater than 28%. The crystalline phases of the PVDF samples is affected by the processing method, where PVDF films mainly crystallize in the non-polar α-phase, while the remaining PVDF membranes are characterized by having high electroactive β-phase contents. The processing temperature is one of the key factors that affect the crystalline structure of PVDF, as PVDF film that was processed at high temperatures, and the remaining PVDF membranes (porous and electrospun membranes) were processed at room temperature. Despite the methodology employed for the design of PVDF membranes, no significant variation was observed in the melting transition, and all PVDF showed hydrophobic behavior. However, surface wettability is affected by the morphology of the PVDF membrane, having a higher hydrophobic behavior the electrospun membranes due to its surface roughness. Finally, cytotoxicity assay proved that, independently of the topography, PVDF maintained high levels of cell viability, and promoted HUVEC cell proliferation, being this higher on the film and electrospun randomly-oriented membranes. All these material characteristics should be taken into account when designing a PVDF membrane for TE applications, including but not limited to cardiovascular system. The results demonstrate that PVDF is a promising candidate to be used for cardiovascular applications.

Data availability statement

The original contributions presented in the study are included in the article/Supplementary Material, further inquiries can be directed to the corresponding author.

Author contributions

DD-R and RB-P: Conceptualization, writing—original draft and methodology; CR, SR, II, and US: Writing—cell culture assays; DD-R, RB-P, and JS-M: Investigation, formal analysis; VC, US, SL-M, and FS-M: Writing—review and; Editing; SL-M and FS-M: Supervision and funding acquisition. The manuscript was written through contributions of all authors. All authors have given approval to the final version of the manuscript.

Funding

This work has been partially funded by the Junta de Extremadura (Spain), the Spanish Ministry of Science and Innovation, the European Social Fund, the European Regional Development Fund, and the European Next Generation Funds (Grant Numbers PD18077, TA18023, and GR21201). The authors also thanks to Portuguese Foundation for Science and Technology (FCT) for financial support under grants SFRH/BD/140698/2018 (RP), 2020.04163. CEECIND (CR). The also authors acknowledge funding by Spanish State Research Agency (AEI) and the European Regional Development Fund (ERFD) through the project PID 2019-106099RB-C43/AEI/10.13039/501100011033 and from the Basque Government Industry Departments under the ELKARTEK program.

Conflict of interest

The authors declare that the research was conducted in the absence of any commercial or financial relationships that could be construed as a potential conflict of interest.

Publisher's note

All claims expressed in this article are solely those of the authors and do not necessarily represent those of their affiliated organizations, or those of the publisher, the editors and the reviewers. Any product that may be evaluated in this article, or claim that may be made by its manufacturer, is not guaranteed or endorsed by the publisher.

References

Ahmed, F., Dutta, N. K., Zannettino, A., Vandyke, K. I., and Choudhury, N. R. (2014). Engineering interaction between bone marrow derived endothelial cells and electrospun surfaces for artificial vascular graft applications. *Biomacromolecules* 15, 1276–1287. doi:10.1021/bm401825c

Balint, R., Cassidy, N. J., and Cartmell, S. H. (2013). Electrical stimulation: A novel tool for tissue engineering. *Tissue Eng. Part B Rev.* 19, 48–57. doi:10.1089/ten.TEB.2012.0183

Benz, M., and Euler, W. B. (2003). Determination of the crystalline phases of poly(vinylidene fluoride) under different preparation conditions using differential scanning calorimetry and infrared spectroscopy. *J. Appl. Polym. Sci.* 89, 1093–1100. doi:10.1002/app.12267

Bergmeister, H., Schreiber, C., Grasl, C., Walter, I., Plasenzotti, R., Stoiber, M., et al. (2013). Healing characteristics of electrospun polyurethane grafts with various porosities. *Acta Biomater.* 9, 6032–6040. doi:10.1016/j.actbio.2012.12.009

Bhardwaj, N., and Kundu, S. C. (2010). Electrospinning: A fascinating fiber fabrication technique. *Biotechnol. Adv.* 28, 325–347. doi:10.1016/j.biotechadv.2010.01.004

Bouaziz, A., Richert, A., and Caprani, A. (1997). Vascular endothelial cell responses to different electrically charged poly(vinylidene fluoride) supports under static and oscillating flow conditions. *Biomaterials* 18, 107–112. doi:10.1016/S0142-9612(96)00114-7

Brito-Pereira, R., Correia, D. M., Ribeiro, C., Francesko, A., Etxebarria, I., Pérez-Álvarez, L., et al. (2018). Silk fibroin-magnetic hybrid composite electrospun fibers for tissue engineering applications. *Compos. Part B Eng.* 141, 70–75. doi:10.1016/j.compositesb.2017.12.046

Brito-Pereira, R., Macedo, A. S., Ribeiro, C., Cardoso, V. F., and Lanceros-Méndez, S. (2022). Natural based reusable materials for microfluidic substrates: The silk road towards sustainable portable analytical systems. *Appl. Mat. Today* 28, 101507. doi:10.1016/j.apmt.2022.101507

Brito-Pereira, R., Macedo, A. S., Tubio, C. R., Lanceros-Méndez, S., and Cardoso, V. F. (2021). Fluorinated polymer membranes as advanced substrates for portable Analytical systems and their proof of concept for colorimetric bioassays. *ACS Appl. Mat. Interfaces* 13, 18065–18076. doi:10.1021/acsami.1c00227

Cai, M., He, H., Zhang, X., Yan, X., Li, J., Chen, F., et al. (2019). Efficient synthesis of PVDF/PI side-by-side bicomponent nanofiber membrane with enhanced mechanical strength and good thermal stability. *Nanomater. (Basel)* 9, 39. doi:10.3390/nano9010039

Cardoso, V. F., Lopes, A. C., Botelho, G., and Lanceros-Méndez, S. (2015). Poly(vinylidene fluoride-trifluoroethylene) porous films: Tailoring microstructure and physical properties by solvent casting strategies. *Soft Mat.* 13, 243–253. doi:10.1080/1539445X.2015.1083444

Cui, L., Li, J., Long, Y., Hu, M., Li, J., Lei, Z., et al. (2017). Vascularization of LBL structured nanofibrous matrices with endothelial cells for tissue regeneration. *RSC Adv.* 7, 11462–11477. doi:10.1039/c6ra26931a

Durán-Rey, D., Crisóstomo, V., Sánchez-Margallo, J. A., and Sánchez-Margallo, F. M. (2021). Systematic review of tissue-engineered vascular grafts. *Front. Bioeng. Biotechnol.* 9, 771400. doi:10.3389/fbioe.2021.771400

Fernandes, M. M., Correia, D. M., Ribeiro, C., Castro, N., Correia, V., and Lanceros-Mendez, S. (2019). Bioinspired three-dimensional magnetoactive scaffolds for bone tissue engineering. *ACS Appl. Mat. Interfaces* 11, 45265–45275. doi:10.1021/acsami.9b14001

Haddadi, S. A., Ghaderi, S., Amini, M., and Ramazani, S. A. A. (2018). Mechanical and piezoelectric characterizations of electrospun PVDF-nanosilica fibrous scaffolds for biomedical applications. *Mater. Today Proc.* 5, 15710–15716. Part 3. doi:10.1016/j.matpr.2018.04.182

Hauser, S., Jung, F., and Pietzsch, J. (2017). Human endothelial cell models in biomaterial research. *Trends Biotechnol.* 35, 265–277. doi:10.1016/j.tibtech.2016.09.007

Heo, S. J., Nerurkar, N. L., Baker, B. M., Shin, J. W., Elliott, D. M., and Mauck, R. L. (2011). Fiber stretch and reorientation modulates mesenchymal stem cell morphology and fibrous gene expression on oriented nanofibrous microenvironments. *Ann. Biomed. Eng.* 39, 2780–2790. doi:10.1007/s10439-011-0365-7

Hitscherich, P., Wu, S., Gordan, R., Xie, L. H., Arinzeh, T., and Lee, E. J. (2016). The effect of PVDF-TrFE scaffolds on stem cell derived cardiovascular cells. *Biotechnol. Bioeng.* 113, 1577–1585. doi:10.1002/bit.25918

Khorshidi, S., Solouk, A., Mirzadeh, H., Mazinani, S., Lagaron, J. M., Sharifi, S., et al. (2015). A review of key challenges of electrospun scaffolds for tissue-engineering applications. *J. Tissue Eng. Regen. Med.* 4, 524–531. doi:10.1002/term.1978

Kitsara, M., Blanquer, A., Murillo, G., Humblot, V., Vieira, S. B., Nogués, C., et al. (2019). Permanently hydrophilic, piezoelectric PVDF nanofibrous scaffolds promoting unaided electromechanical stimulation on osteoblasts. *Nanoscale* 11, 8906–8917. doi:10.1039/c8nr10384d

Kocherova, I., Bryja, A., Mozdziak, P., Volponi, A. A., Dyszkiewicz-Konwińska, M., Piotrowska-Kempisty, H., et al. (2019). Human umbilical vein endothelial cells (HUVECs) co-culture with osteogenic cells: From molecular communication to engineering prevascularised bone grafts. *J. Clin. Med.* 8, 1602. doi:10.3390/jcm8101602

Li, Y., Liao, C., and Tjong, S. C. (2019). Electrospun polyvinylidene fluoride-based fibrous scaffolds with piezoelectric characteristics for bone and neural tissue engineering. *Nanomater. (Basel).* 9, 952. doi:10.3390/nano9070952

Maciel, M. M., Ribeiro, S., Ribeiro, C., Francesko, A., Maceiras, A., Vilas, J. L., et al. (2017). Relation between fiber orientation and mechanical properties of nano-engineered poly(vinylidene fluoride) electrospun composite fiber mats. *Compos. Part B Eng.* 139, 146–154. doi:10.1016/j.compositesb.2017.11.065

Martins, P., Lopes, A. C., and Lanceros-Mendez, S. (2014). Electroactive phases of poly(vinylidene fluoride): Determination, processing and applications. *Prog. Polym. Sci.* 39, 683–706. doi:10.1016/j.progpolymsci.2013.07.006

Mokhtari, F., Azimi, B., Salehi, M., Hashemikia, S., and Danti, S. (2021). Recent advances of polymer-based piezoelectric composites for biomedical applications. *J. Mech. Behav. Biomed. Mat.* 122, 104669. doi:10.1016/j.jmbbm.2021.104669

Motamedi, A. S., Mirzadeh, H., Hajiesmaeilbaigi, F., Bagheri-Khoulenjani, S., and Shokrgozar, M. A. (2017a). Piezoelectric electrospun nanocomposite comprising Au NPs/PVDF for nerve tissue engineering. *J. Biomed. Mat. Res. A* 105, 1984–1993. doi:10.1002/jbm.a.36050

Motamedi, A. S., Mirzadeh, H., Hajiesmaeilbaigi, F., Bagheri-Khoulenjani, S., and Shokrgozar, M. A. (2017b). Piezoelectric electrospun nanocomposite comprising Au NPs/PVDF for nerve tissue engineering. *J. Biomed. Mat. Res. A* 7, 1984–1993. doi:10.1002/jbm.a.36050

Otitoju, T. A., Ahmad, A. L., and Ooi, B. S. (2017). Superhydrophilic (superwetting) surfaces: A review on fabrication and application. *J. Ind. Eng. Chem.* 47, 19–40. doi:10.1016/j.jiec.2016.12.016

Penkala, R. A., and Kim, S. S. (2007). Gastrointestinal tissue engineering. *Expert Rev. Med. Devices* 4, 65–72. doi:10.1586/17434440.4.1.65

Razafiarison, T., Holenstein, C. N., Stauber, T., Jovic, M., Vertudes, E., Loparic, M., et al. (2018). Biomaterial surface energy-driven ligand assembly strongly regulates stem cell mechanosensitivity and fate on very soft substrates. *Proc. Natl. Acad. Sci. U. S. A.* 115, 4631–4636. doi:10.1073/pnas.1704543115

Ribeiro, C., Costa, C. M., Correia, D. M., Nunes-Pereira, J., Oliveira, J., Martins, P., et al. (2018a). Electroactive poly(vinylidene fluoride)-based structures for advanced applications. *Nat. Protoc.* 13, 681–704. doi:10.1038/nprot.2017.157

Ribeiro, C., Sencadas, V., Ribelles, J. L. G., and Lanceros-Méndez, S. (2010). Influence of processing conditions on polymorphism and nanofiber morphology of electroactive poly(vinylidene fluoride) electrospun membranes. *Soft Mat.* 8, 274–287. doi:10.1080/1539445X.2010.495630

Ribeiro, S., Gomes, A. C., Etxebarria, I., Lanceros-Méndez, S., and Ribeiro, C. (2018b). Electroactive biomaterial surface engineering effects on muscle cells differentiation. *Mater. Sci. Eng. C* 92, 868–874. doi:10.1016/j.msec.2018.07.044

Ribeiro, S., Ribeiro, T., Ribeiro, C., Correia, D. M., Farinha, J. P. S., Gomes, A. C., et al. (2018c). Multifunctional platform based on electroactive polymers and silica nanoparticles for tissue engineering applications. *Nanomaterials* 8, 933. doi:10.3390/nano8110933

Seminara, L., Capurro, M., Cirillo, P., Cannata, G., and Valle, M. (2011). Electromechanical characterization of piezoelectric PVDF polymer films for tactile sensors in robotics applications. *Sensors Actuators A Phys.* 169, 49–58. doi:10.1016/j.sna.2011.05.004

Sun, H.-J., Wu, Z.-Y., Nie, X.-W., and Bian, J.-S. (2020). Role of endothelial dysfunction in cardiovascular diseases: The link between inflammation and hydrogen sulfide. *Front. Pharmacol.* 10, 01568. doi:10.3389/fphar.2019.01568

Szewczyk, P. K., Ura, D. P., Metwally, S., Knapczyk-Korczak, J., Gajek, M., Marzec, M. M., et al. (2018). Roughness and fiber fraction dominated wetting of electrospun fiber-based porous meshes. *Polym. (Basel)* 11, 34. doi:10.3390/polym11010034

Veleva, A. N., Heath, D. E., Johnson, J. K., Nam, J., Patterson, C., Lannutti, J. J., et al. (2009). Interactions between endothelial cells and electrospun methacrylic terpolymer fibers for engineered vascular replacements. *J. Biomed. Mat. Res. A* 91, 1131–1139. doi:10.1002/jbm.a.32276

Wang, H. W., Zhou, H. W., Gui, L. L., Ji, H. W., and Zhang, X. C. (2014). Analysis of effect of fiber orientation on Young's modulus for unidirectional fiber reinforced composites. *Compos. Part B Eng.* 56, 733–739. doi:10.1016/j.compositesb.2013.09.020

Weinberger, F., Mannhardt, I., and Eschenhagen, T. (2017). Engineering cardiac muscle tissue: A maturating field of research. *Circ. Res.* 120, 1487–1500. doi:10.1161/CIRCRESAHA.117.310738

Yu, C., Xing, M., Wang, L., and Guan, G. (2020). Effects of aligned electrospun fibers with different diameters on hemocompatibility, cell behaviors and inflammation *in vitro*. *Biomed. Mat.* 15, 035005. doi:10.1088/1748-605X/ab673c

Resultados y Discusión

Bloque I) Estado actual de los injertos vasculares de ingeniería tisular.

A continuación, se presentan los principales resultados hallados en el análisis del momento actual de los injertos vasculares de ingeniería de tejidos obtenidos de la revisión sistemática recogida en la publicación *Systematic review of tissue-engineered vascular grafts* (Durán-Rey et al., 2021) y que aparecen en esta tesis doctoral en el Bloque I.

Como se ha comentado con anterioridad, el tratamiento de las patologías vasculares es la cirugía convencional mediante el uso de injertos autólogos. Sin embargo, pueden no estar disponibles estos injertos en ciertos pacientes. Por otro lado, existen prótesis comerciales diseñadas a partir de materiales sintéticos como el politetrafluoroetileno expandido (ePTFE), los cuales exhiben resultados satisfactorios en anastomosis arteriales de diámetros superiores a 6 mm [8,122]. No obstante, las prótesis comerciales de pequeño diámetro (inferior a 6 mm) están asociadas a la obstrucción del vaso sanguíneo tras un breve periodo de implantación debido a los bajos índices de permeabilidad y posterior formación de trombos [123]. Por consiguiente, los TEVGs representan un área innovadora de investigación que tiene como objetivo ofrecer una disponibilidad continua y tratamiento inmediato para patologías vasculares. Los TEVGs son un campo multidisciplinar que combina ingeniería biomédica, ciencia de los materiales y medicina regenerativa. Por esta razón, este estudio analiza los resultados publicados recientemente en el campo del desarrollo de TEVG, así como la influencia del diámetro del injerto y el uso de heparina en la aparición de trombos y la permeabilidad del injerto. Se utilizaron una serie de criterios de inclusión y exclusión predeterminados, seleccionando finalmente un total de 92 artículos para su análisis.

Modelos experimentales

Se hallaron investigaciones realizados en seis modelos animales diferentes, siendo de mayor a menor frecuencia de uso el roedor, ovino, porcino, conejo, perro y primate. Para poder obtener resultados traslacionales, el modelo experimental seleccionado para estos estudios debería presentar una anatomía y una fisiología cardiovascular muy similar a las del ser humano. Sin embargo, cada uno presenta una serie de peculiaridades, no existiendo un modelo ideal. Aunque los roedores son los más empleados, se debe en gran medida a su bajo coste y por la facilidad de obtener un gran tamaño muestral [8]. Por esta razón, de todos los modelos experimentales y de acuerdo con los resultados hallados, cabe destacar el ovino como un modelo adecuado para el estudio de los TEVGs. Estos animales presentan una endotelización, mecanismos de trombogenicidad y sistema de fibrinólisis muy similares al de los humanos [8,124]. Además, la anatomía de los ovinos les confiere un cuello alargado, facilitando la implantación de los TEVGs [125]. Sin embargo, la principal desventaja de esta especie es que tienen una alta tendencia a la hipercoagulabilidad [8].

Tipos de materiales

Idealmente, del análisis se desprende que los TEVGs deberían parecerse lo más posible a los vasos sanguíneos nativos. En otras palabras, deben tener capacidad de remodelarse, crecer, autorrepararse y responder al entorno inmediato [7]. Se han hallado una amplia variedad de materiales utilizados en el diseño de TEVGs en los artículos analizados, pudiéndolos dividir en materiales naturales y sintéticos. En términos generales, los materiales naturales presentan baja antigenicidad y buena biocompatibilidad, mientras los materiales sintéticos tienen propiedades mecánicas superiores a los naturales, siendo capaces de soportar diferentes presiones, torsiones y estiramientos [25,28,34]. Analizando los artículos seleccionados, hallamos que el colágeno (natural) y el ácido poliglicólico (sintético) son los materiales más ampliamente utilizados, ya que mejoran la adhesión y proliferación celular, y por su alto nivel de flexibilidad y ausencia de respuesta inflamatoria, respectivamente [27,58]. Sin embargo, hay una propensión en el uso de polímeros sintéticos debido a sus

propiedades mecánicas y al crecimiento exponencial de investigaciones destinadas a comprobar la biocompatibilidad de estos materiales, siendo más seguro su uso clínico. Ambas características, mecánicas y biológicas, son esenciales en el diseño de un TEVG. En vista de que cada material, ya sea natural o sintético, tiene una serie de cualidades propias, surgió la posibilidad de crear un injerto híbrido. Este tipo de TEVG está compuesto por la hibridación de materiales sintéticos y biológicos, consiguiendo un injerto vascular con las ventajas de ambos materiales, es decir, presentan unas condiciones biológicas y mecánicas mejoradas [126].

Por otro lado, apreciamos que existe una tendencia en el uso de materiales biodegradables. Cuando se utiliza un TEVG, lo ideal sería que al principio el material otorgue al injerto la suficiente resistencia para poder ser utilizado, pero progresivamente éste se iría degradando y reemplazando al mismo tiempo por el nuevo tejido procedente el propio organismo [7]. Sin embargo, el tiempo de degradación de los materiales puede variar en función de diferentes factores del material, tales como el peso molecular, cristalinidad, entre otros factores [31,127]. Además, hay que tener en cuenta que el tiempo de degradación de los TEVGs es difícil de predecir en los estudios *in vivo*, ya que varía en función de la arquitectura del injerto, lugar de implantación, y el tipo y concentración de enzimas [128].

Metodologías y técnicas

Actualmente existe un amplio abanico de metodologías y técnicas para desarrollar un TEVG, tales como la descelularización de un vaso nativo en la que se obtiene la matriz extracelular y se conserva las propiedades biológicas [67], o la biompresión 3D que proporciona una alta densidad y distribución adecuada [28], entre muchos otros. Sin embargo, la técnica más empleada y con la que mejores resultados se ha obtenido es el *electrospinning* o electrohilado. Esta metodología tiene la capacidad de producir estructuras con nano o microfibras, las cuales pueden tener una orientación o no controlada [129], proporcionando de tal manera porosidad [130]. El electrohilado puede diseñar TEVGs con una topografía muy similar al de la matriz extracelular de los vasos sanguíneos nativos, demostrando tener un gran impacto positivo en el

comportamiento celular y en las propiedades transferencia de nutrientes y residuos [131]. Por todos estos motivos, el electrohilado es una técnica ideal para el desarrollo de estructuras destinadas a aplicaciones biomédicas, incluyendo los TEVGs.

Durante el diseño de los TEVGs, éstos también pueden ser sembrados con células. Las células madre mesenquimales las hiPSCs, son algunas de las células que pueden ser utilizadas en el sembrado celular debido a su capacidad, entre muchas otras, de reducir el rechazo inmunitario [8,31]. Debemos destacar que las células endoteliales son el grupo celular más utilizado entre los autores. Estas células son un componente clave en los vasos sanguíneos, ya que la capa endotelial de los vasos sanguíneos desempeña un papel fundamental en el mantenimiento de la permeabilidad [108]. Cualquier daño o falta de éstas son factores de riesgo que pueden provocar la aparición de trombos [8]. Por esta razón, el cultivo de células endoteliales en TEVGs proporciona efectos anticoagulantes [108] y mejoran la endotelización [35]. No obstante, actualmente existe controversia en el sembrado celular de los TEVGs, ya que se desconoce el número óptimo de células, puede existir falta de unión entre ellas, se puede producir muerte celular durante el procesamiento del injerto, etc. [132]. Además, el uso de estas células conlleva la toma de biopsias a los pacientes y largos tiempos de cultivo celular, no ofreciendo la opción de un tratamiento inmediato. Por otro lado, los artículos analizados mostraron resultados bastante similares entre los TEVGs con y sin sembrado celular, demostrando que ambos tipos de diseño de injerto vascular presentan buena permeabilidad, ausencia de inmunogenicidad y una regeneración tisular funcional.

Desafíos y avances en los TEVGs

Actualmente, los TEVGs diseñados tienen una durabilidad y permeabilidad limitadas. Esto se debe en gran medida a que el enfoque de la ingeniería de tejidos en el ámbito cardiovascular es el desarrollo de injertos vasculares de un diámetro menor a 6 mm, ya que existen prótesis comerciales con resultados óptimos en anastomosis vasculares de un diámetro mayor. Estos TEVGs de pequeño diámetro son especialmente propensos a la aparición de trombos, reducción de la permeabilidad y,

por tanto, la posterior obstrucción vascular [8,31,133]. El uso de sustancias anticoagulantes intraoperatorias, como la heparina, puede ser de utilidad para prevenir la aparición de trombos y evitar una estenosis vascular [102]. Por consiguiente, en el artículo correspondiente a este bloque temático [134], se analizó la influencia del diámetro de los diferentes TEVGs diseñados con respecto a la aparición de trombos y la permeabilidad vascular, así como el uso de heparina durante la cirugía. Los resultados mostraron en general que la tasa de aparición de trombos y la falta de permeabilidad era mayor cuanto más pequeño era el diámetro del injerto vascular desarrollado. Además, parece que existe una correlación positiva entre el uso de heparina, la mejora de permeabilidad y la ausencia de trombos. En esencia, los TEVGs son dispositivos médicos que están en contacto con la sangre del paciente. Por ello, hay una serie de factores de riesgo a tener en cuenta que deben evitarse para prevenir la aparición de trombos y mejorar la permeabilidad del injerto vascular, especialmente en aquellos que presenten un diámetro pequeño. Estos puntos críticos pueden estar asociados principalmente con la técnica quirúrgica, tales como falta de experiencia y habilidad quirúrgica, tensión en la línea de sutura, daños del propio injerto durante la cirugía, factores hemodinámicos por diferencias en el diámetro del injerto con respecto al vaso nativo que provoquen un desajuste en el flujo sanguíneo, etc. [8], o por problemas del propio TEVG, como la falta de porosidad del injerto que provoque una endotelización insuficiente, propiedades mecánicas inadecuadas, reacción inmunitaria por una mala elección del material, mala topografía interna del injerto que provoque adhesión plaquetaria, entre otros [31,35,135].

Como se ha comentado con anterioridad, el uso de anticoagulantes durante la cirugía es necesario para evitar la aparición de trombos y mejorar la permeabilidad vascular. Además, la terapia anticoagulante a largo plazo es requerida cuando se implantan prótesis comerciales [136]. Por otro lado, una de las metas del campo de investigación de los TEVGs es prescindir de dicho tratamiento [137]. No obstante, actualmente sigue siendo relevante el uso de estas terapias para prevenir la aparición de trombos, debido a que aún no existe un diseño ideal de TEVG que presente las condiciones fisicoquímicas y biológicas aptas para estudios clínicos.

Por último, es preciso destacar también los tres estudios en humanos analizados en este bloque temático [37,138,139]. La utilización de estos injertos vasculares en pacientes humanos sigue siendo muy restringida debido a la aparición de patologías asociadas a la implantación, tales como presencia de estenosis, trombos, o escasa permeabilidad, entre otras, además del uso de terapias anticoagulantes durante el período posoperatorio. Ante estos resultados, está claro que más estudios son necesarios plazo para corregir todos los efectos no deseados. No obstante, la existencia de estudios clínicos en humanos es indicativa de los avances logrados en el campo de TEVG.

Bloque II) Análisis fisicoquímicos y biológicos de materiales naturales y sintéticos destinados a ingeniería tisular.

Una vez analizados de forma objetiva y sistemática los diferentes materiales, metodologías, avances y retos hallados en el desarrollo de los TEVGs, abordamos el segundo bloque temático de la presente tesis doctoral. Comparando los resultados del primer bloque, seleccionamos un material natural, fibroína de seda (SF; *silk fibroin*), y un material sintético, fluoruro de polivinilideno (PVDF; *poly(vinylidene fluoride)*). Ambos materiales fueron utilizados para diseñar estructuras básicas, como son las membranas, a partir de diferentes metodologías de ingeniería tisular para analizar sus condiciones fisicoquímicas y biológicas. Los objetivos de estos estudios fueron comprobar si ambos materiales presentan unas condiciones válidad para ser utilizados en la ingeniería de tejidos, y se seleccionó la mejor metodología para el diseño de TEVGs.

A continuación, se muestran los resultados conjuntos del artículo publicado en *Biomacromolecules* (*Durán-Rey et al., "Development of silk fibroin scaffolds for vascular repair"*), y de otro publicado en *Frontiers in Bioengineering and Biotechnology* (*Durán-Rey et al.,* "*Development and evaluation of different electroactive poly(vinylidene fluoride) architectures for endothelial cell culture*"). Dichos artículos científicos forman parte del Bloque II.

Un material natural citado en el bloque temático I es la SF. Esta proteína es biocompatible y no inmunogénica [140]. Además, gracias a sus propiedades piezoeléctricas, promueve la angiogénesis [141]. Este proceso fisiológico está modulado por señales eléctricas que promueven la migración, crecimiento y diferenciación de células endoteliales, las cuales pueden ser moduladas mediante campos eléctricos [142,143]. Debido a este fenómeno, la SF puede promover el crecimiento de células endoteliales, induciendo la regeneración tisular y ayudando a la prevención del desarrollo de trombos durante la implantación de un injerto vascular [141].

Por otra parte, el PVDF (-CH2-CF2-) es un polímero sintético ampliamente utilizado en aplicaciones biomédicas, tales como implantes de hueso [144], músculo [145], nervio [146], entre otros. Su resistencia química, propiedades mecánicas y eléctricas, así como su biocompatibilidad [147], hacen que este material termoplástico sea ideal para aplicaciones de TEVGs. Además, se ha comprobado que las características eléctricas de este material ayudan a la regeneración tisular [146].

Es preciso remarcar que la SF y el PVDF presentan una cualidad común, y es que exhiben propiedades piezoeléctricas [148,149]. Ante una estimulación, ya sea por deformación mecánica o estrés físico, los materiales piezoeléctricos tienen la capacidad de imitar el microambiente electroactivo de las células. Por dicho motivo, este tipo de materiales podrían ser muy útiles para emplearse en diferentes aplicaciones biomédicas de regeneración de tejidos y combinarse con otras particularidades (rigidez, tamaño de poros, grado de porosidad, topografía, etc.) propias de tejidos como la piel, el hueso y el tendón, así como en el ámbito de los injertos vasculares.

Por otro lado, como se indicó en el bloque temático I [134], existe una amplia variedad de metodologías utilizadas en la creación de injertos vasculares, siendo el electrohilado la técnica mayormente empleada y con mejores resultados obtenidos. Por esta razón, quisimos investigar dicha técnica y compararla con otras metodologías utilizadas en ingeniería de tejidos, tales como *solvent-casting* y lixiviación de sales, obteniendo estructuras básicas, como son las membranas electrohiladas, *films* o

películas, y membranas porosas (PM; *porous membrane*), respectivamente. De esta manera, pudimos caracterizar las peculiaridades fisicoquímicas y biológicas de la SF o el PVDF cuando se diseñan morfologías *a priori* similares.

Para analizar dichas propiedades, las diferentes estructuras de SF y PVDF fueron sometidas a estudios de microscopia electrónica de barrido, humectabilidad (capacidad de un líquido para extenderse sobre una superficie), mecánicos, químicos y biológicos.

Estructura microscópica

Una vez diseñadas las estructuras de SF y PVDF, las diferentes morfologías se analizaron mediante un microscopio electrónico de barrido. Las películas presentaban una estructura lisa y sin huecos, las PM resultaron en estructuras porosas, y las membranas electrohiladas estaban compuestas por una superficie lisa compuesta por fibras cilíndricas. La morfología microscópica de estas estructuras es de gran importancia en las aplicaciones biomédicas, ya que estas arquitecturas deberían ser diferentes en función de las condiciones biofísicas del tejido diana. Las películas son morfologías compactas, por lo que su implantación en tejidos que necesiten porosidad se ve dificultada. Por su parte, se puede controlar el tamaño y cantidad de los poros de las PM variando el tamaño y número de las partículas de sal. Sin embargo, dichas partículas se distribuyen aleatoriamente y dificultan la obtención de estructuras con una red de poros regulares no interconectados, resultando en morfologías irregulares y no reproducibles [150,151]. En cuanto a la técnica del electrohilado, las fibras pueden ser diseñadas para que estén orientadas (ES-O; *electrospun oriented fibers*) o aleatorias (ES-NO; *electrospun non-oriented fibers*), proporcionando una porosidad variable. Esta técnica puede modular las propiedades biofísicas de los tejidos, ya que la porosidad, la morfología, dirección, e incluso el diámetro de las fibras pueden ajustarse en función de los parámetros de procesamiento específicos del electrohilado [150,152,153].

Humectabilidad

Por otro lado, también se determinó la humectabilidad o *wettability* de SF y PVDF, la cual es un parámetro clave para la adhesión y la proliferación celular [154,155]. Para ello, se calculó el ángulo que forma la superficie de una gota de agua al entrar en contacto con las diferentes estructuras (ángulo de contacto). Un material se considera que presenta superficies hidrófobas cuando muestran valores superiores a 90°, mientras que los inferiores a 90° corresponden a superficies hidrófilas [156]. Todas las morfologías analizadas en nuestros estudios [157,158] mostraron un ángulo de contacto superior a 90°, por lo que presentan un comportamiento hidrofóbico. La compacidad, composición, cristalinidad, y rugosidad de superficie son factores que afectan en la humectabilidad del material.

Características mecánicas

Las propiedades mecánicas de un material son esenciales para obtener morfologías seguras y duraderas para su aplicación biomédica, ya que dichas características vienen determinadas principalmente por su estructura interna. Por consiguiente, se hallaron las mediciones de tensión-deformación, las cuales son claves para entender el comportamiento de las estructuras diseñadas, tanto de SF como de PVDF. Para una mayor comprensión, cuando a un material se le aplica una fuerza de tensión, éste presenta un primer régimen elástico lineal, en el que la estructura recupera su forma original al cesar la tensión, seguido de un régimen plástico, en el que el material no recupera su forma original, sufriendo una deformación permanente. Si la fuerza continúa, se alcanza el punto de ruptura. Por tanto, dependiendo del comportamiento del mismo, podemos dividirlos en materiales dúctiles, que presentan una zona elástica y plástica típica perfectamente diferenciada, y frágiles, que suelen presentar poca o ninguna deformación plástica. Además, también se calculó el módulo de elasticidad o de Young, el cual caracteriza el comportamiento de un material elástico, aumentando su valor cuando mayor es la rigidez del material [159].

Las películas, tanto de SF como de PVDF, presentaban el valor más alto del módulo de Young. Esta estructura presenta una morfología compacta y densa, siendo por consiguiente más rígido [151]. Por otra parte, las PM de ambos materiales presentaban valores del módulo de elasticidad y de tensión-deformación más bajos que las películas. La rigidez de las PM viene determinada por la deformación de la estructura porosa. Además, estos valores presentan una mayor variabilidad debido a la distribución aleatoria de los poros [151].

Es preciso remarcar que los valores del módulo de Young y de tensión-deformación de la SF también vienen determinados por las características intrínsecas del material. La SF está formada principalmente por regiones amorfas no ordenadas (*random coils*) y una red de enlaces de hidrógeno de cristalitos con estructura β (*β-sheets*). Las primeras estructuras son las encargadas de proporcionar flexibilidad y elasticidad, mientras que las segundas generan la resistencia y rigidez del material [160]. Durante el procesado y preparación de las muestras de las películas y PM de SF, se realizó una evaporación lenta del disolvente para evitar inestabilidades de Marangoni, tales como la aparición de superficies más rugosas [161,162]. Esta evaporación lenta da lugar a estructuras con una buena organización en su cadena polimérica y altamente cristalizada [163], con un contenido mayor en *β-sheets* y menor en *random coils* [161]. Esto puede verse reflejado en los altos valores del módulo Young en las películas y PM, presentando una gran rigidez estas dos estructuras de SF.

Las películas y PM de SF muestran curvas de tensión-deformación típicas de los materiales frágiles, en la que presentan poca o ninguna deformación plástica, respectivamente. Esto es debido al alto contenido en *β-sheets* y bajo en *random coils*, previamente explicado, mostrando una elongación máxima del 4% con respecto al tamaño original de las muestras, valor que corresponde al punto de rotura de las curvas de tensión-deformación. En cuanto a las películas y PM de PVDF presentaban curvas de tensión-deformación típicas de los materiales dúctiles, es decir, tienen una zona elástica y plástica. Esto es indicativo de que el comportamiento mecánico de dichas muestras es intrínseco de la arquitectura de las estructuras, y que no se ven

influenciadas por el tipo de procesamiento llevado a cabo, llegando a elongaciones máximas cercanas al 20%.

En cuanto a las membranas electrohiladas de SF y PVDF, el módulo de Young es mayor en ES-O orientada en la misma dirección de la fuerza ejercida (ES-O (0°)), mientras que ES-NO y ES-O orientada perpendicularmente a la dirección de la fuerza aplicada (ES-O (90°)) presentan valores menores. El módulo de elasticidad varía en función de la orientación relativa de las fibras y la dirección de estiramiento, disminuyendo dicho valor cuando aumenta el ángulo entre la dirección de deformación y la orientación de las fibras [129,164,165]. Cuando se aplica una tensión mecánica en una membrana diseñada por electrohilado, se produce una reorientación de las fibras y un colapso de los poros a medida que las éstas se contraen en la dirección de la fuerza aplicada [164].

Todas las membranas diseñadas con electrohilado, independientemente de que hayan sido desarrolladas con SF o PVDF, mostraron curvas de tensión-deformación de materiales dúctiles. La tensión y límite elástico son mayores en ES-O (0°) que en ES-NO y ES-O (90°). Cuando se ejerce fuerza en el caso de ES-O (0°), la tensión se aplica a lo largo de las fibras. Sin embargo, el efecto inicial en la tensión ejercida en ES-NO y ES-O (90°) produce la reorientación de las fibras a en la dirección de estiramiento [129]. De hecho, ambos materiales presentan puntos de rotura superiores al 20%. En el caso de SF, sus propiedades mecánicas son superiores a las de otros materiales naturales, como la elastina, la resilina o la lana, entre otros [166]. Por su parte, las membranas electrohiladas de PVDF pueden llegar a una elongación del 142%, indicando su gran comportamiento dúctil [167]. En definitiva, las propiedades mecánicas de los materiales de SF y PVDF diseñadas con electrohilado, pueden modificarse en función de la orientación de las fibras, ajustándose en función de la aplicación biomédica.

Finalmente, es preciso destacar que la tecnología de electrohilado provoca que la SF se comporte como un material dúctil, aumentando su régimen plástico. Esto es debido a la rápida evaporación del disolvente durante el proceso de electrohilado, provocando un aumento de los *random coils* y una disminución en la formación de *β-sheets* [161].

Características químicas

Para analizar las características químicas de las diferentes membranas se utilizó la espectroscopía de infrarrojos (FTIR; *Fourier transform infrared spectroscopy*), la cual utiliza la interferometría (método de medición que utiliza el fenómeno de interferencia de ondas) para codificar información sobre una muestra colocada en el haz de infrarrojos, de tal manera que se obtienen datos relativos a la estructura de los materiales. Se hallaron diferencias tanto en SF como en PVDF, indicando que el método de procesado induce ciertos cambios químicos. Por una parte, se encontraron un aumento en las proporciones de *random coils* respecto a las *β-sheets* en las membranas electrohiladas de SF. La conformación *β-sheets* es la que se encuentra en más proporción en todas las morfologías, siendo más del 60% en las películas y PM, y del 35% en las membranas electrohiladas [158]. Además, la presencia de sal en el caso de las PM conlleva un aumento en el contenido β-sheet [168], mostrando solamente un 9% de *random coils*, hallazgo que explica la ausencia de zona plástica en los estudios mecánicos anteriores. Como se comentó anteriormente, estas variaciones en la estructura se deben a la metodología empleada, donde una evaporación lenta del disolvente provoca una mejor organización de la cadena polimérica y, por tanto, la creación de una estructura altamente cristalizada [161,169], como es en el caso de las películas y PM. Por su parte, la fase cristalina del PVDF también se ve afectada por la metodología empleada. El PVDF presenta varias formas dependiendo de la conformación de la cadena molecular [170], destacando la fase α, la cual tiene la energía potencial más baja, y la fase β, responsable de gran parte de la actividad piezoeléctrica del material [171]. La temperatura de procesado es un factor clave que determina la fase cristalina del polímero [147], presentando un mayor contenido en la fase α de las películas por su diseño a altas temperaturas. En el caso del resto de estructuras de PVDF, al ser procesadas a temperatura ambiente, se caracterizan por tener un mayor contenido de fase β electroactiva. Concretamente, aquellas morfologías de PVDF desarrolladas a temperatura ambiente presentaban un contenido de fase β electroactiva superior al 88%, mientras que para las películas obtenidas tras el procesado a alta temperatura se reduce por debajo del 7% [157].

Otra característica química importante es la estabilidad térmica de los materiales, la cual se calcula mediante la calorimetría de barrido diferencial (DSC; *differential scanning calorimetry*). Esta técnica permite determinar el punto de fusión de una muestra, el cual resulta evidenciado por un pico endotérmico. Los termogramas de SF se caracterizaron por tener un pico endotérmico similar, aproximadamente 280°C, demostrando que la estructura física no afecta sustancialmente a las propiedades térmicas del material [172]. Sin embargo, las PM de SF mostraron un pico endotérmico ligeramente superior en torno a los 300°C, probablemente debido a una mayor formación de conformaciones *β-sheets* durante el proceso de difusión de las partículas de sal en agua ultrapura. Por su parte, en las estructuras de PVDF se encontraron pequeñas variaciones en el punto de fusión entre las películas (135.7 ± 3.5°C) y el resto de las membranas (138.8 ± 4.0°C), las cuales se atribuyen a las condiciones de cristalización, previamente explicadas. Además, también se halló el grado de cristalinidad en las estructuras de PVDF, el cual fue calculado mediante la entalpía o calor de fusión obtenida a partir del área bajo el pico de fusión de cada termograma. Todas las morfologías de PVDF presentaron grados de cristalinidad similares (40-55%), por lo que la disminución de la fase β de las películas no provoca cambios significativos en dicho valor [147]. Por consiguiente, las variaciones en los resultados mecánicos de las estructuras de PVDF, previamente explicados, no se ven afectadas por el grado de cristalinidad del material, sino por diferencias en las características morfológicas [159].

Degradación del material

Un dato relevante para tener en cuenta con respecto a SF y PVDF es la degradación del material. Como se comentó en el bloque temático I, los materiales pueden ser o no biodegradables. Sin embargo, lo ideal en el diseño de un TEVG es que sea biodegradable para que se vaya degradando y reemplazando al mismo tiempo por el nuevo tejido procedente el propio organismo [7]. Una de las propiedades de SF es que es un material biodegradable [173], mientras que el PVDF presenta estabilidad química [174]. La mayor o menor pérdida de peso de las muestras se ve afectada por su superficie y arquitectura de la muestra, la cual está a su vez relacionada con la

metodología empleada, ya que varía su morfología y microestructura. Como se explicó en el bloque I, la degradación es difícil de predecir, ya que hay muchos factores que pueden intervenir, tales como la propia arquitectura, cristalinidad, tipo y concentración de enzimas, lugar de implantación, etc. [128]. Esto puede verse reflejado en nuestro estudio [158], donde obtuvimos una tasa de degradación *in vitro* de aproximadamente el 5% a las 4 semanas en todas las membranas de SF, pero un estudio *in vivo* realizado en ratas con *scaffolds* de SF demostraron una degradación completa de los mismos en un año posimplantación [175].

Características biológicas y cultivo celular

Biológicamente, un factor esencial para asegurar el uso seguro de estos materiales en un paciente es conocer cómo afecta el material a la viabilidad celular. De acuerdo con la norma ISO 10993-5, si los valores de viabilidad celular son superiores al 70%, se considera que el material no es citotóxico. Todas las morfologías de SF y PVDF, independientemente de su arquitectura, mediante un ensayo de contacto indirecto, mostraron una viabilidad cercana al 100%, demostrando que ambos materiales no son citotóxicos [128,176]. Conociendo estos datos, se procedió al cultivo de células endoteliales de vena umbilical humana (HUVECs; *Human Umbilical Vein Endothelial Cells*). Como se comentó en el bloque temático I, las células endoteliales forman parte de uno de los principales componentes de los vasos sanguíneos, y cualquier daño o falta de las mismas puede desencadenar la aparición de trombos [8]. Por esta razón, se llevó a cabo el cultivo de las HUVECs en todas las morfologías de SF y PVDF para comprobar la adhesión y proliferación celular de las mismas [157,158]. En general, las HUVECs crecieron en todas las estructuras, obteniendo una mayor tasa de proliferación en las películas y en menor medida en las PM. Dado que todas las estructuras presentan una humectabilidad similar, esta diferencia puede atribuirse a la topografía de la superficie, ya que las estructuras de PM presentan morfologías irregulares [150, 151], dificultando la adhesión y, por tanto, posterior crecimiento celular. En cuanto a las membranas electrohiladas, las ES-NO presentan una mayor tasa de proliferación celular. Estudios anteriores demostraron que, efectivamente, el

electrohilado puede mejorar sustancialmente la proliferación de células endoteliales, especialmente cuando la distribución de las fibras es aleatoria [177]. Nuestros resultados mostraron una tasa de proliferación en SF de las ES-NO muy similares a las de las películas [157]. Debemos destacar que las ES-NO de SF mostraron un crecimiento de las HUVECs de aproximadamente 150% a los 4 días, frente al 70% de las ES-NO de PVDF. En resumen, estos hallazgos demuestran que las células endoteliales son capaces de proliferar en todas las muestras diseñadas con SF y PVDF.

Conclusiones

1. El electrohilado y los polímeros sintéticos son la metodología y materiales más prometedores y ampliamente utilizados en el diseño de injertos vasculares de ingeniería tisular.
2. La principal complicación derivada del uso de los injertos vasculares de ingeniería tisular es la aparición de trombos y la falta de permeabilidad, agravándose en injertos de pequeño diámetro y limitando su implantación en aplicaciones clínicas.
3. Existe una mayor tasa de proliferación de células endoteliales en morfologías diseñadas con fibroína de seda, mientras que las arquitecturas de fluoruro de polivinilideno destacan por sus características mecánicas y comportamiento dúctil.
4. Las propiedades fisicoquímicas y biológicas de la fibroína de seda y el fluoruro de polivinilideno se ven afectadas en función de la metodología de procesamiento.
5. Las estructuras de fibroína de seda y de fluoruro de polivinilideno desarrollados con la técnica del electrohilado muestran propiedades fisicoquímicas y biológicas válidas para el diseño de injertos vasculares de ingeniería de tejidos.

Conclusions

1. Electrospinning and synthetic polymers are the most promising and widely used methodology and materials in the design of tissue-engineered vascular grafts.
2. The main complication of using tissue-engineered vascular grafts is the occurrence of thrombosis and lack of patency, which are exacerbated by the use of small-diameter grafts and limit their use in clinical applications.
3. The proliferation rate of endothelial cells is higher in morphologies with silk fibroin, whereas poly(vinylidene fluoride) architectures are characterized by their mechanical properties and ductile behaviour.
4. Silk fibroin and poly(vinylidene fluoride) have different physicochemical and biological properties depending on processing method.
5. Silk fibroin and poly(vinylidene fluoride) structures developed by electrospinning technology exhibit physicochemical and biological properties suitable for tissue engineering vascular design.

Perspectivas Futuras

Como se ha podido comprobar, el campo de investigación de los TEVGs es muy amplio y crece a un ritmo exponencial, existiendo una gran variedad de materiales y metodologías que se pueden aplicar. Esta tesis doctoral sirve como base para nuevos estudios, especialmente en la aplicabilidad de SF y PVDF en el ámbito vascular. Se ha demostrado que ambos materiales son válidos para el diseño de TEVGs cuando se utiliza la técnica del electrohilado, ya que se obtienen buenas propiedades fisicoquímicas y biológicas. Además, esta metodología tiene la capacidad de crear estructuras formadas por fibras de polímero, las cuales pueden replicar la arquitectura y propiedades mecánicas de los vasos sanguíneos nativos [89,91].

Los siguientes pasos en la investigación de SF y PVDF sería el desarrollo de injertos vasculares mediante la técnica del electrohilado para comprobar que las condiciones halladas se mantienen o cambian. Actualmente, nuestro equipo de investigación ha diseñado y desarrollado prototipos de injertos vasculares de SF y PVDF. Para ello, durante el electrohilado se utilizó un colector cilíndrico con un diámetro de 6 mm, obteniendo TEVGs. Los resultados preliminares hallados en el injerto de SF es que sus cualidades se vieron modificadas, resultando ser muy heterogéneos y relativamente frágiles, los cuales se fracturaban con bastante facilidad, incluso con el paso de la aguja de sutura. Estos hallazgos pueden ser debidos a un alto contenido en *β-sheets* y bajo en *random coils* en la estructura de SF. Por otro lado, el prototipo de PVDF mantuvo las características fisicoquímicas y biológicas halladas en la presente tesis doctoral, procediendo a la evaluación preclínica. Este injerto es el primer prototipo de TEVG fabricado e implantado con PVDF y la tecnología de electrohilado.

El protocolo experimental fue aprobado por el Comité Ético de Investigación Animal del Centro de Cirugía de Mínima Invasión Jesús Usón (Referencia: 004/22) y cumplió íntegramente con la Directiva 2010/63/UE del Parlamento Europeo relativa a la protección de los animales utilizados para fines científicos. El estudio preclínico estuvo constituido por un total de 12 ovejas merinas hembras asignadas aleatoriamente al grupo de PVDF (n=6) y al grupo control (n=6), en el cual se utilizaron

injertos comerciales de ePTFE con un diámetro interno de 6 mm. Ambos tipos de injertos vasculares se implantaron en la arteria carótida común derecha del modelo ovino. Como se comentó en el bloque I, un modelo experimental ideal es aquel que presente una anatomía y fisiología cardiovascular similar o igual a la del humano. De todos ellos, el modelo ovino puede ser apropiado para llevar a cabo las investigaciones de los TEVGs debido a presentan mecanismos de endotelización y trombogenicidad parecidos al ser humano [8,124]. Además, la anatomía de los ovinos les confiere un gran cuello, facilitando la cirugía de implantación de los injertos [125]. Sin embargo, estos animales tienen una alta tendencia a la hipercoagulabilidad [8]. Para reducir la aparición de trombosis, se administró diariamente por vía oral una inhibición plaquetaria dual postoperatoria hasta el final del periodo de investigación del estudio. Tras la cirugía, se llevó a cabo un seguimiento de los animales a las 2, 4 y 6 semanas mediante ecografía. Se obtuvieron imágenes en Modo B y Power-Color de los injertos vasculares para evaluar la existencia de trombos y estenosis, y la permeabilidad vascular, respectivamente. Después de la realización del último estudio con ultrasonidos, se llevaron a cabo angiografías del cuello para determinar la permeabilidad vascular de ambas arterias carótidas y comparar el estado del injerto vascular y el vaso contralateral sano. Tras finalizar el estudio, se extrajeron los injertos y la arteria contralateral, se fijaron en formol al 4% y se reservaron para estudios histológicos. Actualmente los resultados, tanto *in vitro* como *in vivo*, están siendo analizados y, tras su interpretación, serán publicados.

Otra posibilidad de investigación futura es la hibridación de varios materiales, consiguiendo un TEVG con las ventajas de los polímeros utilizados [126]. Un ejemplo sería la hibridación de PVDF y SF, obteniendo las propiedades fisicoquímicas del primero, y las biológicas del segundo. Además, cabe la posibilidad de añadir algún fármaco al propio injerto vascular, como puede ser la heparina. El principal hallazgo encontrado en los TEVGs de es la aparición de trombos. El uso de heparina puede prevenir dicho fenómeno, por lo que el material utilizado puede ser heparinizado mediante adsorción física o conjugación química, y aumentar la permeabilidad vascular [109].

Por otro lado, los estudios analizados en este campo se han llevado a cabo en modelos experimentales jóvenes y sanos. Las patologías cardiovasculares suelen acontecer en pacientes adultos y con comorbilidades. Por esta razón, una vez conseguido resultados óptimos en los modelos experimentales sanos, los TEVGs deberían ser implantados en modelos adultos y que presentaran condiciones similares a las de los pacientes humanos. También sería recomendable realizar estudios a largo plazo, en los cuales se puedan estudiar todos los efectos secundarios de los injertos vasculares. Estos análisis de temporalidad son muy importantes, ya que de esta manera se podrá comprobar el uso satisfactorio y seguro de los TEVGs y, en el futuro, poder implantarlos en el ser humano.

Las futuras investigaciones deberían centrarse en obtener un injerto vascular con características similares a las de los vasos sanguíneos nativos, y especialmente a la zona que se desea realizar la implantación. El uso de diferentes tecnologías o técnicas, como la tomografía computarizada, la resonancia magnética o la angiografía, pueden ayudar a proporcionar datos relativos a las dimensiones del vaso afectado que se quiere sustituir, pudiendo fabricar un TEVG con un tamaño acorde al sitio anatómico. En el futuro, estos injertos podrían superar todas las limitaciones mencionadas, ya que existen una amplia variedad de posibilidades de diseño, probando y combinando las nuevas tecnologías y materiales emergentes. Todas estas cuestiones deben de ser abordadas para desarrollar TEVGs seguros para su aplicación clínica.

Bibliografía

1. World Health Organization (2023). Cardiovascular Disease. Fact sheets. https://www.who.int/health-topics/cardiovascular-diseases#tab=tab_1 (Accedido el 28 de febrero de 2023).

2. Chen S-G, Ugwu F, Li W-C, Caplice NM, Petcu E, Yip SP, et al. (2021). Vascular Tissue Engineering: Advanced Techniques and Gene Editing in Stem Cells for Graft Generation. Tissue Eng Part B Rev; 27(1): 14-28. DOI: 10.1089/ten.TEB.2019.0264.

3. Wei Y, Wang F, Guo Z, Zhao Q. (2022). Tissue-engineered vascular grafts and regeneration mechanisms. J Mol Cell Cardiol; 165: 40-53. DOI: 10.1016/j.yjmcc.2021.12.010.

4. Row S, Santandreu A, Swartz DD, Andreadis ST. (2017). Cell-free vascular grafts: Recent developments and clinical potential. Technology (Singap World Sci); 5(1): 13-20. DOI: 10.1142/S2339547817400015.

5. Mozaffarian D, Benjamin EJ, Go AS, Arnett DK, Blaha MJ, Cushman M, et al. (2015). Heart disease and stroke statistics--2015 update: A report from the american heart association. Circulation; 131(4): e29-322. DOI: 10.1161/CIR.0000000000000152

6. Song H-HG, Rumma RT, Ozaki CK, Edelman ER, Chen CS. (2018). Vascular tissue engineering: progress, challenges, and clinical promise. Cell Stem Cell; 22(3): 340-354. DOI: 10.1016/j.stem.2018.02.009.

7. Chlupáč J, Filová E, Bačáková L. (2009). Blood vessel replacement: 50 years of development and tissue engineering paradigms in vascular surgery. Physiol Res; 58 Suppl 2: S119-S140. DOI: 10.33549/physiolres.931918.

8. Pashneh-Tala S, MacNeil S, Claeyssens F. (2016). The Tissue-Engineered Vascular Graft-Past, Present, and Future. Tissue Eng B Rev; 22(1): 68-100. DOI: 10.1089/ten.teb.2015.0100.

9. Weinberg CB, Bell E. (1986). A blood vessel model constructed from collagen and cultured vascular cells. Science; 231(4736): 397-400. DOI: 10.1126/science.2934816.

10. Syedain ZH, Prunty A, Li J, Tranquillo RT. (2021). Evaluation of the probe burst test as a measure of strength for a biologically-engineered vascular graft. J Mech Behav Biomed Mater; 119: 104527. DOI: 10.1016/j.jmbbm.2021.104527.

11. Konig G, McAllister TD, Dusserre N, Garrido SA, Iyican C, Marini A, et al. (2009). Mechanical properties of completely autologous human tissue engineered blood vessels compared to human saphenous vein and mammary artery. Biomaterials; 30(8): 1542-1550. DOI: 10.1016/j.biomaterials.2008.11.011.

12. L'Heureux N, Pâquet S, Labbé R, Germain L, Auger FA. (1998). A completely biological tissue-engineered human blood vessel. FASEB J; 12(1): 47-56. DOI: 10.1096/fasebj.12.1.47.

13. Hoerstrup SP, Zünd G, Sodian R, Schnell AM, Grünenfelder J, Turina MI (2001). Tissue engineering of small caliber vascular grafts. Eur J Cardiothorac Surg; 20(1): 164-169. DOI: 10.1016/s1010-7940(01)00706-0.

14. L'Heureux N, Dusserre N, Marini A, Garrido S, de la Fuente L, McAllister T. (2007). Technology Insight: the evolution of tissue engineered vascular grafts-from research to clinical practice. Nat Clin Pract Cardiovasc Med; 4(7): 389-395. DOI: 10.1038/ncpcardio0930.

15. Shin'oka T, Imai Y, Ikada Y. (2001). Transplantation of a tissue-engineered pulmonary artery. N Engl J Med; 344(7): 532-533. DOI: 10.1056/NEJM200102153440717.

16. Langer R, Vacanti J. (2016). Advances in tissue engineering. J Pediatr Surg; 51(1): 8-12. DOI: 10.1016/j.jpedsurg.2015.10.022.

17. Stegemann JP, Kaszuba SN, Rowe SL. (2007). Review: Advances in vascular tissue engineering using protein-based Biomaterials. Tissue Eng; 13(11): 2601-2613. DOI: 10.1089/ten.2007.0196.

18. Tortora GJ, Derrickson B. (2018). El aparato circulatorio: vasos sanguíneos y hemodinamia. En: Tortora GJ, Derrickson B. Principios de Anatomía y fisiología. 15ª Edición. Editorial Medica Panamericana. Madrid, España. pp. 802-871.

19. Hasan A, Memic A, Annabi N, Hossain M, Paul A, Dokmeci MR, et al. (2014). Electrospun Scaffolds for Tissue Engineering of Vascular Grafts. Acta Biomater; 10(1): 11-25. DOI: 10.1016/j.actbio.2013.08.022.

20. Milutinović A, Šuput D, Zorc-Pleskovič (2020). Pathogenesis of atherosclerosis in the tunica intima, media, and adventitia of coronary arteries: An updated review. Bosn J Basic Med Sci; 20(1): 21-30. DOI: 10.17305/bjbms.2019.4320.

21. Song Y, Feijen J, Grijpma DW, Poot AA. (2011). Tissue engineering of small-diameter vascular grafts: a literature review. Clin Hemorheol Microcirc; 49(1-4): 357-374. DOI: 10.3233/CH-2011-1486.

22. Jung F, Wischke C, Lendlein A. (2010). Degradable, multifunctional cardiovascular implants: Challenges and hurdles. MRS Bull; 35(8): 607-613. DOI: 10.1557/mrs2010.529.

23. Li S, Sengupta D, Chien S (2014). Vascular tissue engineering: from in vitro to in situ. Willey Interdiscip Rev Syst Biol Med; 6(1): 61-76. DOI: 10.1002/wsbm.1246.

24. Wystrychowski W, Garrido SA, Marini A, Dusserre N, Radochonski S, Zagalski K, et al. (2022). Long-term results of autologous scaffold-free tissue-engineered vascular graft for medodialysis access. J Vasc Access; 11297298221095994. DOI: 10.1177/11297298221095994.

25. Hu K, Li Y, Ke Z, Yang H, Lu C, Li Y, et al. (2022). History, progress and future challenges of artificial blood vessels: a narrative review. Biomater Transl; 3(1): 81-98. DOI: 10.12336/biomatertransl.2022.01.008.

26. Shafiq M, Zhang Q, Zhi D, Wang K, Kong D, Kim D-H, et al. (2018). In Situ Blood Vessel Regeneration Using SP (Substance P) and SDF (Stromal Cell-Derived Factor)-1α Peptide Eluting Vascular Grafts. Arterioscler Thromb Vasc Biol; 38(7): e117-e134. DOI: 10.1161/ATVBAHA.118.310934.

27. Itoh M, Mukae Y, Kitsuka T, Arai K, Nakamura, A, et al. (2019). Development of an immunodeficient pig model allowing long-term accommodation of artificial human vascular tubes. Nat Commun; 10: 2244. DOI: 10.1038/s41467-019-10107-1.

28. Leal BB, Wakabayashi N, Oyama K, Kamiya H, Braghirolli DI, Pranke P. (2021). Vascular Tissue Engineering: Polymers and Methodologies for Small Caliber Vascular Grafts. Front Cardiovasc Med; 7: 592361. DOI: 10.3389/fcvm.2020.592361.

29. Dong C, Lv Y. (2016). Application of Collagen Scaffold in Tissue Engineering: Recent Advances and New Perspectives. Polymers (Basel); 8(2): 42. DOI: 10.3390/polym8020042.

30. Allen AB, Priddy LB, A Li M-T, Guldberg RE. (2015). Functional augmentation of naturally-derived materials for tissue regeneration. Ann Biomed Eng; 43(3): 555-567. DOI: 10.1007/s10439-014-1192-4.

31. Ong CS, Zhou X, Huang CY, Fukunishi T, Zhang H, Hibino N. (2017). Tissue Engineered Vascular Grafts: Current State of the Field. Expert Rev Med Devices; 14(5): 383-392. DOI: 10.1080/17434440.2017.1324293.

32. O'Brien FJ. (2011). Biomaterials & scaffolds for tissue engineering. Materials Today; 14(3): 88-95. DOI: 10.1016/S1369-7021(11)70058-X.

33. Mauri A, Zeisberger SM, Hoerstrup SP, Mazza E. (2013). Analysis of the uniaxial and multiaxial mechanical response of a tissue-engineered vascular graft. Tissue Eng Part A; 19(5-6): 583-592. DOI: 10.1089/ten.tea.2012.0075.

34. Jouda H, Murillo LL, Wang T. (2022). Current progress in vascular engineering and its clinical applications. Cells; 11(3): 493. DOI: 10.3390/cells11030493.

35. Radke D, Jia W, Sharma D, Fena K, Wang G, Goldman J, et al. (2018). Tissue Engineering at the Blood-Contacting Surface: A Review of Challenges and Strategies in Vascular Graft Development. Adv Healthc Mater; 7(15): e1701461. DOI: 10.1002/adhm.201701461.

36. Zhang W.J., Liu W., Cui L., Cao Y. (2007). Tissue Engineering of Blood Vessel. J Cell Mol Med; 11(5): 945-957. DOI: 10.1111/j.1582-4934.2007.00099.x.

37. Herrmann FEM, Lamm P, Wellmann P, Milz S, Hagl C, Juchem G. (2019). Autologous Endothelialized Vein Allografts in Coronary Artery Bypass Surgery - Long Term Results. Biomaterials; 212: 87-97. DOI: 10.1016/ j.biomaterials.2019.05.019.

38. Wang Y, Yin P, Bian G-L, Huang H-Y, Shen H, Yang J-J, et al. (2017). The combination of stem cells and tissue engineering: an advanced strategy for blood vessels regeneration and vascular disease treatment. Stem Cell Res Ther; 8(1): 194. DOI: 10.1186/s13287-017-0642-y.

39. Sundaram S, Echter A, Sivarapatna A, Qiu C, Niklason L. (2014). Small-diameter vascular graft engineered using human embryonic stem cell-derived mesenchymal cell. Tissue Eng Part A; 20(3-4): 740-750. DOI: 10.1089/ten.tea.2012.0738.

40. Volarevic V, Markovic BS, Gazdic M, Volarevic A, Jovicic N, Arsenijevic N, et al. (2018). Ethical and Safety Issues of Stem Cell-Based Therapy. Int J Med Sci; 15(1): 36-45. DOI: 10.7150/ijms.21666.

41. Horwitz EM, Le Blanc K, Dominici M, Mueller I, Slaper-Cortenbach I, Marini FC, et al. (2005). Clarification of the Nomenclature for MSC: The International Society for Cellular Therapy Position Statement. Cytotherapy; 7(5): 393-395. DOI: 10.1080/14653240500319234.

42. Cai Q, Liao W, Xue F, Wang X, Zhou W, Li Y, et al. (2021). Selection of different endothelialization modes and different seed cells for tissue-engineered vascular graft. Bioact Mater; 6(8): 2557-2568. DOI: 10.1016/j.bioactmat.2020.12.021.

43. Lynch K, Pei M. (2014). Age associated communication between cells and matrix: a potential impact on stem cell-based tissue regeneration strategies. Organogenesis; 10(3): 289-298. DOI: 10.4161/15476278.2014.970089.

44. Warrier S, Haridas N, Bhonde R. (2012). Inherent propensity of amnion-derived mesenchymal stem cells towards endothelial lineage: vascularization from an avascular tissue. Placenta; 33(10): 850-858. DOI: 10.1016/j.placenta.2012.07.001.

45. Zhao J, Liu L, Wei J, Ma D, Geng W, Yan X, et al. (2012). A novel strategy to engineer small-diameter vascular grafts from marrow-derived mesenchymal stem cells. Artif Organs; 36(1): 93-101. DOI: 10.1111/j.1525-1594.2011.01231.x.

46. Jiao Y, Zhang Y, Xiao Y, Xing Y, Cai Z, Wang C, et al. (2022). The crescendo pulse frequency of shear stress stimulates the endothelialization of bone marrow mesenchymal stem cells on the luminal surface of decellularized scaffold in the bioreactor. Bioengineered; 13(3): 7925-7938. DOI: 10.1080/21655979.2022.2039502.

47. Faiella W, Atoui R. (2016). Therapeutic Use of Stem Cells for Cardiovascular Disease. Clin Transl Med; 5(1): 34. DOI: 10.1186/s40169-016-0116-3.

48. Wu Z, Zhang S, Zhou L, Cai J, Tan J, Gao X, et al. (2017). Thromboembolism Induced by Umbilical Cord Mesenchymal Stem Cell Infusion: A Report of Two Cases and Literature Review. Transplant Proc; 49(7): 1656-1658. DOI: 10.1016/j.transproceed.2017.03.078.

49. Moll G, Ankrum JA, Kamhieh-Milz J, Bieback K, Ringdén O, Volk H-D., et al. (2019). Intravascular Mesenchymal Stromal/Stem Cell Therapy Product Diversification: Time for New Clinical Guidelines. Trends Mol Med; 25(2): 149-163. DOI: 10.1016/j.molmed.2018.12.006.

50. Wang K, Lin R-Z, Melero-Martin JM. (2019). Bioengineering human vascular networks: trends and directions in endothelial and perivascular cell sources. Cell Mol Life Sci; 76(3): 421-439. DOI: 10.1007/s00018-018-2939-0.

51. Peters EB. Endothelial progenitor cells for the vascularization of engineered tissues. Tissue Eng Part B Rev; 24(1): 1-24. DOI: 10.1089/ten.TEB.2017.0127.

52. Kaushal S, Amiel GE, Guleserian KJ, Shapira OM, Perry T, Sutherland FW, et al. (2001). Functional small-diameter neovessels created using endothelial progenitor cells expanded ex vivo. Nat Med; 7(9): 1035-1040. DOI: 10.1038/nm0901-1035.

53. Allen J, Khan S, Serrano MC, Ameer G. (2008). Characterization of porcine circulating progenitor cells: toward a functional endothelium. Tissue Eng Part A; 14(1): 183-194. DOI: 10.1089/ten.a.2007.0265.

54. Muniswami DM, Reddy LVK, Amirtham SM, Babu S, Raj AN, Sen D, et al. (2020). Endothelial progenitor/stem cells in engineered vessels for vascular transplantation. J Mater Sci Mater Med; 31(12): 119. DOI: 10.1007/s10856-020-06458-7.

55. Shi X, He L, Zhang S-M, Luo J. (2021). Human iPS cell-derived tissue engineered vascular graft: recent advances and future directions. Stem Cell Rev Rep; 17(3): 862-877. DOI: 10.1007/s12015-020-10091-w.

56. Liu G-H, Barkho BZ, Ruiz S, Diep D, Qu J, Yang S-L, et al. (2011). Recapitulation of premature ageing with iPSCs from Hutchinson-Gilford progeria syndrome. Nature; 472(7342): 221-225. DOI: 10.1038/nature09879.

57. Zhang J, Lian Q, Zhu G, Zhou F, Sui L, Tan C, et al. (2011). A human iPSC model of Hutchinson Gilford Progeria reveals vascular smooth muscle and mesenchymal stem cell defects. Cell Stem Cell; 8(1): 31-45. DOI: 10.1016/j.stem.2010.12.002.

58. Luo J, Qin L, Zhao L, Gui L, Ellis MW, Huang Y, et al. (2020). Tissue-engineered vascular grafts with advanced mechanical strength from human iPSCs. Cell Ste, Cell; 26(2): 251-261.e8. DOI: 10.1016/j.stem.2019.12.012.

59. Galat V, Galat Y, Perepitchka M, Jennings LJ, Iannaccone PM, Hendrix MJ. (2016). Transgene reactivation in induced pluripotent stem cell derivatives and reversion to pluripotency of induced pluripotent stem cell-derived mesenchymal stem cells. Stem Cells Dev; 25(14): 1060-1072. DOI: 10.1089/scd.2015.0366.

60. Afra S, Matin MM. (2020). Potential of mesenchymal stem cells for bioengineered blood vessels in comparison with other eligible cell sources. Cell Tissue Res; 130(1): 1-13. DOI: 10.1007/s00441-019-03161-0.

61. Liu C, Niu K, Xiao Q. (2022). Updated perspectives on vascular cell specifation and pluripotent setm cell-derived vascular organoids for studying vasculopathies. Cardiovasc Res; 118(1): 97-114.

62. Vergés E, Ayala D, Grau S, Tost D. (2008). 3D reconstruction and quantification of porous structures. Computers Graphics; 32(4): 438-444. DOI: 10.1016/j.cag.2008.04.001.

63. Wang Z, Mithieux S, Weiss AS. (2019). Fabrication techniques for vascular and vascularized tissue engineering. Adv Healthc Mater; 8(19): e1900742. DOI: 10.1002/adhm.201900742.

64. Jiao W, Liu C, Shan J, Kong Z, Wang X. (2022). Construction and Evaluation of Small-Diameter Bioartificial Arteries Based on a Combined-Mold Technology. Polymers (Basel); 14(15): 3089. DOI: 10.3390/polym14153089.

65. Baba K, Mikhailov A, Sankai Y. (2021). Dynamic flow priming programs allow tuning up the cell layers properties for engineered vascular grafts. Sci Rep; 11: 14666. DOI: 10.1038/s41598-021-94023-9.

66. Crapo PM, Gilbert TW, Badylak SF. (2011). An overview of tissue and whole organ decellularization processes. Biomaterials; 32(12): 3233-3243. DOI: 10.1016/j.biomaterials.2011.01.057.

67. Steffens D, Braghirolli DI, Maurmann N, Pranke P. (2018). Update on the main use of biomaterials and techniques associated with tissue engineering. Drug Discov Today; 23(8): 1474-1488. DOI: 10.1016/j.drudis.2018.03.013.

68. Song JJ, Ott HC. (2011). Organ engineering based on decellularized matrix scaffolds. Trends Mol Med, 17(8): 424-432. DOI: 10.1016/j.molmed.2011.03.005.

69. Syedain Z, Reimer J, Lathi M, Berry J, Johnson S, Bianco R, et al. (2016). Tissue engineering of acellular vascular grafts capable of somatic growth in young lambs. Nat Commun; 7: 12951. DOI: 10.1038/ncomms12951.

70. Dahl SL, Kypson AP, Lawson JH, Blum JL, Strader JT, Li Y, et al. (2011). Readily available tissue-engineered vascular grafts. Sci Transl Med; 3(68): 68ra9. DOI: 10.1126/scitranslmed.3001426.

71. Liu J, Chen D, Zhu X, Liu N, Zhang H, Tang R, et al. (2022). Development of a decellularized human amniotic membrane-based electrospun vascular graft capable of rapid remodeling for small-diameter vascular applications. Acta Biomater; 152: 144-156. DOI: 10.1016/j.actbio.2022.09.009.

72. Badylak SF, Taylor D, Uygun K. (2011). Whole-organ tissue engineering: decellularization and recellularization of three-dimensional matrix scaffolds. Annu Rev biomed Eng; 13: 27-53. DOI: 10.1146/annurev-bioeng-071910-124743.

73. Pellegata AF, Asnaghi MA, Stefani I, Maestroni A, Maestroni S, Dominioni T, et al. (2013). Detergent-enzymatic decellularization of swine blood vessels: insight on mechanical properties for vascular tissue engineering. Biomed Res Int; 2013: 918753. DOI: 10.1155/2013/918753.

74. Rambøl MH, Hisdal J, Sundhagen JO, Brinchmann JE, Rosales A. (2018). Recellularization of Decellularized Venous Grafts Using Peripheral Blood: A Critical Evaluation. EBioMedicine; 32: 215-222. DOI: 10.1016/j.ebiom.2018.05.012.

75. Li J, Cai Z, Cheng J, Wang C, Fang Z, Xiao Y, et al. (2020). Characterization of a heparinized decellularized scaffold and its effects on mechanical and structural properties. J Biomater Sci Polym Ed; 31(8): 999-1023. DOI: 10.1080/09205063.2020.1736741.

76. Lin C-H, Hsia K, Tsai C-H, Ma H, Lu J-H, Tsay R-Y. (2019). Decellularized porcine coronary artery with adipose stem cells for vascular tissue engineering. Biomed Mater; 14(4): 045014. DOI: 10.1088/1748-605X/ab2329.

77. Papaioannou TG, Manolesou D, Dimakakos E, Tsoucalas G, Vavuranakis M, Tousoulis D. (2019). 3D Bioprinting Methods and Techniques: Applications on Artificial Blood Vessel Fabrication. Acta Cardiol Sin; 35(3): 284-289. DOI: 10.6515/ACS.201905_35(3).20181115A.

78. Paul MA, Opyrchał J, Witowski J, Ibrahim AMS, Knakiewicz M, Jaremków P. (2019). The Use of a Three-Dimensional Printed Model for Surgical Excision of a Vascular Lesion in the Head and Neck. J Craniofac Surg; 30(6): e566-e570. DOI: 10.1097/SCS.0000000000005541.

79. Stana J, Grab M, Kargl R, Tsilimparis N. (2022). 3D printing in the planning and teaching of endovascular procedures. Radiologie (Heidelb); 62(Suppl 1): 28-33. DOI: 10.1007/s00117-022-01047-x.

80. Hann SY, Cui H, Esworthy T, Zhou X, Lee S-J, Plesniak MW, et al. (2021). Dual 3D printing for vascularized bone tissue regeneration. Acta Biomater; 123: 263-274. DOI: 10.1016/j.actbio.2021.01.012.

81. Ashammakhi N, Ahadian S, Xu C, Montazerian H, Ko H, Nasiri R, et al. (2019). Bioinks and bioprinting technologies to make heterogeneous and biomimetic tissue constructs. Mater Today Bio; 1: 100008. DOI: 10.1016/j.mtbio.2019.100008.

82. Freeman S, Ramos R, Chando PA, Zhou L, Reeser K, Jin S, et al. (2019). A bioink blend for rotary 3D bioprinting tissue engineered small-diameter vascular constructs. Acta Biomater; 95: 152-164. DOI: 10.1016/j.actbio.2019.06.052.

83. Jin Q, Jin G, Ju J, Xu L, Tang L, Fu Y, et al. (2022). Bioprinting small-diameter vascular vessel with endothelium and smooth muscle by the approach of two-step crosslinking process. Biotechnol Bioeng; 119(6): 1673-1684. DOI: 10.1002/bit.28075.

84. Kong Z, Wang X. (2023). Bioprinting Technologies and Bioinks for Vascular Model Establishment. Int J Mol Sci; 24(1): 891. DOI: 10.3390/ijms24010891.

85. Wu S, Dong T, Li Y, Sun M, Qi M, Liu J, et al. (2022). State-of-the-art review of advanced electrospun nanofiber yarn-based textiles for biomedical applications. Appl Mater Today; 27: 101473. DOI: 10.1016/j.apmt.2022.101473.

86. Rahmati M, Mills DK, Urbanska AM, Saeb MR, Venugopal JR, Ramakrishna S, et al. (2021). Electrospinning for tissue engineering applications. Prog Mater Sci; 117: 100721. DOI: 10.1016/j.pmatsci.2020.100721.

87. Doshi J, Reneker DH. (1995). Electrospinning process and applications of electrospun fibers. J Electrostat; 35(2-3): 151-160. DOI: 10.1016/0304-3886(95)00041-8.

88. Reneker DH, Yarin AL. (2008). Electrospinning jets and polymer nanofibers. Polymer; 49(10): 2387-2425. DOI: 10.1016/j.polymer.2008.02.002.

89. Guo F, Wang N, Wang L, Hou L, Ma L, Liu J, et al. (2015). An electrospun strong PCL/PU composite vascular graft with mechanical anisotropy and cyclic stability. J Mater Chem A; 3: 4782-4787. DOI: 10.1039/C4TA06845A.

90. Kruse M, Greuel M, Kreimendahl F, Scheiders T, Bauer B, Gries T, et al. (2018). Electro-spun PLA-PEG-yarns for tissue engineering applications. Biomed Tech (Berl); 63(3): 231-243. DOI: 10.1515/bmt-2017-0232.

91. Babu R, Reshmi CR, Joseph J, Sathy BN, Nair SV, Varma PK, et al. (2021). Design, Development, and Evaluation of an Interwoven Electrospun Nanotextile Vascular Patch. Macromol Mater Eng; 306(11): 2100359. DOI: 10.1002/mame.202100359.

92. Shenoy SL, Bates WD, Frisch HL, Wnek GE. (2005). Role of chain entanglements on fiber formation during electrospinning of polymer solutions: good solvent, non-specific polymer–polymer interaction limit. Polymer; 46(10): 3372-3384. DOI: 10.1016/j.polymer.2005.03.011.

93. Gu SY, Ren J, Vancso GJ. (2005). Process optimization and empirical modeling for electrospun polyacrylonitrile (PAN) nanofiber precursor of carbon nanofibers. J Macromol Sci Part A; 41(11): 2559-2568. DOI: 10.1016/j.eurpolymj.2005.05.008.

94. Lee KH, Kim HY, Bang HJ, Jung YH, Lee SG. (2003). The change of bead morphology formed on electrospun polystyrene fibers. Polymer; 44(14): 4029-4034. DOI: 10.1016/S0032-3861(03)00345-8.

95. Zarghman S, Bazgir S, Tavakoli A, Rashidi AS, Damerchely R. (2012). The effect of flow rate on morphology and deposition area of electrospun nylon 6 nanofiber. J Eng Fibers Fabr; 7(4): 42-49. DOI: 10.1177/155892501200700414.

96. Deitzel JM, Kleinmeyer J, Harris D, Beck Tan NC. (2001). The effect of processing variables on the morphology of electrospun nanofibers and textiles. Polymer; 42(1): 261-272. DOI: 10.1016/S0032-3861(00)00250-0.

97. Gaumer J, Prasad A, Lee D, Lannutti J. (2009). Structure–function relationships and source-to-ground distance in electrospun polycaprolactone. Acta Biomater; 5(5): 1552-1561. DOI: 10.1016/j.actbio.2009.01.021.

98. Casper CL, Stephens JS, Tassi NG, Chase B, Rabolt JF. (2004). Controlling Surface Morphology of Electrospun Polystyrene Fibers: Effect of Humidity and Molecular Weight in the Electrospinning Process. Macromolecules; 37(2): 573-578. DOI: 10.1021/ma0351975.

99. De Vrieze S, Van Camp V, Nelvig A, Hagström B, Westbroek P, De Clerck K. (2009). The effect of temperature and humidity on electrospinning. J Mater Sci; 44: 1357-1362. DOI: 10.1007/s10853-008-3010-6.

100. Moritz WR, Raman S, Pessin S, Martin C, Li X, Westman A, et al. (2022). The history and innovations of blood vessel anastomosis. Bioengineering (Basel); 9(2): 75. DOI: 10.3390/bioengineering9020075.

101. Ball CG, Feliciano DV. (2009). A simple and rapid vascular anastomosis for emergency surgery: a technical case report. World J Emerg Surg; 4: 30. DOI: 10.1186/1749-7922-4-30.

102. Siemionow MZ, Kwiecien GJ, Uygur S, Bobkiewicz A. (2015). Arterial and venous microanastomosis models. En: Siemionow MZ. Plastic and reconstructive surgery: Experimental models and research designs. Springer. University of Illinois, Chicago, USA. pp. 11-31.

103. Chen YX, Chen LE, Seaber AV, Urbaniak JR. (2001). Comparison of continuous and interrupted suture techniques in microvascular anastomosis. J Hand Surg Am; 26(3): 530-539. DOI: 10.1053/jhsu.2001.22933.

104. de Barros RSM, Leal RA, Teixeira RKC, Yamaki VN, Feijó DH, Gouveia EHH, et al. (2017). Continuous versus interrupted suture technique in microvascular anastomosis in rats. Acta Cir Bras; 32(9): 691-696. DOI: 10.1590/s0102-865020170090000001.

105. He G-W, Taggart DP. (2016). Spasm in arterial grafts in coronary artery bypass grafting surgery. Ann Thorac Surg; 101(3): 1222-1229. DOI: 10.1016/j.athoracsur.2015.09.071.

106. Asada Y, Yamashita A, Sato Y, Hatakeyama K. (2018). Thrombus formation and propagation in the onset of cardiovascular events. J Atheroscler Thromb; 25(8): 653-664. DOI: 10.5551/jat.RV17022.

107. Rehman SM, Yi G, Taggart DP. (2013). The radial artery: current concepts on its use in coronary artery revascularization. Ann Thorac Surg; 96(5): 1900-1909. DOI: 10.1016/j.athoracsur.2013.06.083.

108. Ju YM, Ahn H, Arenas-Herrera J, Kim C, Abolbashari M, Atala A, et al. (2017). Electrospun Vascular Scaffold for Cellularized Small Diameter Blood Vessels: A Preclinical Large Animal Study. Acta Biomater; 59: 58-67. DOI: 10.1016/j.actbio.2017.06.027.

109. Aslani S, Kabiri M, HosseinZadeh S, Hanaee-Ahvaz H, Taherzadeh ES, Soleimani M. (2020). The Applications of Heparin in Vascular Tissue Engineering. Microvasc Res; 131: 104027. DOI: 10.1016/j.mvr.2020.104027.

110. Buntic RF. (2018). Microsurgery essentials. En: Chang J. Global reconstructive surgery. 1ª Edición. Elsevier. pp. 117-125. DOI: 10.1016/B978-0-323-52377-6.00016-1.

111. Osario-da Cruz SM, Aggoun Y, Cikirikcioglu M, Khabiri E, Djebaili K, Kalangos A, et al. (2009). Vascular ultrasound studies for the non-invasive assessment of vascular flow and patency in experimental surgery in the pig. Lab Anim; 43(4): 333-337. DOI: 10.1258/la.2009.0080030.

112. Malik J, Lomonte C, Meola M, de Bont C, Shahverdyan R, Rotmans JI, et al. (2021). The role of Doppler ultrasonography in vascular access surveillance-controversies continue. J Vasc Access; 22(1 Suppl): 63-70. DOI: 10.1177/1129729820928174.

113. Paolinelli P. (2013). Physical principles and clinical indications for doppler ultrasound. Rev Med Clin Las Condes; 24(1): 139-148. DOI: 10.1016/S0716-8640(13)70139-1.

114. Yamamoto M, Ninomiya H, Tashiro M, Sato T, Handa T, Inoue K, et al. (2019). Evaluation of graft anastomosis using time-intensity curves and quantitative near-infrared fluorescence angiography during peripheral arterial bypass grafting. J Artif Organs; 22(2): 160-168. DOI: 10.1007/s10047-018-1083-9.

115. Zhang L, Fu Y, Gong Y, Zhao H, Wu S, Yang, et al. (2021). Graft patency and completeness of revascularization in minimally invasive multivessel coronary artery bypass surgery. J Card Surg; 36(3): 992-997. DOI: 10.1111/jocs.15345.

116. Seldinger DI. Catheter replacement of the needle in percutaneous arteriography; a new technique. Acta radiol; 39(5): 368-376. DOI: 10.3109/00016925309136722.

117. Sheth RA, Ganguli S. (2015). Closure of Alternative Vascular Sites, Including Axillary, Brachial, Popliteal, and Surgical Grafts. Tech Vasc Interv Radiol; 18(2): 113-121. DOI: 10.1053/j.tvir.2015.04.009.

118. Klimek K, Świątek M, Klocek K, Tworek M, Zwolski M, Milewski K, et al. (2021). Comparison of Safety and Efficiency between Tiger-2 Catheter with Right Radial Artery Access and Judkins Catheter with Left Radial Artery Access. J Clin Med; 10(17): 4020. DOI: 10.3390/jcm10174020.

119. Turan B, Erkol A, Mutlu A, Tolga Daşli T, Erden İ. (2016). Effectiveness of Left Judkins Catheter as a Single Multipurpose Catheter in Transradial Coronary Angiography From Right Radial Artery: A Randomized Comparison With Conventional Two-Catheter Strategy. J Interv Cardiol; 29(3): 257-264. DOI: 10.1111/joic.12286.

120. Willson JK. A new technique for cerebral angiography: the variable stiffness guidewire. Radiology; 134(2): 427-430. DOI: 10.1148/radiology.134.2.7352223.

121. Willaert W, Aggarwal R, Bicknell C, Hamady M, Darzi A, Vermassen F, et al. (2010). Patient-specific simulation in carotid artery stenting. J Vasc Surg; 52(6): 1700-1705. DOI: 10.1016/j.jvs.2010.08.015.

122. Lovett M, Cannizzaro C, Daheron L, Messmer B, Vunjak-Novakovic G, Kaplan DL. (2007). Silk Fibroin Microtubes for Blood Vessel Engineering. Biomaterials; 28(35): 5271-5279. DOI: 10.1016/j.biomaterials.2007.08.008.

123. Ehrmann K, Potzmann P, Dworak C, Bergmeister H, Eilenberg M, Grasl C, et al. (2020). Hard Block Degradable Polycarbonate Urethanes: Promising Biomaterials for Electrospun Vascular Prostheses. Biomacromolecules; 21(2): 376-387. DOI: 10.1021/acs.biomac.9b01255.

124. Bergmeister H, Hamza O, Kiss A, Nagel F, Pilz PM, Plasenzotti R, et al. (2019). Animal Models in Cardiovascular Biology. En: Geiger M. Fundamentals of Vascular Biology. Learning Materials in Biosciences. Springer. pp. 271–291. DOI: 10.1007/978-3-030-12270-6_13.

125. Fukunishi T, Best CA, Sugiura T, Opfermann J, Ong CS, Shinoka T, et al. (2017). Preclinical Study of Patient-specific Cell-free Nanofiber Tissue-Engineered Vascular Grafts Using 3-dimensional Printing in a Sheep Model. J Thorac Cardiovasc Surg; 153(4): 924-932. DOI: 10.1016/j.jtcvs.2016.10.066.

126. Hu Y-T, Pan X-D, Zheng J, Ma W-G, Sun L-Z. (2017). In Vitro and In Vivo Evaluation of a Small-Caliber Coaxial Electrospun Vascular Graft Loaded with Heparin and VEGF. Int J Surg; 44: 244-249. DOI: 10.1016/j.ijsu.2017.06.077.

127. Naito Y, Shinoka T, Duncan D, Hibino N, Solomon D, Cleary M, et al. (2011). Vascular Tissue Engineering: towards the Next Generation Vascular Grafts. Adv Drug Deliv Rev; 63(4-5): 312-323. DOI: 10.1016/j.addr.2011.03.001.

128. Kundu B, Rajkhowa R, Kundu SC, Wang X. (2013). Silk fibroin biomaterials for tissue regenerations. Adv Drug Deliv Rev; 65(4): 457-470. DOI: 10.1016/j.addr.2012.09.043.

129. Maciel MM, Ribeiro S, Ribeiro C, Francesko A, Maceiras A, Vilas JL, et al. (2017). Relation between fiber orientation and mechanical properties of nanoengineered poly(vinylidene fluoride) electrospun composite fiber mats. Compos Part B Eng; 139: 146-154. DOI: 10.1016/j.compositesb.2017.11.065.

130. Dvir T, Timko BP, Kohane DS, Langer R. (2010). Nanotechnological Strategies for Engineering Complex Tissues. Nat Nanotech; 6(1): 13-22. DOI: 10.1038/nnano.2010.246.

131. Woods I, Flanagan TC. (2014). Electrospinning of Biomimetic Scaffolds for Tissue-Engineered Vascular Grafts: Threading the Path. Expert Rev Cardiovasc Ther; 12(7): 815-832. DOI: 10.1586/14779072.2014.925397.

132. Villalona GA, Udelsman B, Duncan DR, McGillicuddy E, Sawh-Martínez RF, Hibino N, et al. (2010). Cell-seeding tecniques in vascular tissue engineering. Tissue Eng Part B Rev; 16(3): 341-350. DOI: 10.1089/ten.teb.2009.0527.

133. Iacobazzi D, Swim MM, Albertario A, Caputo M, Ghorbel MT. (2018). Thymus-Derived Mesenchymal Stem Cells for Tissue Engineering Clinical-Grade Cardiovascular Grafts. Tissue Eng Part A; 24(9-10): 794-808. DOI: 10.1089/ten.TEA.2017.0290.

134. Durán-Rey D, Crisóstomo V, Sánchez-Margallo JA, Sánchez-Margallo FM. (2021). Systematic Review of Tissue-Engineered Vascular Grafts. Front Bioeng Biotechnol; 9: 771400. DOI: 10.3389/fbioe.2021.771400.

135. Wu Y, Qin Y, Wang Z, Wang J, Zhang C, Li C, et al. (2018). The Regeneration of Macro-Porous Electrospun Poly(ε-Caprolactone) Vascular Graft during Long-Termin Situimplantation. J Biomed Mater Res; 106(4): 1618-1627. DOI: 10.1002/jbm.b.33967.

136. Kim S-J, Kim W-H, Lim H-G, Lee J-Y. (2008). Outcome of 200 Patients after an Extracardiac Fontan Procedure. J Thorac Cardiovasc Surg; 136(1): 108-116. DOI: 10.1016/j.jtcvs.2007.12.032.

137. Hibino N, McGillicuddy E, Matsumura G, Ichihara Y, Naito Y, Breuer C, et al. (2010). Late-term results of tissue-engineered vascular grafts in humans. J Thorac Cardiovasc Surg; 139(2): 431-436. DOI: 10.1016/j.jtcvs.2009.09.057.

138. Sugiura T, Matsumura G, Miyamoto S, Miyachi H, Breuer CK, Shinoka T. (2018). Tissue-Engineered Vascular Grafts in Children with Congenital Heart Disease: Intermediate Term Follow-Up. Semin Thorac Cardiovasc Surg; 30(2): 175-179. DOI: 10.1053/j.semtcvs.2018.02.002.

139. Kirkton RD, Santiago-Maysonet M, Lawson JH, Tente WE, Dahl SLM, Niklason LE, et al. (2019). Bioengineered Human Acellular Vessels Recellularize and Evolve into Living Blood Vessels after Human. Sci Transl Med; 11(485): eaau6934. DOI: 10.1126/scitranslmed.aau6934.

140. Jin X, Geng X, Jia L, Xu Z, Ye L, Gu Y, et al. (2019). Preparation of Small-Diameter Tissue-Engineered Vascular Grafts Electrospun from Heparin End-Capped PCL and Evaluation in a Rabbit Carotid Artery Replacement Model. Macromol Biosci; 19(8): e1900114. DOI: 10.1002/mabi.201900114.

141. Alessandrino A, Chiarini A, Biagiotti M, Dal Prà I, Bassani GA, Vincoli V, et al. (2019). Three-Layered Silk Fibroin Tubular Scaffold for the Repair and Regeneration of Small Caliber Blood Vessels: From Design to In Vivo Pilot Tests. Front Bioeng Biotechnol; 7: 356. DOI: 10.3389/fbioe.2019.00356.

142. Ribeiro C, Sencadas V, Correia DM, Lanceros-Méndez S. (2015). Piezoelectric polymers as biomaterials for tissue engineering applications. Colloids Surf B Biointerfaces; 136: 46-55. DOI: 10.1016/j.colsurfb.2015.08.043.

143. Chen Y, Ye L, Guan L, Fan P, Liu R, Liu H, et al. (2018). Physiological electric field works via the VEGF receptor to stimulate neovessel formation of vascular endothelial cells in a 3D environment. Biol Open; 7: bio035204. DOI: 10.1242/bio.035204.

144. Ahmed F, Dutta NK, Zannettino A, Vandyke KI, Choudhury NR. (2014). Engineering interaction between bone marrow derived endothelial cells and electrospun surfaces for artificial vascular graft applications. Biomacromolecules; 15(4): 1276-1287. DOI: 10.1021/bm401825c.

145. Mokhtari F, Azimi B, Salehi M, Hashemikia S, Danti S. (2021). Recent advances of polymer-based piezoelectric composites for biomedical applications. J Mech Behav Biomed Mat; 122: 104669. DOI: 10.1016/j.jmbbm.2021.104669.

146. Gryshkov O, Halabi FA, Kuhn AI, Leal-Marin S, Freund LJ, Förthmann M, et al. (2021). PVDF and P(VDF-TrFE) Electrospun Scaffolds for Nerve Graft Engineering: A Comparative Study on Piezoelectric and Structural Properties, and In Vitro Biocompatibility. Int J Mol Sci; 22(21): 11373. DOI: 10.3390/ijms222111373.

147. Ribeiro C, Sencadas V, Ribelles JLG, Lanceros-Méndez S. (2010). Influence of processing conditions on polymorphism and nanofiber morphology of electroactive poly(vinylidene fluoride) electrospun membranes. Soft Mat; 8(3): 274–287. DOI: 10.1080/1539445X.2010.495630.

148. Li Y, Liao C, Tjong SC. (2019). Electrospun Polyvinylidene Fluoride-Based Fibrous Scaffolds with Piezoelectric Characteristics for Bone and Neural Tissue Engineering. Nanomaterials (Basel); 9(7): 952. DOI: 10.3390/nano9070952.

149. Wen D-L, Sun D-H, Huang P, Huang W, Su M, Wang Y, et al. (2021). Recent progress in silk fibroin-based flexible electronics. Microsyst Nanoeng; 7(1): 35. DOI: 10.1038/s41378-021-00261-2.

150. Ribeiro C, Costa CM, Correia DM, Nunes-Pereira J, Oliveira J, Martins P, et al. (2018). Electroactive poly(vinylidene fluoride)-based structures for advanced applications. Nat Protoc; 13(4): 681-704. DOI: 10.1038/nprot.2017.157.

151. Cardoso VF, Lopes AC, Botelho G, Lanceros-Méndez S. Poly(vinylidene fluoride-trifluoroethylene) porous films: Tailoring microstructure and physical properties by solvent casting strategies. Soft Mater; 13: 243-253. DOI: 10.1080/1539445X.2015.1083444.

152. Pereira RFP, Gonçalves HMR, Correia DM, Costa CM, Silva MM, Lanceros-Méndez S, et al. (2020). Plasma-treated Bombyx mori cocoon separators for high-performance and sustainable lithium-ion batteries. Mater Today Sustain; 9: 100041. DOI: 10.1016/j.mtsust.2020.100041.

153. Bhardwaj N, Kundu SC. (2010). Electrospinning: a fascinating fiber fabrication technique. Biotechnol Adv; 28(3): 325-347. DOI: 10.1016/j.biotechadv.2010.01.004.

154. Kitsara M, Blanquer A, Murillo G, Humblot V, Vieira SB, Nogués C, et al. (2019). Permanently hydrophilic, piezoelectric PVDF nanofibrous scaffolds promoting unaided electromechanical stimulation on osteoblasts. Nanoscale; 11(18): 8906-8917. DOI: 10.1039/c8nr10384d.

155. Razafiarison T, Holenstein CN, Stauber T, Jovic M, Vertudes E, Loparic M, et al. (2018). Biomaterial surface energy-driven ligand assembly strongly regulates stem cell mechanosensitivity and fate on very soft substrates. Proc Natl Acad Sci USA; 115(18): 4631-4636. 10.1073/pnas.1704543115.

156. Otitoju TA, Ahmad AL, Ooi BS. (2017). Superhydrophilic (superwetting) surfaces: A review on fabrication and application. J Ind Eng Chem; 47: 19-40. DOI: 10.1016/j.jiec.2016.12.016.

157. Durán-Rey D, Brito-Pereira R, Ribeiro C, Ribeiro S, Sánchez-Margallo JA, Crisóstomo V, et al. (2022). Development and evaluation of different electroactive poly(vinylidene fluoride) architectures for endothelial cell culture. Front Bioeng Biotechnol; 10:1044667. doi: 10.3389/fbioe.2022.1044667

158. Durán-Rey D, Brito-Pereira R, Ribeiro C, Ribeiro S, Sánchez-Margallo JA, Crisóstomo V, et al. (2023). Development of silk fibroin scaffolds for vascular repair. Biomacromolecules; 24(3): 1121-1130. DOI: 10.1021/acs.biomac.2c01124.

159. Brito-Pereira R, Macedo AS, Tubio CR, Lanceros-Méndez S, Cardoso VF. (2021). Fluorinated polymer membranes as advanced substrates for portable Analytical systems and their proof of concept for colorimetric bioassays. ACS Appl Mater Interfaces; 13(15): 18065-18076. DOI: 10.1021/acsami.1c00227.

160. He Y-X, Zhang N-N, Li W-F, Jia N, Chen B-C, Zhou K, et al. (2012). N-Terminal domain of Bombyx mori fibroin mediates the assembly of silk in response to pH decrease. J Mol Biol; 418(3-4): 197-207. DOI: 10.1016/j.jmb.2012.02.040.

161. Reizabal A, Brito-Pereira R, Fernandes MM, Castro N, Correia V, Ribeiro C, et al. (2020). Silk fibroin magnetoactive nanocomposite films and membranes for dynamic bone tissue engineering strategies. Materialia; 12, 100709. DOI: 10.1016/j.mtla.2020.100709.

162. Strawhecker KE, Kumar SK, Douglas JF, Karim A. (2001). The critical role of solvent evaporation on the roughness of spin-cast polymer films. Macromolecules; 34(14): 4669-4672. DOI: 10.1021/ma001440d.

163. Um IC, Kweon HY, Lee KG, Park YH. (2003). The role of formic acid in solution stability and crystallization of silk protein polymer. Int J Biol Macromol; 33(4-5): 203-213. DOI: 10.1016/j.ijbiomac.2003.08.004.

164. Heo S-J, Nerurkar NL, Baker BM, Shin J-W, Elliot DM, Mauck RL. (2011). Fiber stretch and reorientation modulates mesenchymal stem cell morphology and fibrous gene expression on oriented nanofibrous microenvironments. Ann Biomed Eng; 39(11): 2780-2790. DOI: 10.1007/s10439-011-0365-7.

165. Wang HW, Zhou HW, Gui LL, Ji HW, Zhang XC. (2014). Analysis of effect of fiber orientation on Young's modulus for unidirectional fiber reinforced composites. Composites Part B; 56: 733-739. DOI: 10.1016/j.compositesb.2013.09.020.

166. Huang W, Ling S, Li C, Omenetto FG, Kaplan DL. (2018). Silkworm silk-based materials and devices generated using bionanotechnology. Chem Soc Rev; 47(17): 6486-6504. DOI: 10.1039/c8cs00187a.

167. Cai M, He H, Zhang X, Yan X, Li J, Chen F, et al. (2019). Efficient synthesis of PVDF/PI side-by-side bicomponent nanofiber membrane with enhanced mechanical strength and good thermal stability. Nanomaterials (Basel); 9(1): 39. DOI: 10.3390/nano9010039.

168. Reizabal A, Gonçalves R, Fidalgo-Marijuan A, Costa CM, Pérez L, Vilas JL, et al. (2020). Tailoring silk fibroin separator membranes pore size for improving performance of lithium ion batteries. J Membr Sci; 598: 117678. DOI: 10.1016/j.memsci.2019.117678.

169. Brito-Pereira R, Correia DM, Ribeiro C, Francesko A, Etxebarria I, Pérez-Álvarez L, et al. (2018). Silk fibroin-magnetic hybrid composite electrospun fibers for tissue engineering applications. Composites Part B; 141: 70-75. DOI: 10.1016/j.compositesb.2017.12.046.

170. Cai X, Lei T, Sun D, Lin L. (2017). A critical analysis of the α, β and γ phases in poly(vinylidene fluoride) using FTIR. RSC Adv; 7(25): 15382-15389. DOI: 10.1039/c7ra01267e.

171. Simona E, Monticelli O, Marsano E, Cebe P. (2013). On the electrospinning of PVDF: Influence of the experimental conditions on the nanofiber properties. Polymer International; 62(1): 41-48. DOI: 10.1002/pi.4314.

172. Cebe P, Partlow BJ, Kaplan DL, Wurm A, Zhuravlev E, Schick C. (2017). Silk I and Silk II studied by fast scanning calorimetry. Acta Biomater; 55: 323-332. DOI: 10.1016/j.actbio.2017.04.001.

173. Li G, Sun S. (2022). Silk fibroin-based biomaterials for tissue engineering applications. Molecules; 27(9): 2757. DOI: 10.3390/molecules27092757.

174. Marshall JE, Zhenova A, Roberts S, Petchey T, Zhu P, Dancer CEJ, et al. (2021). On the Solubility and Stability of Polyvinylidene Fluoride. Polymers (Basel); 13(9):1354. DOI: 10.3390/polym13091354.

175. Wang Y, Rudym DD, Walsh A, Abrahamsen L, Kim HJ, Kim HS, et al. (2008). In vivo degradation of three-dimensional silk fibroin scaffolds. Biomaterials; 29(24-25): 3415-3428. DOI: 10.1016/j.biomaterials.2008.05.002.

176. Ribeiro S, Ribeiro T, Ribeiro C, Correia DM, Farinha JPS, Gomes AC, et al. (2018). Multifunctional platform based on electroactive polymers and silicananoparticles for tissue engineering applications. Nanomaterials (Basel); 8(11): 933. DOI: 10.3390/nano8110933.

177. Veleva AN, Heath DE, Johnson JK, Nam J, Patterson C, Lannutti JJ, et al. (2009). Interactions between endothelial cells and electrospun methacrylic terpolymer fibers for engineered vascular replacements. J Biomed Mater Res A; 91(4): 1131-1139. DOI: 10.1002/jbm.a.32276.

ANEXOS

Anexo I: Iconografía

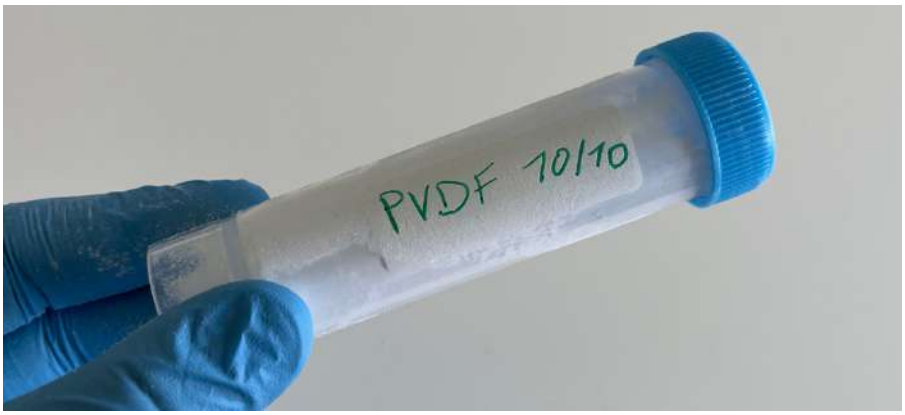

Figura 7. Formato comercial de PVDF 10/10 en polvo.

Figura 8. Diferentes perspectivas del instrumental *Doctor Blade* para diseñar películas con un grosor de 200, 450, 700 o 950 mm mediante *solvent-casting*.

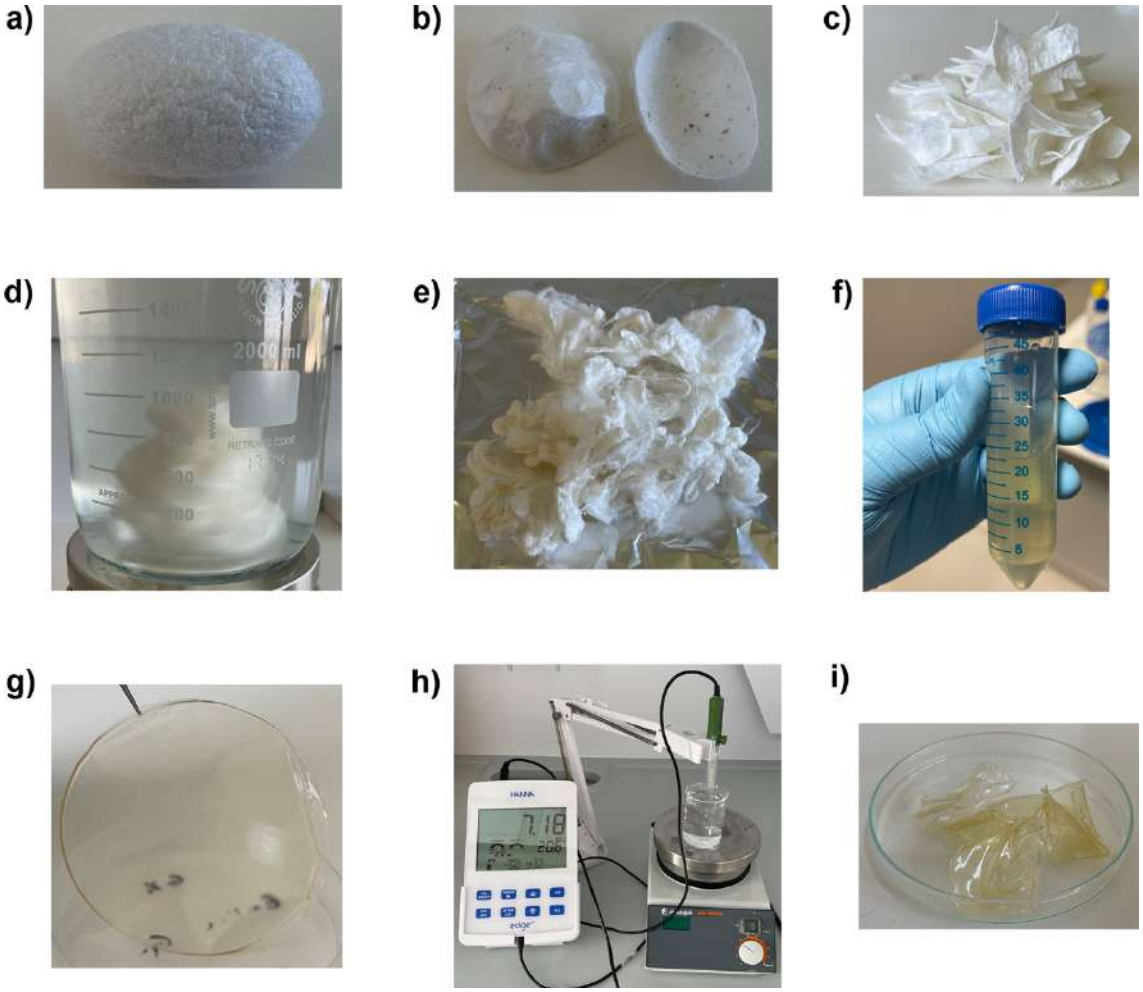

Figura 9. Procesado de SF, donde: **a)** se obtienen huevos de *Bombyx mori* comerciales; **b)** extracción de la crisálida y eliminación de las impurezas macroscópicas; **c)** troceado del huevo en tamaños de aproximadamente 1 cm^2; **d)** separación de la sericina de SF mediante una disolución de carbonato de calcio o el uso de agua destilada en autoclave; **e)** lavado con agua destilada y secado de la muestra a 30°C en un horno; **f)** disolución de la muestra con ácido fórmico y cloruro cálcico, y centrifugación para separar SF de las impurezas; **g)** el sobrenadante proveniente del centrifugado se vierte en placas de Petri y se dejan secar a temperatura ambiente bajo una mampara; **h)** eliminación de sales e igualar el pH a valores neutros o cercanos a 7 mediante lavados en agua destilada; **i)** secado de las muestras en un horno a 30°C y obtención de SF lista para usarse.

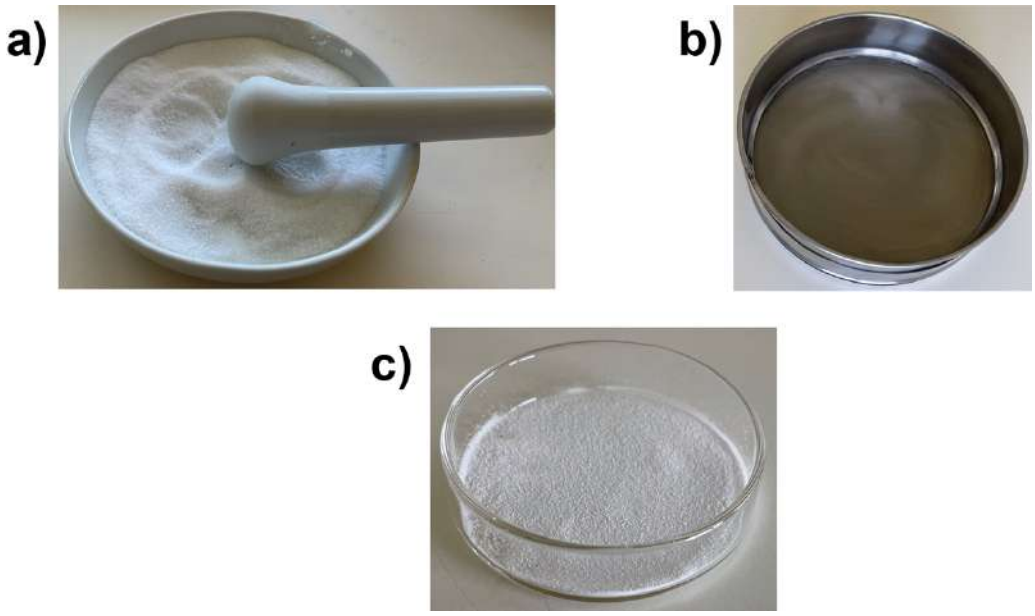

Figura 10. Proceso de tamizado de la sal para obtener membranas porosas, donde: **a)** utilización de un mortero para disminuir el tamaño de las partículas de sal; **b)** tamizador con tamaños de poros de 2 mm; **c)** partículas de sal con un tamaño aproximado de 2 mm listas para ser usadas en el diseño de membranas porosas.

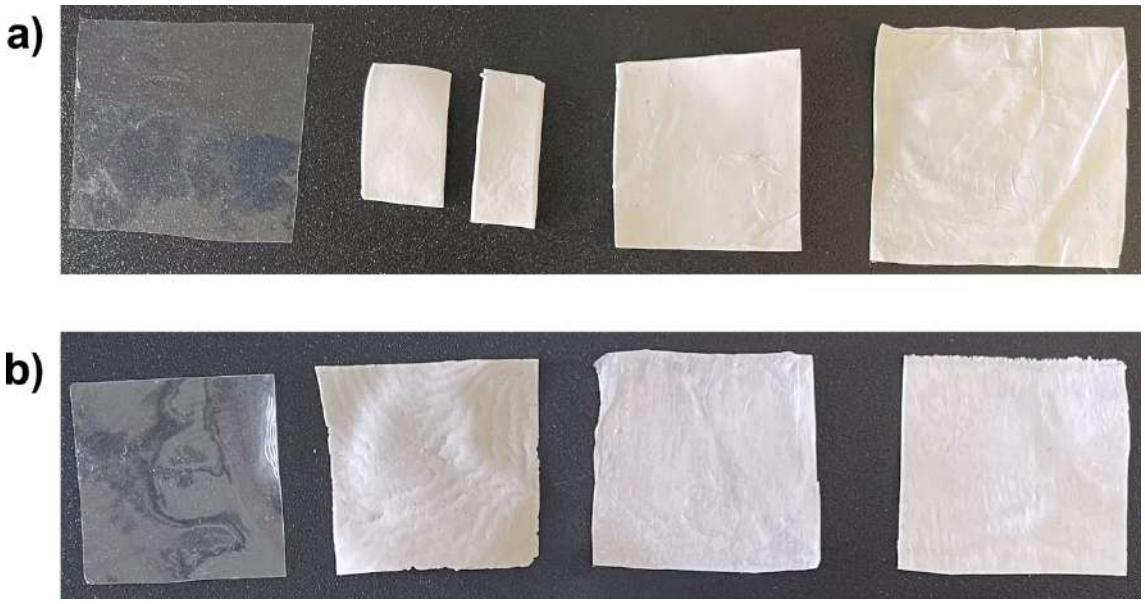

Figura 11. De izquierda a derecha, películas, membranas porosas, membranas electrohiladas aleatorias, y membranas electrohiladas orientadas, siendo el material: **a)** PVDF; y **b)** SF.

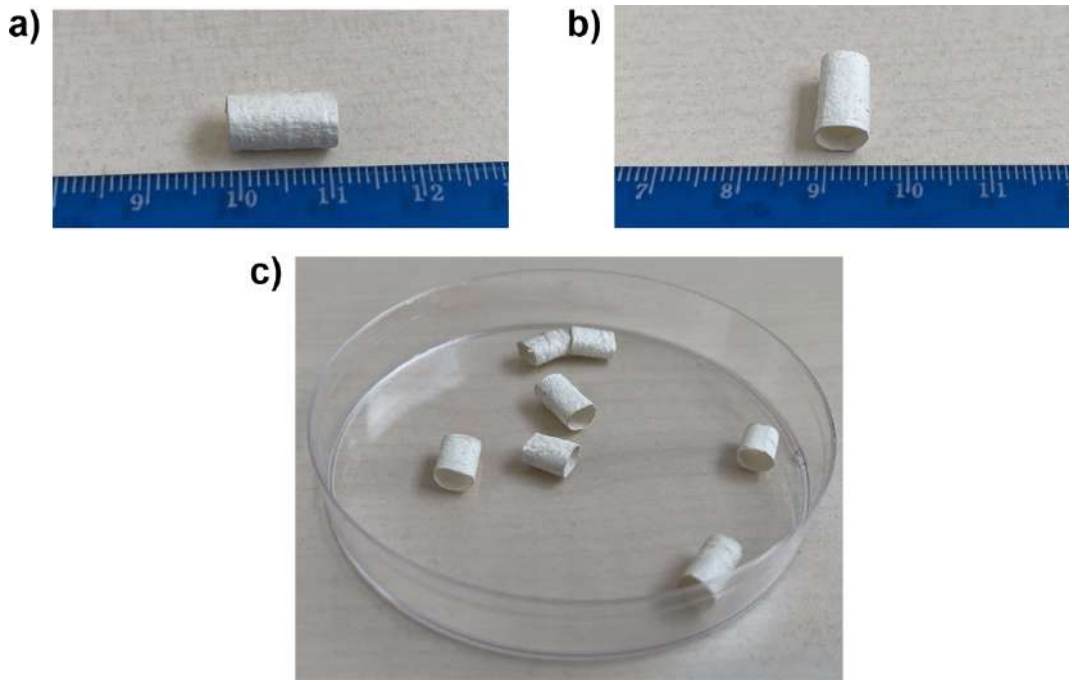

Figura 12. a-c) TEVGs de SF diseñados con la técnica de electrohilado.

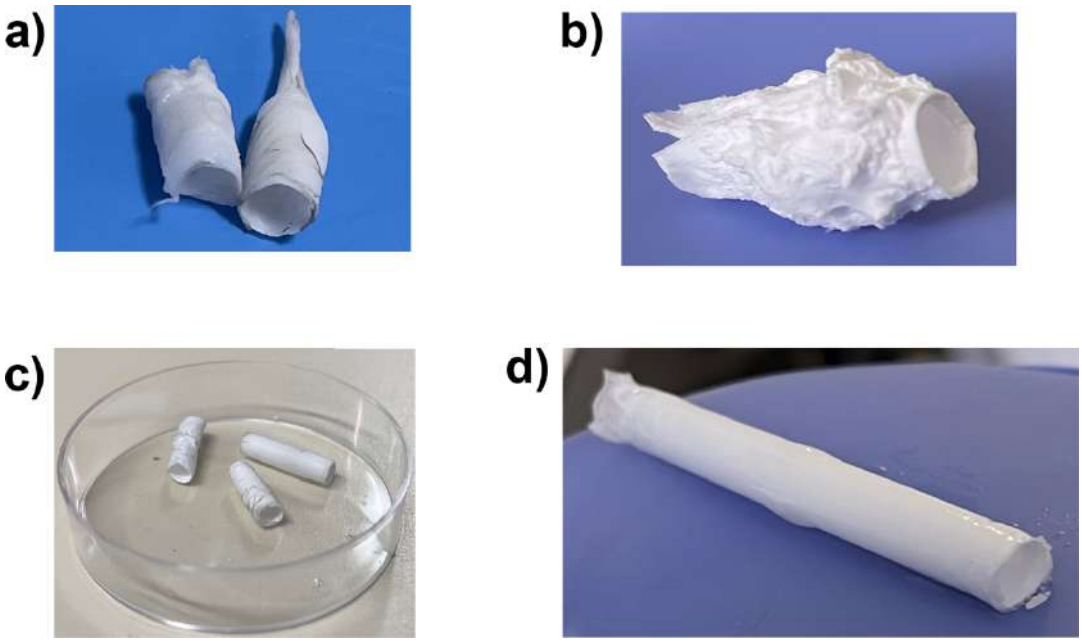

Figura 13. TEVGs diseñados con PVDF mediante la técnica de electrohilado. **a-c)** Diferentes desarrollos de injertos vasculares variando las configuraciones del electrohilado; **d)** prototipo final de injerto vascular de PVDF.

Anexo II: Contribuciones Científicas

Artículos originales publicados en revistas científicas indexadas en JCR

- **Histological and Immunohistochemical Study of Wounds in Sheep Skin in Maggot Therapy by Using Protophormia terraenovae (Diptera: Calliphoridae)**

  Durán-Rey D, Galapero J, Frontera E, Bravo-Barriga D, Blanco J, Gómez L.

  Larvae J Med Entomol. **2020**; 57(2): 369-376. DOI: 10.1093/jme/tjz185.

- **Comparative Study of the Influence of Three-Dimensional Versus Two-Dimensional Urological Laparoscopy on Surgeons' Surgical Performance and Ergonomics: A Systematic Review and Meta-Analysis**

  Sánchez-Margallo FM, Durán-Rey D, Pascual AS, Martínez JAM, Sánchez-Margallo JA.

  J Endourol. **2021**; 35(2): 123-137. DOI: 10.1089/end.2020.0284.

Libros o Capítulos de libro

- **Wearable technology for assessment and surgical assitance in minimally invasive surgery. En: Sanna A. Advances in Minimally Invasive Surgery**

  Sánchez-Margallo JA, Rabazo JC, de Miguel CP, Gloor P, Durán-Rey D, González-Portillo MR, et al.

  IntechOpen. **2021**. DOI: 10.5772/intechopen.100617.

- **Educational models for training in minimally invasive colorectal surgery. En: Państwo i Społeczeństwo: State and Society**

  Sánchez-Margallo FM, Durán-Rey D, González-Portillo MR, López-Agudelo I, Sánchez-Margallo JA.

  CEJSH. **2021**; 1: 115-140. DOI: 10.48269/2451-0858-pis-2021-1-010.

- **Cirugía de cráneo y columna en pequeños animales**

  Sánchez-Margallo FM, Usón-Gargallo J, Vérez-Fraguela JL,, Latorre-Reviriego R, Köstlin R, Climent-Peris S, et al.

  SERVET. **2022**. ISBN: 9788418339462.

Abstracts publicados en revistas científicas indexadas en JCR

- **Evaluation of the effect of 3D imaging in the European Training in Basic Laparoscopic Urological Skills (E-BLUS) program**

  Sánchez-Margallo JA, Durán-Rey D, Sánchez-Margallo FM.

  28th International Congress of the European Association for Endoscopic Surgery (EAES) Virtual Congress 23-26 June 2020. Surg Endosc. **2020**. DOI: 10.1007/s00464-020-07834-8.

- **Evaluation of a robotic emulator laparoscopic instrument**

  Sánchez-Margallo JA, Durán-Rey D, Sánchez-Margallo FM.

  28th International Congress of the European Association for Endoscopic Surgery (EAES) Virtual Congress 23-26 June 2020. Surg Endosc. **2020**. DOI: 10.1007/s00464-020-07834-8.

- **O-061 - Revisión del estado actual de la ingeniería tisular cardiovascular**

  Sánchez-Margallo FM, Durán-Rey D, Sánchez-Margallo JA, Crisóstomo V.

  Cir Esp. **2020**; 98(Espec Congr 1): 17.

- **O-162 - Análisis de la curva de aprendizaje de un nuevo diseño de instrumento laparoscópico articulado**

  Sánchez-Margallo FM, Durán-Rey D, Sánchez-Margallo JA.

  Cir Esp. **2020**; 98(Espec Congr 1): 454.

- **O-179 - Uso de dispositivos inteligentes para la predicción de la carga de trabajo durante la práctica laparoscópica**

  Sánchez-Margallo FM, Gloor PA, Durán-Rey D, Sánchez-Margallo JA

  Cir Esp. **2020**; 98(Espec Congr 1): 471.

- **Dispositivo laparoscópico mecánico articulado: Análisis de la curva de aprendizaje**

  Sánchez-Margallo JA, Durán-Rey D, Sánchez-Margallo FM.

  XXXVIII Congreso Anual de la Sociedad Española de Ingeniería Biomédica CASEIB. 25-27 Nov. **2020**; pp. 129-132. ISBN: 978-84-09-25491-0.

- **Relationship between surgeon's physiological and kinematic parameters and the quality of surgical performance and workload in laparoscopic training**

  Sánchez Margallo JA, Rabazo JC, Durán-rey D, López-Agudelo I, González-Portillo MR, Gloor PA, et al.

  Br J Surg. **2021**; 108 (Supplement 3). DOI: 10.1093/bjs/znab160.042.

- **Design and study of different silk fibroin structures**

  Durán-Rey D, Brito-Pereira R, Ribeiro C, Sánchez-Margallo JA, Crisóstomo V, Lanceros-Méndez S, et al.

  Br J Surg. **2023**; 110 (Supplement 1). DOI: 10.1093/bjs/znac443.014.

- **Design and study of different PVDF structures**

  Durán-Rey D, Brito-Pereira R, Ribeiro C, Sánchez-Margallo JA, Crisóstomo V, Lanceros-Méndez S, et al.

  Br J Surg. **2023**; 110 (Supplement 1). DOI: 10.1093/bjs/znac443.013.

Comunicaciones científicas en Congresos y Jornadas

- **Terapia larvaria con Protophormia terraenovae en ovinos: Estudio Histológico e Inmunohistoquímico**

  Durán-Rey D.

  VI Jornadas Veterinarias de Estudiantes y V Jornadas de Ciencias de la Salud, celebradas en Cáceres durante los días 28, 29 y 30 de marzo de 2019.

- **Evaluación objetiva del instrumento laparoscópico FlexDex®: ergonomía y desempeño quirúrgico**

  Durán-Rey D, Sánchez-Margallo JA, Sánchez-Margallo FM.

  7º Simposio Nacional de Actualización en Formación de Cirugía Laparoscópica y Robótica en el ámbito multidisciplinario, celebrado en Cáceres el 4 de diciembre de 2019.

- **Predicting the surgical workload during laparoscopy using body sensors of smartwatches**

  Sánchez-Margallo JA, Gloor PA, Durán-Rey D, Sánchez-Margallo FM.

  European Association for Endoscopic Surgery and other Interventional Techniques, celebrado en formato online del 23 al 26 de junio de 2020.

- **Estado actual de los injertos vasculares de ingeniería tisular: Revisión Sistemática**

  Durán-Rey D, Sánchez-Margallo JA, Crisóstomo V, Sánchez-Margallo FM.

  XVIII Congreso Nacional de la Sociedad Española de Cirugía Laparoscópica y Robótica, celebrado en formato online del 15 al 17 de octubre de 2020.

- **Predicción de la carga de trabajo quirúrgico durante la práctica laparoscópica mediante el uso de tecnología wearable**

  Sánchez-Margallo JA, Gloor PA, Durán-Rey D, Sánchez-Margallo FM.

  XVIII Congreso Nacional de la Sociedad Española de Cirugía Laparoscópica y Robótica, celebrado en formato online del 15 al 17 de octubre de 2020.

- **Nuevo diseño de instrumentos laparoscópicos articulados: Análisis de la curva de aprendizaje**

  Sánchez-Margallo JA, Durán-Rey D, Sánchez-Margallo FM.

  XVIII Congreso Nacional de la Sociedad Española de Cirugía Laparoscópica y Robótica, celebrado en formato online del 15 al 17 de octubre de 2020.

- **Injertos vasculares de ingeniería tisular**

  Durán-Rey D.

  IV Semana de la Ciencia y la Tecnología en Extremadura, celebrado en formato online del 26 de octubre al 9 de noviembre de 2020.

- **Revisión del estado actual de la ingeniería tisular cardiovascular**

  Sánchez-Margallo FM, Durán-Rey D, Sánchez-Margallo JA, Crisóstomo V.

  33 Congreso Nacional de Cirugía, celebrado en formato online del 11 al 14 de noviembre de 2020.

- **Análisis de la curva de aprendizaje de un nuevo diseño de instrumento laparoscópico articulado**

  Sánchez-Margallo JA, Durán-Rey D, Sánchez-Margallo FM.

  33 Congreso Nacional de Cirugía, celebrado en formato online del 11 al 14 de noviembre de 2020.

- **Uso de dispositivos inteligentes para la predicción de la carga de trabajo durante la práctica laparoscópica**

  Sánchez-Margallo JA, Gloor PA, Durán-Rey D, Sánchez-Margallo FM.

  33 Congreso Nacional de Cirugía, celebrado en formato online del 11 al 14 de noviembre de 2020.

- **Injertos vasculares de ingeniería tisular**

  Durán-Rey D.

  IV Jornadas Doctorales de la Universidad de Extremadura, celebrado en formato online el 27 de noviembre de 2020.

- **Systematic review of vascular grafts by tissue engineering composition and production technologies**

  Durán-Rey D, Sánchez-Margallo JA, Crisóstomo V, Sánchez-Margallo FM.

  32nd Annual SMIT Congress, celebrado en formato online los días 3, 4 5, 9 y 10 de diciembre de 2020.

- **Surgical workload prediction during laparoscopic practice using wearable technology**

  Sánchez-Margallo JA, Gloor PA, Durán-Rey D, Sánchez-Margallo FM.

  32nd Annual SMIT Congress, celebrado en formato online los días 3, 4 5, 9 y 10 de diciembre de 2020.

- **Robotic emulator laparoscopic instruments: A learning curve analysis**

  Sánchez-Margallo JA, Durán-Rey D, Sánchez-Margallo FM.

  32nd Annual SMIT Congress, celebrado en formato online los días 3, 4 5, 9 y 10 de diciembre de 2020.

- **Relación entre los parámetros cinemáticos y fisiológicos de los cirujanos y el desempeño quirúrgico y la carga de trabajo en el entrenamiento en cirugía laparoscópica**

  Sánchez-Margallo JA, Castillo-Rabazo J, Durán-Rey D, López-Agudelo I, González-Portillo MR, Gloor PA, et al.

  1er Congreso Virtual de la Sociedad Española de Investigaciones Quirúrgicas, celebrado en formato online del 11 al 12 de marzo de 2021.

- **Injertos vasculares de ingeniería tisular**

  Durán-Rey D.

  IV Jornadas de Divulgación Científica G-9 y IX Jornadas Doctorales G-9, celebradas en Bilbao del 18 al 20 de mayo de 2022.

- **Diseño y estudio de diferentes estructuras de fibroína de seda**

  Durán-Rey D, Brito-Pereira R, Ribeiro C, Sánchez-Margallo JA, Crisóstomo V, Lanceros-Méndez S, et al.

  26 Congreso de la Sociedad Española de Investigaciones Quirúrgicas, celebrado en Gijón del 29 al 30 de septiembre de 2022.

- **Diseño y estudio de diferentes estructuras de PVDF**

  Durán-Rey D, Brito-Pereira R, Ribeiro C, Sánchez-Margallo JA, Crisóstomo V, Lanceros-Méndez S, et al.

  26 Congreso de la Sociedad Española de Investigaciones Quirúrgicas, celebrado en Gijón del 29 al 30 de septiembre de 2022.

- **Desarrollo de injertos vasculares de ingeniería tisular**

  Durán-Rey D.

  VI Jornadas Doctorales de la Universidad de Extremadura, celebrado en Cáceres el 4 de noviembre de 2022.

Experiencia docente y formadora

- **Tutor de Trabajo Fin de Máster en el Máster Oficial Universitario en Endoscopia y Cirugía de Mínima Invasión en Pequeños Animales**

  2020-2021, Universidad de Extremadura.

- **Profesor en el Curso de Especialista Universitario en Técnicas Endoscópicas y de Endocirugía en Pequeños Animales**

  2021-2022, Universidad de Extremadura.

- **Profesor y organizador de Cursos de Laparoscopia**

  2019-2023, Centro de Cirugía de Mínima Invasión Jesús Usón (Cáceres, España).

Anexo III: Informes de los Directores

Dr. D. Francisco Miguel Sánchez Margallo y Dra. Dña. Verónica Crisóstomo Ayala como directores de la tesis doctoral titulada "**ANÁLISIS Y VALIDACIÓN DE MATERIALES DESTINADOS AL DISEÑO DE INJERTOS VASCULARES DE INGENIERÍA TISULAR**", certificamos el factor de impacto y la categorización de las siguientes publicaciones incluidas en la tesis doctoral. Del mismo modo, se especifica cuál ha sido la participación del doctorando.

Durán-Rey D, Crisóstomo V, Sánchez-Margallo JA, Sánchez-Margallo FM. (**2021**). Systematic review of tissue-engineered vascular graft. *Front Bioeng Biotechnol*; 9:771400. DOI: 10.3389/fbioe.2021.771400. PMID: 34805124.

IF (JCR): 6.064

Categoría: Multidisciplinary sciences

Revista dentro del 25%: Sí

Contribución del doctorando: Desarrollo experimental, análisis y discusión de los resultados, elaboración y escritura del manuscrito.

Durán-Rey D, Brito-Pereira R, Ribeiro C, Ribeiro S, Sánchez-Margallo JA, Crisóstomo V, Irastorza I, Silván U, Lanceros-Méndez S, Sánchez-Margallo FM. (**2022**). Development and evaluation of different electroactive poly(vinylidene fluoride) architectures for endothelial cell culture. *Front Bioeng Biotechnol*; 10:1044667. DOI: 10.3389/fbioe.2022.1044667. PMID: 36338140.

IF (JCR): 6.064

Categoría: Multidisciplinary sciences

Revista dentro del 25%: Sí

Contribución del doctorando: Desarrollo experimental, análisis y discusión de los resultados, elaboración y escritura del manuscrito.

Durán-Rey D, Brito-Pereira R, Ribeiro C, Ribeiro S, Sánchez-Margallo JA, Crisóstomo V, Irastorza I, Silván U, Lanceros-Méndez S, Sánchez-Margallo FM. (**2023**). Development of silk fibroin scaffolds for vascular repair. *Biomacromolecules*; 24(3): 1121-1130. DOI: 10.1021/acs.biomac.2c01124. PMID: 36754364.

IF (JCR): 6.979

Categoría: Polymer science

Revista dentro del 25%: Sí

Contribución del doctorando: Desarrollo experimental, análisis y discusión de los resultados, elaboración y escritura del manuscrito.

Dr. D. Francisco Miguel Sánchez Margallo

Dra. Dña. Verónica Crisóstomo Ayala